UNIVERSITÀ DEGLI STUDI DI PISA

Facoltà di Scienze Matematiche, Fisiche e Naturali

Corso di Laurea Magistrale in Matematica

Tesi di Laurea

ON THE LINEAR STABILITY OF SOME PERIODIC ORBITS OF THE N-BODY PROBLEM WITH THE SIMMETRY OF PLATONIC POLYHEDRA

Relatore:
Prof. GIOVANNI FEDERICO GRONCHI

Candidato:
MARCO FENUCCI

Controrelatore:
Prof. ANDREA MILANI COMPARETTI

ANNO ACCADEMICO 2015/2016

CONTENTS

LIST OF FIGURES

LIST OF TABLES

INTRODUCTION

In the last few years, many interesting periodic motions of the classical Newtonian N-body problem have been discovered as minimizers of the action functional

$$\mathcal{A} : \Lambda \to \mathbb{R} \cup \{+\infty\},$$
$$\mathcal{A}(u) = \int_0^T \left(\frac{1}{2} \sum_{i=1}^{N} m_h |\dot{u}_h|^2 + \sum_{1 \leqslant h < k \leqslant N} \frac{m_h m_k}{|u_h - u_k|} \right) dt,$$

on a particular subset $\Lambda \subseteq H^1_T(\mathbb{R}, \mathbb{R}^{3N})$ of T-periodic loops. The interest in this classical problem was revived by the numerical discovery of the now famous *figure eight* solution of the three-body problem, by C. Moore in 1993 ([15]). In 2000 A. Chenciner and R. Montgomery rediscover this particular orbit, giving a formal proof of its existence that uses the direct method of Calculus of Variations. The figure eight is a first example of a N-body *choreography*, that is a solution of the classical N-body problem in which N equal masses chase each other around a fixed closed curve, equally spaced in phase along the curve: since 2000 many other choreographies that present a strong symmetrical structure have been found. Moreover, in [13] and [19] the authors proved the linear stability of the figure eight: this fact is quite surprising, since that no other stable choreographies are known ("All the choreographies found, except the eight, are unstable", see [20]).

In this thesis, following [5], we prove the existence of a number of periodic motions of the classical N-body problem which, up to relabeling of the N particles, are invariant under the rotation group $\mathcal{R}$ of one of the five Platonic polyhedra. The number N coincides with the order of the rotation group $\mathcal{R}$ and the particles have all the same mass. We use again variational techniques to minimize the Lagrangian action $\mathcal{A}$ on a suitable subset $\mathcal{K}$ of the H^1 T-periodic maps $u : \mathbb{R} \to \mathbb{R}^{3N}$. The set $\mathcal{K}$ is a cone and it is determined by imposing on u both topological and symmetry constraints which are defined in terms of the rotation group $\mathcal{R}$. For a certain number of cones $\mathcal{K}$, using level estimates and local perturbations, we show that minimizers are free of collisions and therefore they are classical solutions on the N-body problem.

A natural question that comes out in presence of a periodic orbit is whether it is stable or not. To perform a study of the linear stability we use numerical methods, since our problem is not integrable. In fact we know only that periodic orbits with the previous symmetries exist, but we do not have their analytic expression. These particular solutions were found numerically (see the website [8]), using a method described in [15] and called *relaxation dynamics*. The numerical implementation of this method reduces to a gradient search of the minima in some finite-dimensional approximation of the path space: in short, it is a numerical implementation of a direct method of Calculus of Variations. Starting from these numerical solutions, we can propagate numerically the *variational equation* in order to produce an approximation

of the *monodromy matrix*, from which we can determine the linear stability studying its spectral properties: this is a first method that we develop. However, since the convergence of the gradient search is slow, especially when the orbit presents some close approaches, this method can be inefficient. An alternative approach is to find an initial condition of the periodic orbit and then propagate numerically the equation of motion and the variational equation coupled together. A classical method to find an initial condition is the well known *multiple shooting method*, described for example in [22]. This method has been successfully used in [13] to find an initial condition for the figure eight and some other non-symmetric choreographies. However, since this is an iterative method too, it could fail to converge and this typically happens when the orbit passes close to a collisions. Therefore, it is clear that the problem of close approaches must be treated with more care.

The thesis is structured as follows:

CHAPTER 1 It contains results on the existence of periodic orbits of the classical N-body problem with the symmetries of Platonic polyhedra, as treated in [5].

CHAPTER 2 In this chapter we try to develop an automatic procedure in order to find all the periodic orbits described in Chapter 1, in a way to complete the lists present in [5].

CHAPTER 3 Following [10] and [17], we present the classical theory of linear stability for periodic solutions of autonomous systems. In particular, we introduce here the monodromy matrix, the Floquet multipliers and the Poincaré map.

CHAPTER 4 It is the heart of the work, in which we develop the two different numerical methods to study the linear stability of periodic orbits found in Chapters 1 and 2. Some tests of the software written are reported in this Chapter, in a way to study the performances of each one. At the end, we present all the results obtained for the orbits found in Chapter 2.

CHAPTER 5 In this Chapter we suggest some improvements of the methods of Chapter 4 and of the software, which could represent a continuation of the present work, in order to produce a true computer assisted proof of the stability or instability of these orbits. Moreover, on the basis of [6], we could study the stability and bifurcations of these orbits in the case of non-Newtonian potentials of the form $1/r^\alpha$.

1

PERIODIC ORBITS WITH THE SYMMETRY OF PLATONIC POLYHEDRA

In this chapter we present results appearing in [5] and [9], in particular prove the existence of smooth periodic orbits of the classical Newtonian N-body problem which, up to relabeling of the N particles, are invariant under the rotation group $\mathcal{R}$ of one of the five Platonic polyhedra. The number N coincides with the order of $\mathcal{R}$ and the particles have all the same mass. The authors use variational techniques that permit to find such orbits as minimizers of the Lagrangian action on a suitable subset $\mathcal{K}$ of the H^1 T-periodic maps $u : \mathbb{R} \to \mathbb{R}^{3N}$. The set $\mathcal{K}$ is a cone and it is determined by imposing both symmetrical and topological constraints. We shall see that the action functional is coercive on this subset, therefore the existence of minimizers is ensured by standard arguments of Calculus of Variations. The subsequent problem that we have to deal with is the exclusion of both total and partial collisions: we recall here the methods used to avoid these singularities. After that, we are sure that our minimum points are true solutions of the classical Newtonian N-body problem.

THE N-BODY PROBLEM AND CALCULUS OF VARIATIONS

Consider N point masses $m_1, \dots, m_N$ subject to their mutual gravitational interaction. The equations of motion for this problem are

$$m_i \ddot{u}_i = \frac{\partial U}{\partial u_i}(u), \quad i = 1, \dots, N \tag{1.1}$$

where

$$U(u) = \sum_{1 \leqslant h < k \leqslant N} \frac{m_h m_k}{|u_h - u_k|}$$

is the potential. The map $\mathbb{R} \ni t \mapsto u = (u_1, \dots, u_N) \in \mathbb{R}^{3N}$ describes the evolution of the positions of the N bodies in the three dimensional space $\mathbb{R}^3$. If we introduce the kinetic energy

$$K(\dot{u}) = \frac{1}{2} \sum_{i=1}^{N} m_i |\dot{u}_i|^2,$$

for a fixed period $T > 0$ we can give a variational formulation to the search for periodic orbits of (1.1): this solutions are stationary points of the Lagrangian action functional

$$\mathcal{A}(u) = \int_0^T K(\dot{u}(t)) + U(u(t)) dt, \tag{1.2}$$

on a particular set of admissible closed curves. In particular, we can search for periodic solutions which are minimum points of $\mathcal{A}$.

It is well known that for this type of problems, a natural environment where we can search for minima is the Sobolev space $H^1_T(\mathbb{R}, \mathbb{R}^{3N})$ of T- periodic loops (i.e. closed curves) in H^1, with norm

$$\|u\|_{H^1_T} = \left[\int_0^T |u(t)|^2 + |\dot{u}(t)|^2 dt \right]^{1/2},$$

where $\dot{u} \in L^2$ is the weak derivative of u in H^1. Using the integral of the center of mass we can assume $\sum_{h=1}^N m_h u_h = 0$ and introduce the configuration space as

$$X = \left\{ x = (x_1, \dots, x_N) \in \mathbb{R}^{3N} : \sum_{h=1}^N m_h x_h = 0 \right\}.$$

In this way we restrict the domain of (1.2) to the loop space $\Lambda = H^1_T(\mathbb{R}, X)$.

Searching for minima

To ensure the existence of minimum points of a functional we use standard methods of Calculus of Variations: we recall briefly these results.

DEFINITION 1.1 - Let $E \subseteq \Lambda$ be a set of loops. A functional $\mathcal{J} : \Lambda \to \mathbb{R}$ is COERCIVE on E if

$$\lim_{k \to +\infty} \mathcal{J}(u^{(k)}) = +\infty$$

for each sequence $\left\{ u^{(k)} \right\}_{k \in \mathbb{N}} \subset E$ such that $\lim_{k \to \infty} \left\| u^{(k)} \right\| = +\infty$.

The following theorem, due to L. Tonelli, will be critical in the searching for periodic orbits.

THEOREM 1.2 - *Let $\mathcal{J} : E \to \mathbb{R}$ a coercive functional on $E \subseteq \Lambda$ and suppose that it is also lower-semicontinuous on E. Then there exists a minimum point of $\mathcal{J}$ on $\overline{E}$.*

Proof. Let $I = \inf_{\overline{E}} \mathcal{J} \in \mathbb{R} \cup \{-\infty\}$. From the definition of inf, there exists a sequence $\left\{ u^{(k)} \right\} \subseteq E$ such that $\lim_{k \to \infty} \mathcal{J}(u^{(k)}) = I$. Since $I \in \mathbb{R} \cup \{-\infty\}$, there exist $M \in \mathbb{R}$ and a subsequence k_n such that $\mathcal{J}(u^{(k_n)}) \leqslant M$, then from the definition of coercivity we have that $\left\| u^{(k_n)} \right\|_{H^1_T}$ is bounded. So, up to subsequences, there exists $v \in L^2$ such that $\dot{u}^{(k_n)} \rightharpoonup v$. From Ascoli-Arzelà's theorem we have that, up to subsequences, there exists $u_* \in \overline{E}$ such that $u^{(k_n)} \to u_*$ uniformly and $\dot{u}_* = v$. Using the lower-semicontinuity property we see that $I \in \mathbb{R}$ and u is actually a minimum point, in fact

$$I \leqslant \mathcal{J}(u_*) \leqslant \liminf_{n \to \infty} \mathcal{J}(u^{(k_n)}) = \lim_{k \to \infty} \mathcal{J}(u^{(k)}) = I.$$

□

The functional (1.2) results to be lower-semicontinuous: in fact, if $\dot{u}^{(k)}$ weakly converges to $\dot{u}_*$ with $u_* \in \Lambda$, then $u^{(k)}$ converges uniformly to u_*, up to subsequences. Then from the Cauchy-Schwartz inequality we have

$$\liminf_{k \to \infty} \left\| \dot{u}^{(k)} \right\|^2_{H^1_T} \geqslant \|\dot{u}_*\|^2_{H^1_T},$$

so the kinetic part of $\mathcal{A}$ is lower-semicontinuous. Furthermore, the uniform convergence of $u^{(k)}$ and the continuity of the potential U ensure that

$$\lim_{k\to\infty}\int_0^T U(u^{(k)}(t))dt = \int_0^T U(u_*(t))dt,$$

so the functional (1.2) is lower-semicontinuous.

However, $\mathcal{A}$ is not coercive on the whole space Λ: consider for example the problem of 4 bodies and take the sequence

$$u^{(n)}(t) = (u_1^n(t), u_2^n(t), u_3^n(t), u_4^n(t)),$$

defined by

$$\begin{cases} u_1^n(t) = \left(n + \frac{1}{n}\cos\frac{2\pi t}{T}, n + \frac{1}{n}\sin\frac{2\pi t}{T}, 0\right) \\ u_2^n(t) = \left(-n + \frac{1}{n}\cos\frac{2\pi t}{T}, n + \frac{1}{n}\sin\frac{2\pi t}{T}, 0\right) \\ u_3^n(t) = \left(n + \frac{1}{n}\cos\frac{2\pi t}{T}, -n + \frac{1}{n}\sin\frac{2\pi t}{T}, 0\right) \\ u_4^n(t) = \left(-n + \frac{1}{n}\cos\frac{2\pi t}{T}, -n + \frac{1}{n}\sin\frac{2\pi t}{T}, 0\right) \end{cases}$$

They represent four circles of radius $1/n$ around the points $(\pm n, \pm n)$, covered in a time T with uniform motion: in this way we have that $\left\|u^{(n)}\right\|_{H^1_T} \to +\infty$. Since the mutual distances between the particles become larger and larger, the contribute of the potential part to the action is zero at the limit. Furthermore, for the kinetic part we can compute directly that

$$|\dot{u}_i^n|^2 = \frac{4\pi^2}{n^2T^2}, \quad i = 1, 2, 3, 4,$$

and then also the kinetic part becomes zero: this is enough to show the non-coercivity of $\mathcal{A}$. Later we shall see that we can recover the coercivity introducing some constraints on the space of admissible loops: in particular we will use both symmetrical constraints and topological constraints.

Another obstruction is that the minimizers of $\mathcal{A}$ may have collisions: in fact if u_* is a minimizer with a collision at time t_c, then from Sundman's estimates we have that

$$|u_*(t)| = O(|t_c - t|^{2/3}), \quad |\dot{u}_*(t)| = O(|t_c - t|^{-1/3}),$$

near t_c, and then

$$K = O(|t_c - t|^{-2/3}), \quad U = O(|t_c - t|^{-2/3}).$$

Therefore the contribution of collisions to the action is finite, that is $\mathcal{A}(u_*) < +\infty$: to find minimizers that are solution of the classical N-body problem, we must find some results that excludes both partial and total collisions.

Recovering coercivity by symmetry constraints

A general formulation for the use of the symmetry constraints to prove the existence of periodic orbits is given in [3]. Assume that $m_i = m_j$ for $1 \leqslant i < j \leqslant N$, and consider a finite group G and two representations

$$\tau : G \to O(2), \quad \rho : G \to O(3),$$

and a homomorphism $\sigma : G \to \Sigma_N$, where Σ_N is the group of permutations of $\{1, \dots, N\}$. Through τ, ρ, σ we can define an action of G on the loop space Λ

$$\begin{array}{rcl} G \times \Lambda & \to & \Lambda \\ (g, u) & \mapsto & g \cdot u \end{array}$$

where

$$(g \cdot u)_j(t) = \rho(g) u_{\sigma(g^{-1})(j)}(\tau(g^{-1})t), \quad j = 1, \dots, N. \tag{1.3}$$

Since we work on closed loops, we can identify the time interval $[0, T]$ to a circle S^1 in the two dimensional space, so the action of τ on the time t is well defined and it represents a time shift. We define also an action on the configuration space

$$\begin{array}{rcl} G \times \mathcal{X} & \to & \mathcal{X} \\ (g, x) & \mapsto & g \cdot x \end{array}$$

where

$$(g \cdot x)_j = \rho(g) x_{\sigma(g^{-1})_j}, \quad j = 1, \dots, N. \tag{1.4}$$

A motion $u : \mathbb{R} \to \mathcal{X}$ is said to be EQUIVARIANT if $g \cdot u(t) = u(t)$ for all $g \in G$ and for all $t \in \mathbb{R}$: we denote by Λ_G the set of equivariant loops in Λ. Moreover, let $\mathcal{X}^G$ be the set of configurations which are fixed by every element of G, that is

$$\mathcal{X}^G = \{ x \in \mathcal{X} : g \cdot x = x \text{ for all } g \in G \}.$$

The coercivity condition formulated and proven in [3] is expressed by the following Theorem.

THEOREM 1.3 - *The action functional $\mathcal{A}$ is coercive on Λ_G if and only if $\mathcal{X}^G = \{0\}$.*

We observe that if the group action satisfies the coercivity condition, then for a loop $u \in \Lambda_G$ we have that

$$\bar{u} = \frac{1}{T} \int_0^T u(t) dt = 0. \tag{1.5}$$

In fact from the definition of equivariant loop, follows that

$$\int_0^T u_i(t) dt = \int_0^T u_i(\tau(g)(t)) dt = \rho(g) \int_0^T u_{\sigma(g^{-1})(i)}(t) dt,$$

which is equivalent to $\bar{u}_i = \rho(g) \bar{u}_{\sigma(g^{-1})(i)}$ for all $g \in G$: this means that $\bar{u} \in \mathcal{X}^G$, therefore $\bar{u} = 0$.

Clearly, the equivariant relation poses symmetrical conditions on the admissible loops and the zero mean condition defines other geometric restrictions on the motion. However, for the problem we are going to consider, we will see that the coercivity condition imposed by the Theorem 1.3 will not be satisfied: in our case we shall recover coercivity imposing some topological constraints, in addition to the symmetrical ones.

SYMMETRY OF PLATONIC POLYHEDRA

Following [5], first we introduce the symmetry constraints of Platonic polyhedra. Let P one of the five Platonic polyhedra, that is $P \in \{\mathfrak{T}, \mathfrak{C}, \mathfrak{O}, \mathfrak{D}, \mathfrak{I}\}$ where $\mathfrak{T}, \mathfrak{C}, \mathfrak{O}, \mathfrak{D}, \mathfrak{I}$ denote *Tetrahedron, Cube, Octahedron, Dodecahedron, Icosahedron* respectively. Let $\mathcal{T}, \mathcal{O}, \mathcal{I}$ be the groups of rotations of $\mathfrak{T}$, of $\mathfrak{C}$ and $\mathfrak{O}$, of $\mathfrak{D}$ and $\mathfrak{I}$ respectively, and denote by $\mathcal{R} \in \{\mathcal{T}, \mathcal{O}, \mathcal{I}\}$ the group of rotation of P and by $|\mathcal{R}|$ the order of $\mathcal{R}$. We search for T-periodic motions of the classical N-body problem, with $N = |\mathcal{R}|$ and $m_i = m_j$ for $1 \leqslant i < j \leqslant N$, that satisfies the following condition:

(a) At each time $t \in \mathbb{R}$ the set of the positions of the N masses coincides with an orbit of $\mathcal{R}$: there is a $1-1$ correspondence between masses and elements of the group $\mathcal{R}$ and the motion $u_R : \mathbb{R} \to \mathbb{R}^3$ of the particle corresponding to $R \in \mathcal{R}$ is determined by

$$u_R(t) = Ru_I(t) \tag{1.6}$$

where u_I is the motion of the GENERATING PARTICLE, that is the particle corresponding to the identity. We denote with $\Lambda^{(a)} \subseteq \Lambda$ the set of loops that satisfy this condition.

Imposing condition (a) has important implications for the set of possible collisions. In fact, for a map u that satisfies (a), $u_{R_1} = u_{R_2}$ for some $R_1 \neq R_2$ is equivalent to $u_I = Ru_I$ with $R = R_1^{-1}R_2$. Therefore, there is a collision at a time t_c if and only if $u_I(t_c)$ belongs to the axis $r(R)$ of some rotation $R \in \mathcal{R} \setminus \{\mathrm{Id}\}$. Then it follows that a motion u satisfying (a) is collision free if it satisfies

$$u_I(\mathbb{R}) \cap \Gamma = \emptyset, \quad \Gamma = \bigcup_{R \in \mathcal{R} \setminus \{\mathrm{Id}\}} r(R). \tag{1.7}$$

Using (1.6), the action functional restricted to the loop space $\Lambda^{(a)}$ becomes

$$\mathcal{A}(u) = \frac{N}{2} \int_0^T \left(|\dot{u}_I|^2 + \sum_{R \in \mathcal{R} \setminus \{\mathrm{Id}\}} \frac{1}{|(R - I)u_I|} \right) dt. \tag{1.8}$$

We note that the symmetry constraints are not sufficient to recover coercivity of the action functional. In fact, set O the center of the Platonic polyhedron and C the center of a face $\mathcal{F}$. If we fix the motion u_I of the generating particle and we set $u_I^{(k)} = u_I + ke_1$, $e_1 = OC/|OC|$, clearly we have $\lim_{k\to\infty} \left\|u^{(k)}\right\|_{H_T^1} = +\infty$, but

$$\lim_{k\to\infty} \mathcal{A}(u^{(k)}) = \lim_{k\to\infty} \frac{N}{2} \int_0^T \left(|\dot{u}_I|^2 + \sum_{R \in \mathcal{R} \setminus \{\mathrm{Id}\}} \frac{1}{|(R - I)(u_I + ke_1)|} \right) dt$$

is finite: this shows the non-coercivity of $\mathcal{A}$.

Another way to check the non-coercivity of the functional is to use the equivalent condition proposed in the Theorem 1.3. Let L one side of a face $\mathcal{F}$ of the Platonic polyhedron and M the midpoint of L and set $\mathcal{C} \subseteq \mathcal{R}$ the cyclic subgroup of rotations around OC. For the loop space $\Lambda^{(a)}$, the group G is the subgroup G_P of $O(2) \times O(3) \times \Sigma_N$ generated by

$$\begin{cases} g_1 = (I, R_C, R_C \cdot), \\ g_2 = (I, R_M, R_M \cdot), \end{cases} \tag{1.9}$$

where R_C is a generator of $\mathcal{C}$, R_M is the rotation of π around OM. Here we have identified $\{1, \dots, N\}$ with $\mathcal{R}$ and the notation $R \cdot (\cdot R)$ refers to the permutation induced on $\mathcal{R}$ by left (right) multiplication by R. The homomorphisms τ, ρ and σ are the projections of G_P onto the first, second and third factor of $O(2) \times O(3) \times \Sigma_N$.

Let us now show that $\Lambda^{(a)} = \Lambda_{G_P}$. We observe first that to check if a loop u is equivariant, it is sufficient to check condition (1.3) only over a set of generators of the group G. The symmetry condition (a) can be viewed as follows

$$u_{R_i} = R_i u_I \Leftrightarrow u_{R^{-1}R_i} = R^{-1} R_i u_I \Leftrightarrow R u_{R^{-1}R_i} = u_{R_i} \quad \forall R, R_i \in \mathcal{R}.$$

If we took a loop $u \in \Lambda^{(a)}$, then

$$\begin{aligned} \rho(g_1) u_{\sigma(g_1^{-1})(i)}(t) &= R_C u_{R_C^{-1} R_i}(t) = u_{R_i}(t) = u_i(t), \\ \rho(g_2) u_{\sigma(g_2^{-1})(i)}(t) &= R_M u_{R_M^{-1} R_i}(t) = u_{R_i}(t) = u_i(t), \end{aligned}$$

or else, $u \in \Lambda_{G_P}$. On the other hand, if $u \in \Lambda_{G_P}$, relation (1.3) holds for $g_i, i = 1, 2$, but this is equivalent to $R_i u_I = u_{R_i}$, so $u \in \Lambda^{(a)}$: this proves that $\Lambda^{(a)} = \Lambda_{G_P}$.

Now, if $R_j \in \mathcal{R} \setminus \{\mathrm{Id}\}$, $j = 2, \dots, N$ is the rotation corresponding to the j-th particle and we take the nonzero vector $x \in \mathcal{X}$ defined by

$$x = (x_1, \dots, x_N), \quad x_1 = e_1, \, x_j = R_j e_1, \, j = 2, \dots, N,$$

we have that $x \in \mathcal{X}^{G_P}$, so the condition in the Theorem 1.3 is not satisfied and we do not have coercivity. However, the fact that on the loop space $\Lambda^{(a)}$ the action functional is not coercive does not exclude a priori the existence of motions satisfying condition (a). In fact, these motions may correspond to local minimizers, that may exist even though the condition $\mathcal{X}^{G_P} = \{0\}$ is not satisfied.

TOPOLOGICAL CONSTRAINTS

We denote with $\mathfrak{S} \subset \Lambda^{(a)}$ the subset of the loops that present collisions, that is

$$\mathfrak{S} = \left\{ u \in \Lambda^{(a)} : \exists \, t_c \in \mathbb{R}, h \neq k \in \{1, \dots, N\}, \, u_h(t_c) = u_k(t_c) \right\}. \tag{1.10}$$

This is a subset of $\Lambda^{(a)}$ closed in the C^0 topology. The idea to find some local minimizers of the action functional (1.8) is to select an *open cone* $\mathcal{K} \subset \Lambda^{(a)}$ with the property

$$\partial\mathcal{K} \subset \mathfrak{S}, \tag{1.11}$$

where $\partial\mathcal{K}$ is the C^0 boundary of $\mathcal{K}$. If we consider $\mathcal{A}$ defined only over the cone $\mathcal{K}$, it could be coercive even if the zero mean condition (1.5) is not satisfied. Therefore, if we are able to prove that a minimizer u_* of $\mathcal{A}|_{\overline{\mathcal{K}}}$ exists and is collision free, then automatically we have $u_* \in \mathcal{K}$ and then a genuine solution of the N-body problem. We remark that restricting the action to a cone $\mathcal{K} \subset \Lambda^{(a)}$ that satisfies (1.11) corresponds to the introduction of some *topological constraints* beside the *symmetry constraints* imposed by the equivariance condition. The next step is introduce the topological constraints for our problem and define the right cones $\mathcal{K}$.

Cones $\mathcal{K}$ for Platonic polyhedra

If the motion u_I of the generating particle is collision free, let $[u_I]$ the free homotopy class in $\mathbb{R}^3 \setminus \Gamma$. Exploiting the symmetry condition (1.6), we can associate to $[u_I]$ a cone $\mathcal{K}(u)$ of equivariant collision free loops defined as

$$\mathcal{K}(u) = \{v \in \Lambda^{(a)} : v_I \in [u_I]\} \subset \Lambda^{(a)}. \tag{1.12}$$

We denote by $\mathcal{U}$ the set of the classes $\mathcal{K}(u)$ that satisfy the following condition:

(C) u_I is not homotopic to any map $v_I \in H^1_T(\mathbb{R}, \mathbb{R}^3)$ of the form

$$v_I(t) = e'_1 + \delta\left[\cos\left(2\pi k\frac{t}{T}\right)e'_2 + \sin\left(2\pi k\frac{t}{T}\right)e'_3\right], \tag{1.13}$$

where e'_j, $j = 1, 2, 3$ is an orthonormal basis, with e'_1 parallel to one of the axis of Γ, $0 < \delta \ll 1$, $k \in \mathbb{N} \cup \{0\}$.

The condition (C) means that the generating particle u_I does not wind around one rotation axis only. For cones $\mathcal{K} \in \mathcal{U}$ we can state the existence of minimizers for $\mathcal{A}|_{\overline{\mathcal{K}}}$, on the basis of the Theorem 1.2: in fact, restricting the action functional to this type of cones permits to recover the coercivity.

PROPOSITION 1.4 - *Each $\mathcal{K} \in \mathcal{U}$ satisfies* (1.11) *and $\mathcal{A}|_{\mathcal{K}}$ is coercive.*

Proof. We have $u \in \partial\mathcal{K}$ if and only if there exists a time $\bar{t}$ and $R \in \mathcal{R}$ such that $u_I(\bar{t}) \in r(R)$. Then for (1.6) we have $u_I(\bar{t}) = Ru_I(\bar{t}) = u_R(\bar{t})$ and therefore a collision: this establishes (1.11).

To show coercivity we observe that condition (C) implies the existence of a constant $c_{\mathcal{K}} > 0$ such that

$$\max_{t_1,t_2\in[0,T]} |u_I(t_1) - u_I(t_2)| \geqslant c_{\mathcal{K}} \min_{t\in[0,T]} |u_I(t)|, \quad \text{for all } u \in \mathcal{K}.$$

Therefore, if t_m satisfies $|u_I(t_m)| = \min_{t\in[0,T]}|u_I(t)|$, we have

$$u_I(t) \leqslant |u_I(t_m)| + |u_I(t) - u_I(t_m)| \leqslant (1/c_{\mathcal{K}} + 1) \max_{t_1,t_2\in[0,T]} |u_I(t_1) - u_I(t_2)|.$$

Now, if $\{u^{(k)}\}_{k\in\mathbb{N}} \subset \mathcal{K}$ is a sequence such that $\left\|u^{(k)}\right\|_{H^1_T} \to \infty$, then there exists a sequence $\{t_k\}_{k\in\mathbb{N}} \subseteq [0,T]$ such that $|u_I^{(k)}(t_k)| = \left\|u_I^{(k)}\right\|_{C^0} \to \infty$. If $t_k^1, t_k^2 \in [0,T]$ satisfies

$$|u_I^{(k)}(t_k^1) - u_I^{(k)}(t_k^2)| = \max_{t_1,t_2\in[0,T]} |u_I^{(k)}(t_1) - u_I^{(k)}(t_2)|,$$

from the inequality above we have

$$|u_I^{(k)}(t_k)| \leqslant (1/c_{\mathcal{K}} + 1)|u_I^{(k)}(t_k^1) - u_I^{(k)}(t_k^2)|,$$

and then $|u_I^{(k)}(t_k^1) - u_I^{(k)}(t_k^2)| \to \infty$: this ensures that the kinetic part is unbounded. In fact if we set

$$L^k = \int_0^T |\dot{u}_I^{(k)}(t)|dt,$$

to be the length of the curve $u_I^{(k)}$, then $L^k \to \infty$. But from the Cauchy-Schwarz inequality we get

$$L^k = \int_0^T |\dot{u}_I|dt \leqslant \left(\int_0^T |\dot{u}_I|^2 dt\right)^{1/2} \left(\int_0^T 1 dt\right)^{1/2} = T^{1/2}\sqrt{K},$$

and then the kinetic part of the action is unbounded, so the action functional is coercive. □

Therefore, for the cones defined above we have that there exists a minimizer $u_* \in \overline{\mathcal{K}}$: to prove that this is a smooth periodic motion of the Newtonian N-body problem we must prove that it does not present both partial and total collisions. For the detailed analysis of singularities we use two different ways to characterizing the equivariant free homotopy classes $\mathcal{K}(u)$, by means of periodic sequences of symbols.

Encoding the cones $\mathcal{K} \in \mathcal{U}$

First we introduce some notations. We denote with $\mathcal{R}$ the reflection group of P. Let Π be the union of all symmetry planes of P and $\mathcal{S}$ be the collection of the connected components of $\Pi \setminus \Gamma$. Then

$$\mathbb{R}^3 \setminus \Pi = \bigcup_{\tilde{R}\in\tilde{\mathcal{R}}} \tilde{R}D, \tag{1.14}$$

and

$$\mathbb{S}^2 \setminus \Pi = \bigcup_{\tilde{R}\in\tilde{\mathcal{R}}} \tilde{R}\tau, \tag{1.15}$$

where $D \subset \mathbb{R}^3$ is an open fundamental region of the action of $\tilde{\mathcal{R}}$ on $\mathbb{R}^3$ and $\tau = \mathbb{S}^2 \cap D$. Equation (1.14) corresponds to the fact that $\mathbb{R}^3 \setminus \Gamma$ is divided into $2|\mathcal{R}|$ non-overlapping chambers that coincide with the orbit $\mathcal{D} = \{\tilde{R}D\}_{\tilde{R}\in\tilde{\mathcal{R}}}$ of D. Similarly $\mathbb{S}^2 \setminus \Pi$ is tasselled by the orbit $\{\tilde{R}\tau\}_{\tilde{R}\in\tilde{\mathcal{R}}}$ of the Möebius triangle τ. The set of vertexes of the tessellation coincides with the set $\mathcal{P} = \mathbb{S}^2 \cap \Gamma$ of the poles. We also remark that $\mathcal{S}$ coincides with the set of the walls of all elements in the orbit $\mathcal{D}$ of D.

Let now s be the side of τ defined as $s = \overline{\tau} \cap S$, where S is the wall of D opposite to the right dihedral angle of D. Given $q \in s \cup \tau$, the graph with vertexes $\{\tilde{R}q\}_{\tilde{R}\in\tilde{\mathcal{R}}}$ and edges the segments with extrema in adjacent triangles of the tessellation $\{\tilde{R}\tau\}_{\tilde{R}\in\tilde{\mathcal{R}}}$ is homotopically equivalent to $\mathbb{R}^3 \setminus \Gamma$ or $S^2 \setminus \mathcal{P}$. We make use of two choices of $q \in s \cup \tau$, namely $q \in \tau$ and $q \in s$. We denote by $\mathcal{L}_{\tilde{\mathcal{R}}}$ and $\mathcal{L}_{\mathcal{R}}$ the graphs corresponding to these two choices of q; these graphs coincides with the union of the edges of the polyhedron $\mathcal{Q}_{\tilde{\mathcal{R}}}$ ($\mathcal{Q}_{\tilde{R}}$) defined as the convex hull of the orbit $\{\tilde{R}q\}_{\tilde{R}\in\tilde{\mathcal{R}}}$ of $q \in \tau$ ($\{Rq\}_{R\in\mathcal{R}}$ of $q \in s$). $\mathcal{Q}_{\tilde{\mathcal{R}}}$ and $\mathcal{Q}_{\tilde{R}}$ have $\#\mathcal{P}$ faces and the axis of each face is one of the axes $r(R)$ of some $R \in \mathcal{R}$. For later application we take $q \in s$ the point having equal distances from its mirror images q_i, $i = 1, 2$ with respect to the other walls $S_i \neq S$, $i = 1, 2$ of D (see figure 1). For this particular choice, $\mathcal{Q}_{\tilde{R}}$ is an Archimedean polyhedron:

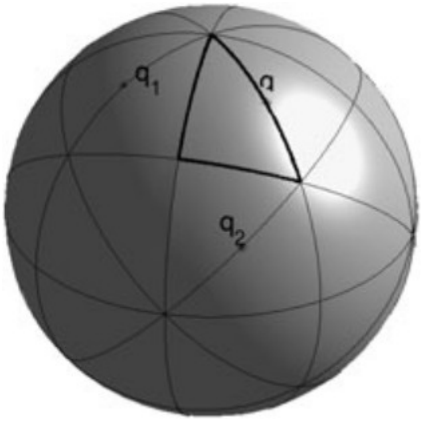

Figure 1: The point $q \in s$, with the tessellation of S^2, $\mathcal{R} = \mathcal{O}$.

in fact this is a special case of the Wythoff construction, that can be found in [2]. The three Archimedean polyhedra $\mathcal{Q}_{\mathcal{R}}$, $\mathcal{R} \in \{\mathcal{T}, \mathcal{O}, \mathcal{I}\}$, are shown in Figure 2. We can use this construction to describe the free homotopy classes of loops and consequently encode the cones $\mathcal{K}$.

PROPOSITION 1.5 - *Each $\mathcal{K} \in \mathcal{U}$ uniquely determines a number $n \in \mathbb{N}$ and (up to translations) a periodic sequence $\nu = \{\nu_k\}_{k\in\mathbb{Z}}$ of vertexes of $\mathcal{Q}_{\mathcal{R}}$ such that:*

(i) for each $k \in \mathbb{Z}$ the segment $[\nu_k, \nu_{k+1}]$ coincides with one of the edges of $\mathcal{Q}_{\mathcal{R}}$.

(ii) $\nu_{\nu+1} \neq \nu_{k-1}$, that is we can not go forth and back on the same edge.

(iii) $\nu \not\subset \overline{\mathcal{F}}$ for all the faces $\mathcal{F}$ of $\mathcal{Q}_{\mathcal{R}}$, that is ν does not wind around one axis only.

Conversely each pair (n, ν), ν a periodic sequence of vertexes of $\mathcal{Q}_{\mathcal{R}}$ that satisfies (i), (ii), (iii) uniquely determines a cone $\mathcal{K} \in \mathcal{U}$.

Proof. A free homotopy class on $\mathcal{L}_{\mathcal{R}}$ uniquely determines, up to translations, a periodic sequence $\nu = \{\nu_k\}_{k\in\mathbb{Z}}$ of vertexes of $\mathcal{Q}_{\mathcal{R}}$ that satisfy (i) and (ii). The integer n is the ratio between the period κ of ν and its minimal period κ_ν.

Conversely a pair (n, ν), with $n \in \mathbb{N}$ and ν a periodic sequence of vertexes that satisfies (i) and (ii), determines a free homotopy class of $\mathcal{L}_{\mathcal{R}}$.

The proposition follows from this and from the homotopic equivalence of $\mathbb{R}^3 \setminus \Gamma$ and $\mathcal{L}_{\mathcal{R}}$, after observing that a map of the form (1.13) represents an

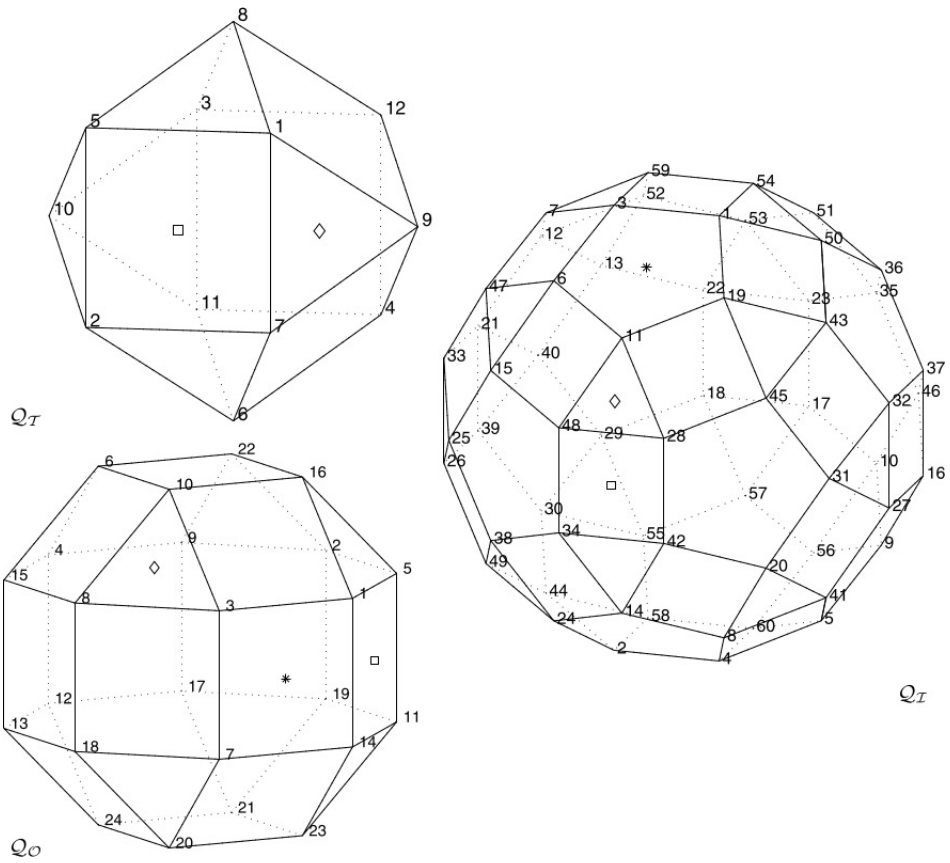

Figure 2: The Archimedean polyhedra $\mathcal{Q}_\mathcal{T}, \mathcal{Q}_\mathcal{O}, \mathcal{Q}_\mathcal{I}$

homotopy class that corresponds to a sequence $\nu \subset \overline{\mathcal{F}}$ for some face $\mathcal{F}$ of $\mathcal{Q}_\mathcal{R}$. □

Another way to encode a cone is by using the tessellation of the sphere, or equivalently the split of $\mathbb{R}^3 \setminus \Gamma$ into non-overlapping chambers.

PROPOSITION 1.6 - *Each $\mathcal{K} \in \mathcal{U}$ uniquely determines a number $n \in \mathbb{N}$ and (up to translations) a periodic sequence $\sigma = \{D_k\}_{k\in\mathbb{Z}} \subset \mathcal{D}$ such that:*

(I) D_{k+1} *is the mirror image of* D_k *with respect to one of the walls of* D_k.

(II) $D_{k+1} \neq D_{k-1}$

(III) $\cap_{k\in\mathbb{Z}} D_k = O$

Conversely each pair (n, σ), $\sigma = \{D_k\}_{k\in\mathbb{Z}}$ a periodic sequence that satisfies (I), (II), (III) uniquely determines a cone $\mathcal{K} \in \mathcal{U}$.

Proof. The argument in the Proposition 1.5 can be applied to $\mathcal{L}_{\tilde{\mathcal{R}}}$ and $\mathcal{Q}_{\tilde{\mathcal{R}}}$. Therefore the statement of the Proposition 1.5 still holds if we replace $\mathcal{Q}_\mathcal{R}$ with $\mathcal{Q}_{\tilde{\mathcal{R}}}$. The $1-1$ correspondence between the set of vertexes of $\mathcal{Q}_{\tilde{\mathcal{R}}}$ and $\mathcal{D}$ concludes the proof. □

Given (n, ν), ν a periodic sequence of vertexes of $\mathcal{Q}_{\mathcal{R}}$ satisfying (i), (ii) and (iii), we denote by $\mathcal{K}^{(n,\nu)} \in \mathcal{U}$ the corresponding cone. We also define the T-periodic map $v^{(n,\nu)} \in \mathcal{K}^{(n,\nu)}$ by setting

$$\begin{cases} \gamma^{(n,\nu)} = \prod_{j=1}^{n\kappa_\nu} \gamma_{\nu,j} \\ \gamma_{\nu,j} = (1-s)\nu_j + s\nu_{j+1}, \quad s \in [0,1] \\ v_I^{(n,\nu)}(t) = \gamma^{(n,\nu)}(t/T) \end{cases} \tag{1.16}$$

that is, $v_I^{(n,\nu)}$ moves along the sides defined by ν with constant speed, where κ_ν is the minimal period of ν. We say that the map $v^{(n,\nu)}$ is the CANONICAL REPRESENTATIVE of $\mathcal{K}^{(n,\nu)}$. Moreover, we set $\mathcal{K}^\nu = \mathcal{K}^{(1,\nu)}$ and $v^\nu = v^{(1,\nu)}$.

Furthermore, we want to add another symmetry to the motion. Given a rotation $R \in \mathcal{R} \setminus \{Id\}$, we denote as η_R the permutation induced by R on the set of vertexes of the Archimedean polyhedron $\mathcal{Q}_{\mathcal{R}}$. We are interested to closed paths ν that satisfy the condition

$$\eta_R \nu_j = \nu_{j+k}, \tag{1.17}$$

for some $k \neq 0$. From Equation (1.16) and condition (1.17) follow that

$$v_I^\nu\left(t + \frac{k}{\kappa_\nu}T\right) = v_I^{\eta_\nu}(t) = Rv_I^\nu(t).$$

Therefore v_I^ν satisfies the symmetry condition

$$u_I\left(t + \frac{T}{M}\right) = Ru_I(t), \quad M = \frac{\kappa_\nu}{k}, \tag{1.18}$$

for all t, where κ_ν is the minimal period of the sequence ν. Moreover, since we want that condition (a) holds, this implies that M particles follow the same trajectory with a time shift of T/M, thereby producing a *choreography* of M particles. Given a sequence ν that satisfies condition (1.17), we denote by $\tilde{\mathcal{K}}^\nu \subseteq \mathcal{K}^\nu$ the subset of loops that satisfy condition (1.18) and we search for minimizers of the action on this loops set. Actually, the latter cone $\tilde{\mathcal{K}}^\nu$ can be defined as the intersection between $\mathcal{K}^\nu$ and the set Λ_G, with $G \subseteq O(2) \times O(3) \times S_N$ the group generated by

$$g_1, g_2, \left(\begin{pmatrix} \cos(2\pi/M) & -\sin(2\pi/M) \\ \sin(2\pi/M) & \cos(2\pi/M) \end{pmatrix}, I, \cdot R^{-1}\right)$$

where g_1, g_2 are defined in (1.9).

From the coercivity of the action functional restricted to the cone $\mathcal{K} = \tilde{\mathcal{K}}^\nu$ and from results given in Section 1.1, at this point we have proven the existence of a minimizer $u_* \in H_T^1(\mathbb{R}, X) \cap \overline{\mathcal{K}}$, where $\overline{\mathcal{K}}$ denotes the closure of $\mathcal{K}$ in the C^0 topology. To prove that this minimizer is actually a solution of the classical Newtonian N-body problem, we must show that it does not present collisions: this will be the purpose of sections 1.4 and 1.5. Before proceeding with this, we can prove the regularity of collision-free minimizers and some interesting geometric properties of them. We also remark that when the minimizer u_* is collision-free, by Palais principle of symmetric criticality (see [23], Appendix B for brief description), we deduce that u_* actually is a critical point of the unconstrained action functional.

Regularity and geometric structure of collision-free minimizers

By standard arguments of Calculus of Variations we can prove that each minimizer $u_* \in \mathcal{K}$ collision-free is a smooth function, and therefore a solution of the gravitational N-body problem. In general, let us consider a functional $\mathcal{A} : \Lambda \to \mathbb{R}$ defined by

$$\mathcal{A}(u) = \int_0^T L(u(t), \dot{u}(t))dt,$$

where $\Lambda \subseteq H^1_T(\mathbb{R}, \mathbb{R}^n)$ is a set of T-periodic loops, where the period $T > 0$ is fixed. Moreover, assume that we have a mechanical system, so that the Lagrangian function is of the form

$$L(u, \dot{u}) = \frac{1}{2}|\dot{u}|^2 + U(u),$$

where the potential U is defined on $\mathbb{R}^n \setminus \Gamma$ and is regular enough (it will be sufficient continuous differentiable). The set Γ plays the role of the collision set defined before. Let us now assume that $u_* \in \Lambda$ is a minimizer of $\mathcal{A}$ and it is "collision free", that is $u_*([0, T]) \cap \Gamma = \emptyset$: we want to show that, under these conditions, $u_* \in C^\infty_T(\mathbb{R}, \mathbb{R}^n)$. If we take as set of variations

$$\tilde{V} = \{v \in C^2_T(\mathbb{R}, \mathbb{R}^n) : v(0) = v(T) = 0\},$$

then fixed $v \in \tilde{V}$, the curve $u_* + \lambda v$ is still T-periodic for small values of λ and collision free: therefore we assume that it belongs to the loop space Λ. Since u_* is a minimizer, its first variation will be zero, that is

$$\frac{d}{d\lambda}\mathcal{A}(u_* + \lambda v)\bigg|_{\lambda=0} = \int_0^T \left[\dot{u}_*(t) \cdot \dot{v}(t) + \frac{\partial U(u_*(t))}{\partial u} \cdot v(t)\right] dt = 0, \quad \text{for all } v \in \tilde{V}.$$

Using integrations by parts on the second term of the integral and using the periodic boundary conditions, we obtain

$$\int_0^T \left[\dot{u}_*(t) - \int_0^t \frac{\partial U(u_*(s))}{\partial u} ds\right] \cdot \dot{v}(t) dt = 0, \quad \text{for all } v \in \tilde{V}.$$

Since v is zero at the extrema, the mean of its time derivative $\dot{v}$ is zero, then from the well known Du Bois-Reymond Lemma, we have that the integrating function is constant, that is

$$\dot{u}_*(t) - \int_0^t \frac{\partial U(u_*(s))}{\partial u} ds = c \in \mathbb{R},$$

and finally we get

$$\dot{u}_*(t) = F(t) + c, \quad F(t) = \int_0^t \frac{\partial U(u_*(s))}{\partial u} ds.$$

Since we have assumed that U is a continuous differentiable function, its derivative $\partial U/\partial u$ is a continuous function, and because of u_* is a Lipschitz's function, we have that $F(t)$ is a differentiable function: from this we get that $\dot{u}_* \in C^1_T(\mathbb{R}, \mathbb{R}^n)$ and therefore $u_* \in C^2_T(\mathbb{R}, \mathbb{R}^n)$. Furthermore, by induction

we obtain that $u_* \in C^\infty_\Gamma(\mathbb{R}, \mathbb{R}^n)$. Using this argument we can prove that if $u_* \in \overline{\mathcal{K}}$ is a collision-free minimizer, then it is smooth and therefore a solution of the classical Newtonian N-body problem. In fact, we can choose as set of variation the set

$$\tilde{V} = \big\{v = (v_1, \dots, v_N) \in C^2_\Gamma(\mathbb{R}, \mathbb{R}^{3N}) : \\ v_1(0) = v_1(T) = 0,\ v_i(t) = R_i v_1(t),\ i = 2, \dots, N,\ R_i \in \mathcal{R} \setminus \{\mathrm{Id}\}\big\},$$

and, take a variation $v \in \tilde{V}$, the sum $u_* + \lambda v$ is collision-free for small values of λ, belongs to the same free homotopy class of u_* and satisfies the condition $(u_* + \lambda v)_i(t) = R_i(u_* + \lambda v)_I(t)$, that is $u_* + \lambda v \in \mathcal{K}$. Since the Lagrangian function of the action (1.8) is of the form mentioned above and acts only on the particle u_I, we are exactly in the case discussed: therefore u_* is a smooth function.

Collision-free minimizers also have an interesting geometric feature, that is: the motion of the generating particle, when projected on the sphere $\mathbb{S}^2$, crosses the minimum number of triangles in a period. This statement is clarified in the following theorem.

THEOREM 1.7 - *Given a cone $\mathcal{K} \in \mathcal{U}$, let (n, σ), $\sigma = \{D_k\}_{k\in\mathbb{Z}}$ be the associated pair given by the Proposition 1.6. If $u_* \in \mathcal{K}$ is a collision-free minimizer of the action functional $\mathcal{A}$, then there exist two sequences $\{S_k\}_{k\in\mathbb{Z}} \subseteq \mathcal{S}$ and $\{t_k\} \subseteq \mathbb{R}$ such that*

(i) $S_k \subseteq \overline{D}_k$, $S_{k+1} \neq S_k$

(ii) $u_{*,I}$ *crosses transversally* S_k *at time* t_k *(that is* $u_{*,I}(t_k) \in S_k$ *and* $\dot{u}_{*,I}(t_k)$ *is transversal to* S_k*) and* $u_{*,I}((t_k, t_{k+1})) \subseteq D_k$.

Therefore, the number

$$m_* = \#\{t \in [0, T) : u_{*,I}(t) \in S,\ S \in \mathcal{S}\}$$

is finite and it is the minimum compatible with the membership in $\mathcal{K}$, that is $m_* = n\kappa_\sigma$ (κ_σ the minimum period of σ).

For the proof of this statement we need the following Proposition.

PROPOSITION 1.8 - *Let $\mathcal{K} \in \mathcal{U}$ and $\sigma = \{D_k\}_{k\in\mathbb{Z}}$ be the sequence associated to $\mathcal{K}$. Then, given $u \in \mathcal{K}$, there exists $\hat{u} \in \mathcal{K}$ and a two sequences $\{t_k\}_{k\in\mathbb{Z}} \subseteq \mathbb{R}$, $\{S_k\}_{k\in\mathbb{Z}}$ such that $t_k < t_{k+1}$, $S_k \subseteq \overline{D}_k$ for all $k \in \mathbb{Z}$ and*

(i) $\hat{u}_I([t_k, t_{k+1}]) \subseteq \overline{D}_k \setminus \Gamma$,

(ii) $u_I(t_k) \in S_k$, $S_{k+1} \neq S_k$,

(iii) $\mathcal{A}(\hat{u}) \leqslant \mathcal{A}(u)$.

Proof. The proof is divided in two steps. First, we see that applying some reflections to the path u, the action does not change; second we construct the new path $\hat{u}$ using reflections.

For the first step, fixed $S \in \mathcal{S}$, we note that the map $\mathcal{R} \setminus \{\mathrm{Id}\} \ni R \mapsto R^S \in \mathcal{R} \setminus \{\mathrm{Id}\}$ defined by $R^S = \tilde{R}_S R \tilde{R}_S$ (where $\tilde{R}_S$ is the reflection with respect to the plane S) is a bijection. We also note that

$$|R^S \tilde{R}_S x - \tilde{R}_S x| = |\tilde{R}_S(Rx - x)| = |Rx - x|, \quad \text{for all } x \in \mathbb{R}^3,$$

and therefore we have, for all $t \in \mathbb{R}$ and $S \in \mathcal{S}$

$$\sum_{R \in \mathcal{R}\setminus\{Id\}} \frac{1}{|R\tilde{R}_S u_I(t) - \tilde{R}_S u_I(t)|} = \sum_{R \in \mathcal{R}\setminus\{Id\}} \frac{1}{|R^S \tilde{R}_S u_I(t) - \tilde{R}_S u_I(t)|} = \sum_{R \in \mathcal{R}\setminus\{Id\}} \frac{1}{|R u_I(t) - u_I(t)|}.$$

This shows that if $u_I(t_i) \in S$, $i = 1,2$ for some $t_1 < t_2 + T$, then the arch $u_I|_{[t_1,t_2]}$ and the reflected one $\tilde{R}_S u_I|_{[t_1,t_2]}$ give the same contribution to the potential term of the action. The same is true also for the kinetic part, since reflections does not change the norms.

Now it suffice to show that $\hat{u}$ can be constructed with a finite number of reflections of this type, without changing the free homotopy class of u_I. So, let $\mathcal{I}_u$ be the set of intervals (t^-, t^+) such that for some $D' \in \mathcal{D}$ and $S^\pm \in \mathcal{S}$ it results:

(a) $u_I(t^\pm) \in S^\pm$, $S^\pm \subseteq \overline{D}'$, $S^- \neq S^+$,

(b) $u_I([t^-, t^+]) \subseteq \overline{D}' \setminus \Gamma$,

(c) if $\tau^- \leqslant t^- < t^+ \leqslant \tau^+$ and (τ^-, τ^+) satisfies (a) and (b) then $\tau^\pm = t^\pm$.

The number m_u of the intervals $(t^-, t^+) \in \mathcal{I}_u$ that lie in an interval of size T is finite: this follows from the fact that there is a positive lower bound for the time needed for $u_I(t)$ to travel between two different walls (remember that u is a fixed loop without collisions). Let the intervals in $\mathcal{I}_u$ and the corresponding $D', S^\pm$ be enumerated so that $t_k^+ < t_{k+1}^+$. Note that this implies

$$S_k^+ = S_{k+1}^-, \quad k \in \mathbb{Z}. \tag{1.19}$$

Let ζ_u be the set of $k \in \mathbb{Z}$ such that $t_k^+ < t_{k+1}^-$ and define $\hat{u}$ by setting

$$\hat{u}_I = \begin{cases} \tilde{R}_{S_k^+} u_I(t) & t \in [t_k^+, t_{k+1}^-],\ u_I(t) \in \tilde{R}_{S_k^+} \overline{D}_k',\ k \in \zeta_u \\ u_I(t) & \text{otherwise.} \end{cases} \tag{1.20}$$

An example of construction of such loop is presented in Figure 3. From the first step, we have that $\mathcal{A}(\hat{u}) = \mathcal{A}(u)$. Moreover $\hat{u}$ belongs to the same homotopy class of u_I: in fact $\overline{D}_k' \cup \tilde{S}_{S_k^+} \overline{D}_k'$ is a convex set and then the function $h(s,t) = s\hat{u}_I(t) + (1+s)u_I(t)$ is an homotopy that transforms u_I into $\hat{u}_I$ without crossing any collision.

It remains to be proved that this new path satisfies conditions (i) and (ii). Assume first that

$$D'_{k+1} \neq D_k,\ k \in \mathbb{Z}. \tag{1.21}$$

Then it follows that

$$D_{k+1} \neq D_{k-1},\ k \in \mathbb{Z}. \tag{1.22}$$

Therefore the sequence $\{D'_k\}_{k\in\mathbb{Z}}$ satisfies conditions (I) and (II) of the Proposition 1.6 that characterize our free homotopy classes: then, by uniqueness, the sequence $\{D'_k\}_{k\in\mathbb{Z}}$ coincides (up to translation) with the sequence $\sigma = \{D_k\}_{k\in\mathbb{Z}}$ corresponding to u. Moreover, from the definition (1.20), we have that $\hat{u}_I([t_k^+, t_{k+1}^-]) \subseteq \overline{D}_k' \setminus \Gamma$, $k \in \zeta_u$ and therefore for all $k \in \mathbb{Z}$ we have

$$\hat{t}_{k+1}^- = t_{k+1}^- \leqslant \hat{t}_k^+, \tag{1.23}$$

where we have denoted with $\{\hat{t}^{\pm}\}_{k\in\mathbb{Z}}$ the sequences corresponding to $\hat{u}_I$. It follows that $\hat{u}_I$ satisfies (i) and (ii) with $S_k = S_k^+ = S_{k+1}^-$ and $t_k = (\hat{t}_{k+1}^- + \hat{t}_k^+)/2$. We also observe that for each $D_k \in \sigma$ there is an interval (t_k^-, t_k^+) and a corresponding interval (t_k, t_{k+1}), therefore we have $m_{\hat{u}} = m_u = n\kappa_\sigma$.

Assume now that there is a k such that $D'_{k+1} = D'_k$. Then, the definition (1.20) implies that $\hat{u}_I([t_k^-, t_{k+1}^+]) \subseteq \overline{D}'_k \setminus \Gamma$ and therefore $m_{\hat{u}} < m_u$. In fact, the interval (t_k^-, t_{k+1}^+) contains at most one of the intervals $(\hat{t}_k^-, \hat{t}_k^+) \in \mathcal{I}_{\hat{u}}$, while it contains the two intervals (t_k^-, t_k^+), $(t_{k+1}^-, t_{k+1}^+) \in \mathcal{I}_u$. It follows that we can replace u with $\hat{u}$ and iterate. After a finite number of steps, we end up with a map $\hat{u}$ that satisfies (1.21) and we are back to the previous situation. □

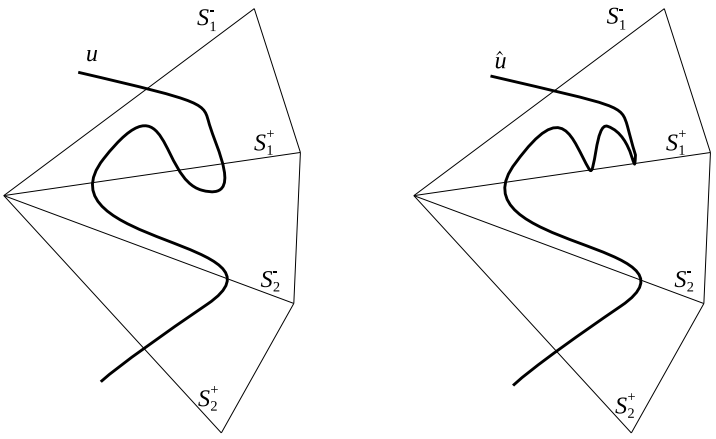

Figure 3: Construction of the loop $\hat{u}$.

Now we are ready to prove the Theorem 1.7. First, assume that u_I does not cross transversally some S: then there exists $\bar{t}$ such that $\dot{u}_I(t)$ is parallel to S. This implies

$$\begin{cases} \tilde{R}_S R u_{*,I}(\bar{t}) = R^S \tilde{R}_S u_{*,I}(\bar{t}) = R^S u_{*,I}(\bar{t}) \\ \tilde{R}_S R \dot{u}_{*,I}(\bar{t}) = R^S \tilde{R}_S \dot{u}_{*,I}(\bar{t}) = R^S \dot{u}_{*,I}(\bar{t}) \end{cases} \tag{1.24}$$

These equations say that at time $t = \bar{t}$ the set of positions and velocities of the particles is mapped into itself by the reflection $\tilde{R}_S$: therefore for the symmetry of the equations of motion it follows that $u_{*,I}(t) \in S$ for each t in some maximal interval (t_α, t_β). But the minimizer is collision free for our assumption, therefore $(t_\alpha, t_\beta) = \mathbb{R}$, and this is incompatible with the membership in $\mathcal{K}$, so the transversality condition must holds. If we assume now that (i) and (ii) does not hold and we take $\hat{u}_*$ given by the Proposition 1.8, then $\hat{u}_* \neq u_*$ and $\hat{u}_*$ is a minimizer collision-free, so it is a smooth function. But from the construction of this new loop, we have that there exists $\bar{t} \in \mathbb{R}$ and $S \in \mathcal{S}$ such that $\hat{u}_{*,I}(\bar{t}) = u_{*,I}(\bar{t}) \in S$ and

$$\lim_{t\to\bar{t}^-} \dot{\hat{u}}_{*,I}(t) = \dot{u}_{*,I}(\bar{t}) \neq \tilde{R}_S \dot{u}_{*,I}(\bar{t}) = \lim_{t\to\bar{t}^+} \dot{\hat{u}}_{*,I}(t).$$

This means that $\hat{u}_*$ is not a smooth function, which is a contradiction: therefore conditions (i) and (ii) must hold and this proves the theorem.

This geometric property has a consequence in the search of minimizers. In fact, to each minimizer of $\mathcal{A}|_{\mathcal{K}}$ we can associate a minimizer u_* which is the C^0 limit of a minimizing sequence $\{\hat{u}^\ell\}_{\ell\in\mathbb{N}} \subseteq \mathcal{K}$ of loops with properties (i), (ii) and (iii) of the Proposition 1.8. On the other hand, the Theorem 1.7 implies that, if a collision-free minimizer exists, it has to be a minimizer of this type. Therefore, in the search of smooth solutions in $\mathcal{K}$, minimizing on this cone is equivalent to minimizing on the subset of the loops $u \in \mathcal{K}$ such that the generating particle u_1 visits, one after the other, the chambers D_k in the sequence $\{D_1, \dots, D_{n\kappa_\sigma}\}$ entering D_k from S_k and exiting D_k from S_{k+1} without crossing the third wall $S^k \notin \{S_k, S_{k+1}\}$ of D_k. Furthermore, we associate to the generating particle the sequence $k \mapsto r_k = (\overline{S_{k+1}} \cap \overline{S^k}) \setminus O$: this sequence will be useful in the next, especially in the exclusion of partial collisions. A sketch of this sequence is shown if Figure 4.

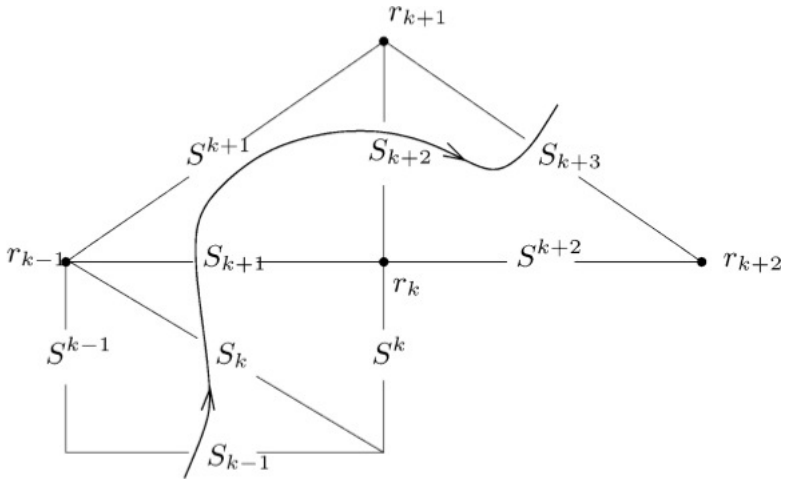

Figure 4: The sequence $k \mapsto r_k$.

EXCLUDING TOTAL COLLISIONS

In this section we want to give some sufficient conditions that exclude total collisions. Our strategy is based on *level estimates*, that is we will show that:

(a) The assumption that u_* has a total collision implies a bound of the form
$$\mathcal{A}(u_*) \geqslant a > 0.$$

(b) There exists $v \in \mathcal{K}$ such that
$$\mathcal{A}(v) < a.$$

This approach is quite natural in our contest. In fact a total collision implies $u_* \in \partial\mathcal{K}$ and therefore any attempt to perturb u_* into a competing function v such that $\mathcal{A}(v) < \mathcal{A}(u_*)$ to show that u_* is free of total collisions runs against the difficulty of respecting the topological constraints that characterize the membership in $\mathcal{K}$. To derive level estimates we use the following result, based on [7].

PROPOSITION 1.9 - *Let* $u : (0,T) \to \mathbb{R}^{3N}$, $u = (u_1, \dots, u_N)$, *be a motion of* N *masses* $m_1, \dots, m_N$ *connecting a total ejection at time* $t = 0$ *to a total collision at time* $t = T$. *Then, for the action*

$$\mathcal{A}(u) = \int_0^T \left(\frac{1}{2} \sum_{h=1}^{n} m_h |\dot{u}_h|^2 + \sum_{1 \leqslant h < k \leqslant N} \frac{m_h m_k}{|u_h - u_k|} \right) dt,$$

we have the estimate

$$\mathcal{A}(u) \geqslant \frac{3}{2} \mathcal{M} (\pi U_0)^{2/3} T^{1/3}, \quad \mathcal{M} = \sum_{i=1}^{N} m_i,$$

where

$$U_0 = \min_{\rho(u)=1} U(u), \quad U(u) = \frac{1}{\mathcal{M}} \sum_{h \neq k}^{N} \frac{m_h m_k}{|u_h - u_k|}, \quad \rho(u) = \left(\sum_{h=1}^{N} \frac{m_h}{\mathcal{M}} |u_h|^2 \right).$$

Proof. It is easy to prove that bilinear form of the masses

$$\langle u, v \rangle = \sum_{h=1}^{N} \frac{m_h}{M} u_h \cdot v_h, \tag{1.25}$$

defines a scalar product of $\mathbb{R}^{3N}$, where $\cdot$ denotes the usual scalar product in the three dimensional space. From the Cauchy-Schwarz inequality $|\langle u, v \rangle| \leqslant \|u\| \, \|v\|$ we have

$$\sum_{h=1}^{N} \frac{m_h}{M} |\dot{u}_h|^2 \geqslant \dot{\rho}(u)^2.$$

In fact, we have that $\rho(u) = \langle u, u \rangle^{1/2}$ and $\dot{\rho}(u) = \langle u, \dot{u} \rangle / \rho(u)$, so applying the Cauchy-Schwarz inequality to $\rho(u)\rho(\dot{u})$ we obtain

$$\rho(u)^2 \dot{\rho}(u)^2 = |\langle u, \dot{u} \rangle|^2 \leqslant \|u\|^2 \, \|\dot{u}\|^2 = \rho(u)^2 \sum_{h=1}^{N} \frac{m_h}{M} |u_h|^2,$$

that is the above relation. We can use this result to obtain an estimate on the action. Since the potential U is an homogeneous function of degree -1, we get

$$\begin{aligned} \mathcal{A}(u) &\geqslant \frac{M}{2} \int_0^T \dot{\rho}(u)^2 + U(u) \, dt \\ &= \frac{M}{2} \int_0^T \dot{\rho}(u)^2 + \frac{1}{\rho(u)} U\left(\frac{u}{\rho(u)} \right) dt \\ &\geqslant \frac{M}{2} \int_0^T \dot{\rho}(u)^2 + \frac{U_0}{\rho(u)} \, dt. \end{aligned}$$

The latter functional represents a unidimensional Kepler problem with gravitational constant equals to U_0. The bound of the action follows from the Gordon's Theorem (see [7]). The value

$$\frac{3}{2} M (\pi U_0)^{(2/3)} T^{1/3},$$

corresponds to the action of an homographic motion that goes from a total ejection to a total collision in the interval $(0, T)$ with a central configuration that minimizes the potential on the ellipsoid $\rho(u) = 1$. □

Now we use this Proposition to derive an estimate on the Lagrangian action of our problem. Let $p_j \in \mathcal{P}$, $j = 1, 2, 3$ be the vertexes of the Möebius triangle $\tau = \mathbb{S}^2 \cap D$. We denote the order of each pole $p \in \mathcal{P}$ by o_p and set

$$\alpha_p = \sum_{j=1}^{o_p - 1} \frac{1}{\sin\left(\frac{j\pi}{o_p}\right)}.$$

An estimate on the action of a loop that presents total collisions is given by the following Proposition.

PROPOSITION 1.10 - *Assume that* $u \in H^1_T(\mathbb{R}, \mathcal{X})$ *satisfies condition (a) and has* M *(equally spaced) total collisions per period. Then*

$$\mathcal{A}(u) \geqslant \frac{3}{2}|\mathcal{R}|(\pi M \tilde{U}_0)^{2/3} T^{1/3}, \tag{1.26}$$

where

$$\tilde{U}_0 = \frac{1}{4} \sum_{p \in \mathcal{P}} \frac{\alpha_p}{\max_{j \in \{1,2,3\}} |p_j \times p|}.$$

Proof. If we set

$$U(u) = \sum_{R \in \mathcal{R} \setminus \{Id\}} \frac{1}{|(R - Id)u_I|},$$

we have that the potential is

$$\begin{aligned}
\frac{1}{2} \sum_{\substack{h,k=1 \\ h \neq k}}^{N} \frac{1}{|u_h - u_k|} &= \frac{1}{2} \sum_{R,R' \in \mathcal{R} \setminus \{Id\}} \frac{1}{|Ru_I - R'u_I|} \\
&= \frac{1}{2} \sum_{R,R' \in \mathcal{R} \setminus \{Id\}} \frac{1}{|R'^{-1}Ru_I - u_I|} \\
&= \frac{1}{2} \sum_{R'' \in \mathcal{R} \setminus \{Id\}} \frac{1}{|R''u_I - u_I|} = \frac{N}{2} U(u).
\end{aligned}$$

But it is easy to prove that

$$U(u) = \frac{1}{4} \sum_{p \in \mathcal{P}} \frac{\alpha_p}{|u_I \times p|},$$

and $\rho(u) = |u_I|$. Therefore, from the invariance of $U(u)$ under $\tilde{\mathcal{R}}$, it follows

$$U_0 = \frac{1}{4} \min_{|u_I|=1} \sum_{p \in \mathcal{P}} \frac{\alpha_p}{|u_I \times p|} = \frac{1}{4} \min_{u_I \in \overline{\tau}} \sum_{p \in \mathcal{P}} \frac{\alpha_p}{|u_I \times p|},$$

where τ is a Möebius triangle. From the equation

$$\max_{u_I \in \overline{\tau}} |u_I \times p| = \max_{j \in \{1,2,3\}} |p_j \times p|,$$

we obtain $U_0 \geqslant \tilde{U}_0$. Then the Proposition 1.9 implies the thesis for $M = 1$. The case $M > 1$ follows trivially applying the previous case. □

Table 1: Lower bounds for $\alpha_{\mathcal{R},M}$ for loops with M total collisions.

$\mathcal{R}\setminus M$	1	2	3	4	5
$\mathcal{T}$	132.69547	210.64093	276.01771	/	/
$\mathcal{O}$	457.18432	725.73487	950.98171	1152.03230	/
$\mathcal{I}$	2296.89241	3646.08943	4777.72875	/	7616.15416

We denote by $\alpha_{\mathcal{R},M}$ the right-hand side of (1.26) corresponding to $T = 1$: in Table 1 we list these values, obtained in [5]. To find minimizers $u_* \in \overline{\mathcal{K}}, \mathcal{K} = \tilde{\mathcal{K}}^\nu$ that are free of total collisions, we can show that there exists $v \in \mathcal{K}$ which is collision free and has a value $\mathcal{A}(v)$ of the action below the lower bounds discussed above. To do this, we can choose simple loops for that the action is explicitly computable: for example we can take the linear piecewise loop $v = \lambda v^\nu$ that defines the cone, with $\lambda > 0$ a constant that will be chosen later. For this type of loop we have that $\mathcal{A}(v^\nu) = A_U + A_K$, where

$$A_U = \frac{N}{2}\int_0^T \sum_{R\in\mathcal{R}\setminus\{Id\}} \frac{1}{|(R-Id)v_I^\nu|}dt, \tag{1.27}$$

$$A_K = \frac{N}{2}\int_0^T |\dot{v}_I^\nu|^2 dt = \frac{N}{2}\frac{\ell k_\nu^2}{T}. \tag{1.28}$$

Here ℓ is the length of a side of the Archimedean polyhedron $\mathcal{Q}_\mathcal{R}$, k_ν is the minimal period of ν and we have used that $|\dot{v}_I^\nu| = \ell k_\nu/T$. Therefore, the value of the action is $\mathcal{A}(v) = \mathcal{A}(\lambda v^\nu) = \lambda^2 A_K + A_U/\lambda$: considered as function of λ, we obtain that the minimal value is obtained for $\lambda = \left(\frac{A_U}{2A_K}\right)^{1/3}$. Then the minimal value of the action for a piecewise linear loop is given by

$$\mathcal{A}(v) = 3\left(\frac{A_K A_U^2}{4}\right)^{1/3}. \tag{1.29}$$

Action of piecewise loops

The action of the linear piecewise loop can be expressed with a simple formula, for instance

$$\mathcal{A}(v) = \frac{3}{2\cdot 4^{1/3}} N\ell^{2/3}(k_1\zeta_1 + k_2\zeta_2)^{2/3}T^{1/3}, \tag{1.30}$$

where k_1 and k_2 are the numbers of sides of the sequence ν of type one and two respectively, while ζ_1, ζ_2 are integrals expressed by elementary function (these values, obtained in [5], are listed in Table 2). In fact, going back

Table 2: Numerical values of ℓ, ζ_1, ζ_2.

$\mathcal{R}$	$\mathcal{T}$	$\mathcal{O}$	$\mathcal{I}$
ℓ	1.0	0.7149	0.4479
ζ_1	9.5084	20.3225	53.9904
ζ_2	9.5084	19.7400	52.5762

to the Wythoff construction, we recall that we have set $q_i = \tilde{R}_i q$, $i = 1, 2$, where $\tilde{R}_1, \tilde{R}_2 \in \tilde{\mathcal{R}}$ are the reflections associated to the walls of D that form

a right angle. The set $\mathcal{L}_{\mathcal{R}}$ of the sides of $\mathcal{Q}_{\mathcal{R}}$ is the union of the two orbits $\{R[q,q_i]\}_{R\in\mathcal{R}}$, $i=1,2$ of the segments $[q,q_1]$ and $[q,q_2]$. It follows that we can associate to each $j\in\mathbb{Z}$ a uniquely determined pair $(R_j,i_j)\in\mathcal{R}\times\{1,2\}$ such that $[v_{j-1},v_j]=R_j[q,q_{i_j}]$. For each rotation $R'\in\mathcal{R}$ we set

$$\zeta_i(R')=\int_0^1\frac{ds}{|(R-Id)R'[(1-s)q+sq_i]|},\quad i=1,2.$$

Since

$$|(R-Id)R'[(1-s)q+sq_i]|=|(R'^{-1}RR'-Id)[(1-s)q+sq_i]|,$$

and the map $R\mapsto R'^{-1}RR'$ is an isomorphism of $\mathcal{R}$ onto itself, we have that the values of $\zeta_i(R')$ does not depend on the given rotation, but only from the type of side considered, that is $\zeta_i(R')=\zeta_i(Id):=\zeta_i$. From this and from the fact that the linear piecewise loop travels each side $[v_{j-1},v_j]$ in a time interval of size T/k_v, it follows that the potential part of the Lagrangian action is given by

$$\begin{aligned}A_U&=\frac{N}{2}\frac{T}{k_v}\sum_{j=1}^{k_v}\int_0^1\sum_{R\in\mathcal{R}\setminus\{Id\}}\frac{ds}{|(R-Id)R_j[(1-s)q]-sq_i|}\\&=\frac{N}{2}\frac{T}{k_v}(k_1\zeta_1+k_2\zeta_2).\end{aligned}$$

Therefore, from equations (1.28) and (1.29) follow the equation (1.30).

Then, if we take a linear piecewise loop on the Archimedean polyhedron $\mathcal{Q}_{\mathcal{R}}$ that satisfies the additional symmetry condition $v_I^\nu(t+T/M)=Rv_I^\nu(t)$, if it has the right number of sides in order to satisfy the condition $\mathcal{A}(v^\nu)<\alpha_{\mathcal{R},M}$, the corresponding minimizer $u_*\in\overline{\mathcal{K}}$, $\mathcal{K}=\tilde{\mathcal{K}}^\nu$ is free of total collisions. At this point, to show the existence of minimizers that are smooth solutions of the classical Newtonian N−body problem, we have to find some conditions that exclude partial collisions.

EXCLUDING PARTIAL COLLISIONS

Assume now that the minimizer $u_*\in\overline{\mathcal{K}}$ has a partial collision at time $t=t_c$. From results present in [3] we can assume that collisions are isolated in time. To find sufficient conditions that exclude partial collisions we show that, under certain hypotheses, we can construct a local perturbation v such that $\mathcal{A}(v)<\mathcal{A}(u_*)$. We base our analysis on the fact that partial collisions can be regarded as binary collisions and can take advantage of the knowledge of the structure of this latter type of collisions.

Since u_* is a minimizer, if (t_1,t_2) is an interval of regularity, then the generating particle $u_{*,I}$ solves the Euler-Lagrange equations associated to the functional (1.8), which results to be

$$\ddot{w}=\sum_{R\in\mathcal{R}\setminus\{Id\}}\frac{(R-Id)w}{|(R-Id)|^3},\quad t\in(t_1,t_2).\tag{1.31}$$

If a partial collision occurs, the generating particle must collide on a rotation axis r of some rotation $R\in\mathcal{R}$ and let $\mathcal{C}$ be the subgroup (of order $o_{\mathcal{C}}$) of the

rotations with axis r; we can rewrite equation the (1.31) and the first integral of the energy in the form

$$\ddot{w} = \alpha \frac{(R_\pi - \mathrm{Id})w}{|(R_\pi - \mathrm{Id})w|^3} + V_1(w), \quad \alpha = \sum_{j=1}^{o_\mathcal{C}-1} \frac{1}{\sin\left(\frac{j\pi}{o_\mathcal{C}}\right)}, \tag{1.32}$$

$$|\dot{w}|^2 - \alpha \frac{1}{|(R_\pi - \mathrm{Id})w|} - V(w) = h, \tag{1.33}$$

where R_π is the rotation of π around r, $V_1(w)$ and $V(w)$ are smooth functions defined in an open set $\Omega \subseteq \mathbb{R}^3$ that contains $r \setminus \{0\}$. Moreover, if $\tilde{R} \in \tilde{\mathcal{R}}$ is a reflection such that $\tilde{R}r = r$, then V_1, V satisfy the conditions

$$V_1(\tilde{R}w) = \tilde{R}V_1(w), \quad V(\tilde{R}w) = V(w). \tag{1.34}$$

The form (1.32) of the Newton's equation is well suited for the analysis of partial collisions occurring on r and in particular implies that all the partial collisions a minimizer $u_* \in \overline{\mathcal{K}}$ may present can be regarded as binary collisions.

Collision and ejection solutions

We list now some known properties of collision ejection solutions of the equation (1.32), that is solutions such that

$$\lim_{t \to t_c^+} w(t) = w(t_c) \in r \setminus \{0\}.$$

Up to translations of time and space, we can assume that $w(t_c) = 0$ and $t_c = 0$ and we consider w defined on a maximal interval $(0, \bar{t})$. In this conditions, if we denote with e_r a unit vector parallel to the axis r, there exist a constant $b \in \mathbb{R}$ and a unit vector n^+, orthogonal to r, such that

$$\lim_{t \to 0^+} \frac{\dot{w}(t) + R_\pi \dot{w}(t)}{2} = b e_r, \tag{1.35}$$

$$\lim_{t \to 0^+} \frac{w(t) - R_\pi w(t)}{|w(t) - R_\pi w(t)|} = \lim_{t \to 0^+} \frac{w(t)}{|w(t)|} = n^+. \tag{1.36}$$

The vector n^+ corresponds to the ejection limit direction. Furthermore, the rescaled functions

$$w^\lambda : [0,1] \to \mathbb{R}^3, \quad w^\lambda(\tau) = \lambda^{2/3} w(\tau/\lambda),$$

with $\lambda > 1/\bar{t}$, satisfy

$$\lim_{\lambda \to +\infty} w^\lambda(\tau) = s^\alpha(\tau) n \text{ uniformly in } [0,1], \tag{1.37}$$

$$\lim_{\lambda \to +\infty} \dot{w}^\lambda(\tau) = \dot{s}^\alpha(\tau) n \text{ uniformly in } [\delta, 1],\ 0 < \delta < 1, \tag{1.38}$$

where $s^\alpha(\tau) = (3^{2/3}/2)\alpha^{1/3}\tau^{2/3}$, $\tau \in [0, +\infty)$: this is the parabolic ejection motion, that is the solution of

$$\dot{s} = (\alpha/2)^{1/2} s^{-1/2},$$

that satisfies $\lim_{\tau\to 0^+} s(\tau) = 0$. Therefore, our singularity can be regarded asymptotically as a parabolic ejection.

Analogous statements hold for collision solutions, that is solutions such that (up to translations of time and space) $\lim_{t\to 0^-} w(t) = 0$, with a unit vector n^-, orthogonal to the axis r, corresponding to the collision limit direction. These results are well know and we refer to [3] for a proof.

Direct and indirect Keplerian arcs

If $u_* \in \overline{\mathcal{K}}$ is a minimizer of the action with a partial collision at time t_c, we can associate to the collision an axis r and two unit vectors $n^\pm$ orthogonal to r, defined by the one-sided limits

$$n^\pm = \lim_{t\to t^+} \frac{u_{*,I}(t_c \pm t) - u_{*,I}(t_c)}{|u_{*,I}(t_c \pm t) - u_{*,I}(t_c)|}. \tag{1.39}$$

We also associate to the collision the ejection-collision parabolic motion $\omega : \mathbb{R} \to \mathbb{R}^3$ defined by

$$\omega(\pm t) = n^\pm s^\alpha(t), \quad t \geqslant 0. \tag{1.40}$$

Set $\Theta_d = \arccos(n^+ \cdot n^-)$ and let $\Theta_i = 2\pi - \Theta_d$. If $\Theta_d \in (0, \pi)$, given $\tau > 0$, there exist unique Keplerian arcs $\omega_d : [-\tau, \tau] \to \mathbb{R}^3$ and $\omega_i : [-\tau, \tau] \to \mathbb{R}^3$ that connect $\omega(-\tau)$ and $\omega(\tau)$ in the time interval $[-\tau, \tau]$ and satisfy

$$\begin{cases} \omega_d((-\tau,\tau)) \subseteq \{a_1 n^- + a_2 n^+,\ a_i > 0\}, \\ \omega_i((-\tau,\tau)) \subseteq \mathrm{Span}\{n^-, n^+\} \setminus \{a_1 n^- + a_2 n^+,\ a_i \geqslant 0\}. \end{cases}$$

The arcs ω_i and ω_d are called *indirect* and *direct* Keplerian arc, respectively. In the boundary case $\Theta_d = \Theta_i = \pi$ (this situation occurs when $n^+ \cdot n^- = -1$) a similar statement holds, but the distinction between ω_d and ω_i does not make sense. In the other boundary case $\Theta_d = 0$, $\Theta_i = 2\pi$ (this situation occurs when $n^+ \cdot n^- = 1$) the indirect arc does not exist at all and $\omega_d([-\tau, \tau]) \subseteq \{an^+, a > 0\}$. We will see that the possibility of choosing between the direct and the indirect arc allows us to perturb the minimizer u_* inside the cone $\mathcal{K}$. A result that will be critical in the exclusion of partial collisions is the Marchal Theorem, that gives relations between the action over the direct and indirect Keplerian arcs and the action over the parabolic motion. A more precise statement is as follows.

THEOREM 1.11 (Marchal Theorem) - *The following inequalities hold:*

(i) $A(\omega_d) < A(\omega|_{[-\tau,\tau]})$ *for all* $n^\pm$,

(ii) $A(\omega_i) < A(\omega|_{[-\tau,\tau]})$ *for all* $n^\pm$ *such that* $n^+ \cdot n^- < 1$,

where the functional A *is*

$$A(w) = \int_{-\tau}^{\tau} \left(\frac{|\dot{w}|^2}{2} + \frac{\alpha}{4|w|} \right) dt.$$

We note that the functional A is the one of a unidimensional Kepler problem, with gravitational constant equals to $\alpha/4$. A proof of this Theorem can be found in [5], Appendix 2.

Excluding partial collisions by local perturbations

To state a first result that excludes partial collisions we introduce a definition. Let $\mathcal{K} \in \mathcal{U}$ an admissible cone, σ the sequence given by the Proposition 1.6 and k_σ its minimal period.

DEFINITION 1.12 - The cone $\mathcal{K}$ is said to be SIMPLE if the sequence σ does not contain a string $D_k, \dots, D_{k+2\sigma}$ such that

$$\mathrm{Span}\left(\bigcap_{j=0}^{2\sigma} \overline{D}_{k+j}\right) = r(R), \qquad \text{for some } R \in \mathcal{R} \setminus \{I\},$$

where σ is the order of the poles determined by $r(R)$.

We can explain this definition also in a physical way: in fact, the simple cone condition says that the deflection angle of the generating particle during a close approach with a rotation axis is less than 2π, that is reasonable for the classical Newtonian gravitational problem.

The possibility of choosing between the direct and indirect arcs allows to perturb a minimizer u_* inside the cone $\mathcal{K}$ and the Theorem 1.11 will give the desired estimates. In the special case $n^+ \cdot n^- = 1$ the indirect Keplerian arc does not exists at all and therefore we can not construct a perturbation inside the cone: this situation will be treated in the next subsection and motivates us to introduce another definition that allows us to distinguish the two different situations.

DEFINITION 1.13 - Let $u_* \in \overline{\mathcal{K}}$ be a minimizer of the action $\mathcal{A}|_{\mathcal{K}}$ and assume that it has a partial collision at a time t_c. Let r be the axis on which the collision of the generating particle takes place and n^+, n^- be the unit vectors associated to the collision. We say that the collision is of type $(\rightrightarrows)$ if

1. $n^+ = n^-$.
2. The plane generated by $r, n = n^\pm$ is fixed by some reflection $\tilde{R} \in \tilde{\mathcal{R}}$.

The first main result that excludes partial collisions is stated in the following Proposition.

PROPOSITION 1.14 - *Let $u_* \in \overline{\mathcal{K}}$ be a minimizer of the action and assume that u_* has a partial collision at time t_c. If the cone $\mathcal{K}$ is simple, then the collision is of type $(\rightrightarrows)$.*

The proof is by contradiction. If we assume that the collision is not of type $(\rightrightarrows)$, we will find a loop $v \in \overline{\mathcal{K}}$ such that $\mathcal{A}(v) < \mathcal{A}(u_*)$, against the minimality of u_*. The loop v is constructed by local perturbations, using Keplerian direct and indirect arcs as explained above and the blow-up technique. The next step will be the exclusion of $(\rightrightarrows)$ collisions, making use of an uniqueness result.

To construct the loop v it is sufficient to define it over a fundamental interval $I_{\mathcal{K}} = [t_0, t_0 + T/M]$ that contains the collision time t_c: the remaining part of v will be defined by the symmetry. So, assume that r is the collision

axis and let $\mathcal{C} \subseteq \mathcal{R}$ the subgroup of rotations with axis r and let $w(t) = u_{*,I}(t_c + t) - u_{*,I}(t_c)$. For every fixed $\lambda \gg 1$, the map $w|_{[-1/\lambda,1/\lambda]}$ is a minimizer of the functional

$$\mathcal{A}^\lambda(\phi) = \lambda^{1/3}\frac{N}{2}\int_{-1/\lambda}^{1/\lambda}\left(|\dot{\phi}|^2 + \frac{\alpha}{2|\phi|} + \sum_{R\in\mathcal{R}\setminus\mathcal{C}}\frac{1}{|(R-\mathrm{Id})(\phi + u_{*,I}(t_c))|}\right)dt,$$

defined on the set of functions $\phi \in H^1\left((-1/\lambda, 1/\lambda), \mathbb{R}^3\right)$ such that $\phi(\pm 1/\lambda) = w(\pm 1/\lambda)$. The map

$$f : H^1\left(\left(\frac{-1}{\lambda}, \frac{1}{\lambda}\right), \mathbb{R}^3\right) \to H^1((-1,1), \mathbb{R}^3),$$

defined by

$$\begin{cases} f(\phi) = \psi, \\ \phi(t) = \lambda^{-2/3}\psi(\lambda t) \end{cases} \tag{1.41}$$

is a bijection. Moreover, we have that $\mathcal{A}^\lambda(\phi) = \hat{\mathcal{A}}^\lambda(\psi)$, with

$$\begin{aligned} \hat{\mathcal{A}}(\psi) &= \frac{N}{2}\int_{-1}^{1}\left|\frac{d\psi}{d\tau}\right|^2 + \frac{\alpha}{2|\psi|} + \sum_{R\in\mathcal{R}\setminus\mathcal{C}}\frac{1}{|(R-\mathrm{Id})(\psi + \lambda^{2/3}u_{*,I}(t_c))|}d\tau \\ &:= N(A(\psi) + A^\lambda(\psi)), \end{aligned} \tag{1.42}$$

where

$$A(\psi) = \int_{-1}^{1}\frac{1}{2}\left|\frac{d\psi}{d\tau}\right|^2 + \frac{\alpha}{4|\psi|}d\tau,$$

is the action of a Kepler problem with gravitational constant equals to $\alpha/4$. Therefore, we have that $w^\lambda(\tau) = \lambda^{2/3}w(t/\lambda)$ is a minimizer of $\hat{\mathcal{A}}^\lambda(\psi)$. From the results of the previous subsections, w^λ converges uniformly in $[-1,1]$ to the parabolic motion ω defined by (1.40). Since we have assumed that $n^+ \cdot n^- < 1$, there exist the two Keplerian arcs ω_d, ω_i connecting $\omega(-1)$ to $\omega(+1)$. We can construct a perturbation using these arcs, defining

$$\hat{w}_i^\lambda = \omega_i + \delta^\lambda, \quad \hat{w}_d^\lambda = \omega_d + \delta^\lambda,$$

where

$$\delta^\lambda(\tau) = \left(w^\lambda(-1) - \omega(-1)\right)\frac{1-\tau}{2} + \left(w^\lambda(1) - \omega(1)\right)\frac{1+\tau}{2}, \quad \tau \in [-1,1].$$

To understand how the perturbation acts, see Figure 5. Since ω_i, ω_d are bounded and w^λ uniformly converges, then w_d^λ, w_i^λ are bounded. Therefore, from Lebesgue's dominate convergence theorem and from uniformly convergence we have

$$\begin{cases} \lim_{\lambda\to+\infty}\hat{\mathcal{A}}^\lambda(w^\lambda) = NA(\omega), \\ \lim_{\lambda\to+\infty}\hat{\mathcal{A}}^\lambda(\hat{w}_i^\lambda) = NA(\omega_i), \\ \lim_{\lambda\to+\infty}\hat{\mathcal{A}}^\lambda(\hat{w}_d^\lambda) = NA(\omega_d). \end{cases} \tag{1.43}$$

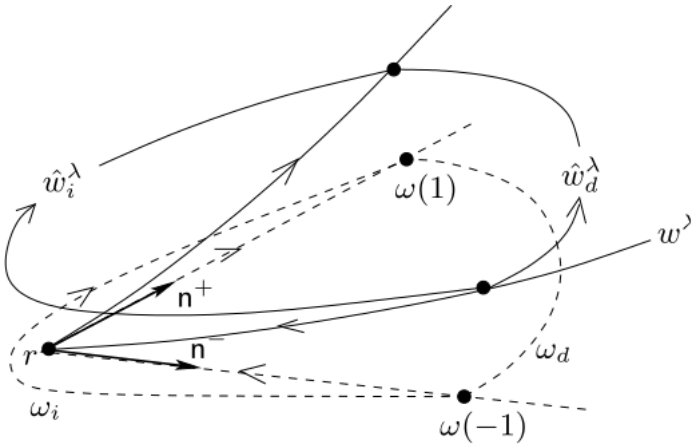

Figure 5: Perturbations of the indirect and direct arcs.

Now we construct local variations of the parabolic ejection-collision v_β^λ, $\beta \in \{i, d\}$, through

$$v^\lambda_{\beta,I}(t) = \begin{cases} u_{*,I}(t), & t \in I_{\mathcal{K}} \setminus \left[t_c - \frac{1}{\lambda}, t_c + \frac{1}{\lambda}\right], \\ \lambda^{-2/3}\hat{w}^\lambda_\beta(\lambda(t-t_c)) + u_{*,I}(t_c), & t \in \left[t_c - \frac{1}{\lambda}, t_c + \frac{1}{\lambda},\right] \end{cases} \tag{1.44}$$

if t_c is in the interior of $I_{\mathcal{K}}$, and by (1.44) with $[t_c - 1/\lambda, t_c + 1/\lambda]$ replaced by $[t_c - 1/\lambda, t_c + 1/\lambda] \cap I_{\mathcal{K}}$ if t_c is on the boundary of $I_{\mathcal{K}}$. Then, from the Theorem 1.11 we have that, for λ finite but large enough

$$\mathcal{A}(v_i^\lambda) < \mathcal{A}(u_*), \quad \mathcal{A}(v_d^\lambda) < \mathcal{A}(u_*). \tag{1.45}$$

To complete the proof of the Proposition 1.14 it is sufficient to show that we can choose $\beta \in \{i, d\}$ such that $v_\beta^\lambda \in \mathcal{K}$ for $\lambda \gg 1$. Note that in the case $n^+ = n^-$, the indirect arc does not exists and therefore we can define only v_d^λ.

From the results shown in Section 1.3, we can assume that the minimizer u_* is the C^0 limit of a minimizing sequence $\{\hat{u}^\ell\}_{\ell\in\mathbb{N}}$ that satisfies the special geometric condition discussed before. Therefore, if u_* has a collision at a time t_c, necessarily $u_{*,I}(t_c) \in r_h$ for some r_h in the sequence $k \mapsto r_k$ defined at the end of Section 1.3. Let $\tilde{h} > h$ be defined by

$$\begin{cases} r_h \subseteq \overline{S^h} \cap \overline{S^{\tilde{h}}}, \\ h < k < \tilde{h} \Rightarrow \overline{S^h} \cap \overline{S^k} = O. \end{cases}$$

In particular, $S^{\tilde{h}}$ is the wall that borders with S^h along r_h, as shown in Figure 6. Since the cone is simple, we have that

$$\tilde{h} - h + 1 \leqslant 2o_h, \tag{1.46}$$

where o_h is the order of the pole $r_s \cap \mathbb{S}^2$, and we note that the equality is attained if and only if $S^h = S^{\tilde{h}}$. From now on, with $\mathfrak{p}, \mathfrak{p}^\pm, \mathfrak{p}^\ell(t)$ we always refer to an open half plane with origin the line of r_h. We take as positive the versus of rotation around r_h defined by D_k when k increases from h to $\tilde{h}$. Let

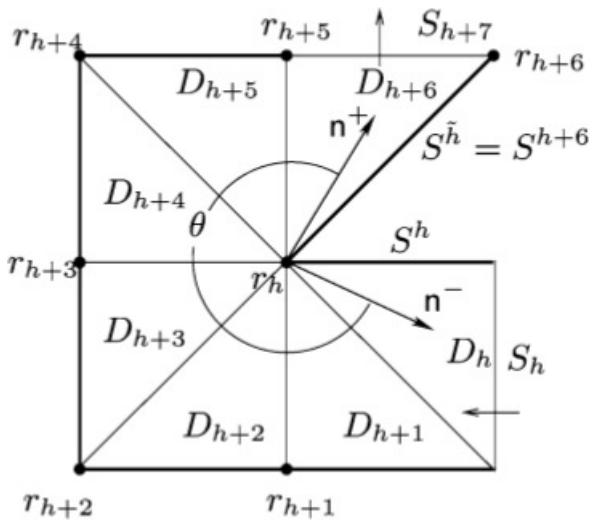

Figure 6: The definition of $S^{\tilde{h}}$.

$\mathfrak{p}^{\pm}$ be the half plane parallel to $n^{\pm}$. Let $\{t_k^\ell\}_{\ell\in\mathbb{N}}$ be the sequence associated to $\hat{u}^\ell$, defined in the proof of the Proposition 1.8: up to subsequences, we can assume that $t_k^* = \lim_{\ell\to+\infty} t_k^\ell$ exists for all $k \in \mathbb{N}$. Let i (j) be the largest (smallest) integer such that $t_i^* < t_c$ ($t_c < t_j^*$) and observe that

$$i + 1 \leqslant j, \quad h \leqslant i \leqslant \tilde{h}, \quad h < j \leqslant \tilde{h} + 1. \tag{1.47}$$

For each $t \in [t_i^\ell, t_j^\ell]$ denote by $\mathfrak{p}^\ell(t)$ the half plane through $\hat{u}_I^\ell(t)$ and let θ^ℓ be the (signed) angle swept by $\mathfrak{p}^\ell(t)$ while t increasing from t_i^ℓ to t_j^ℓ. Let $\theta^{\ell,+}$ ($\theta^{\ell,-}$) be the (signed) angle swept by the generic half plane $\mathfrak{p}$ to rotate from $\mathfrak{p}^\ell(t_j^\ell)$ ($\mathfrak{p}^\ell(t_i^\ell)$) to $\mathfrak{p}^+$ ($\mathfrak{p}^-$). It results

$$-\frac{\pi}{\mathfrak{o}_h} \leqslant \theta^{\ell,\pm} \leqslant \frac{\pi}{\mathfrak{o}_h}. \tag{1.48}$$

In fact, for $\theta^{\ell,+}$ we note that for $t \in (t_c, t_j^*)$ and $\ell \gg 1$ result $t \in (t_{j-1}^\ell, t_j^\ell)$ and therefore $\hat{u}_I^\ell(t) \in \overline{D_{j-1}} \setminus \Gamma$. It follows that $\lim_{\ell\to+\infty} \hat{u}_I^\ell(t) = u_{*,I}(t) \in \overline{D_{j-1}}$ and in turn $\mathfrak{p}^+ \cap \overline{D_{j-1}} \neq \emptyset$: this and $\hat{u}_I^\ell(t_j^\ell) \in S_j$ imply that $\theta^{\ell,+}$ satisfies (1.48); the argument for $\theta^{\ell,-}$ is similar. From the definitions of $\theta^\ell, \theta^{\ell,\pm}$ it follows that the expression $\theta^\ell + \theta^{\ell,+} - \theta^{\ell,-}$ does not depend from ℓ, therefore we can associate to the collision time t_c a well determined *collision angle* θ (see Figure 7)

$$\theta = \theta^\ell + \theta^{\ell,+} - \theta^{\ell,-}. \tag{1.49}$$

The collision angle θ satisfies the inequalities

$$-\frac{\pi}{\mathfrak{o}_h} \leqslant \theta \leqslant 2\pi, \tag{1.50}$$

and moreover, a necessary condition for $\theta = 2\pi$ is that the collision is of type ($\rightrightarrows$). A proof of this statement can be found in [5], Section 5. From the hypotheses of the Proposition 1.14 we can assume $-\frac{\pi}{\mathfrak{o}_h} \leqslant \theta < 2\pi$. It follows that, for each θ in this interval, there is a choice of $\beta \in \{d, i\}$ (precisely $\beta = d$ if $-\frac{\pi}{\mathfrak{o}_h} \leqslant \theta \leqslant \pi$ and $\beta = i$ if $\pi \leqslant \theta < 2\pi$) such that, for $\lambda \gg 1$, the interval $(t_c - 1/\lambda, t_c + 1/\lambda)$ does not contains other collision times beside t_c and,

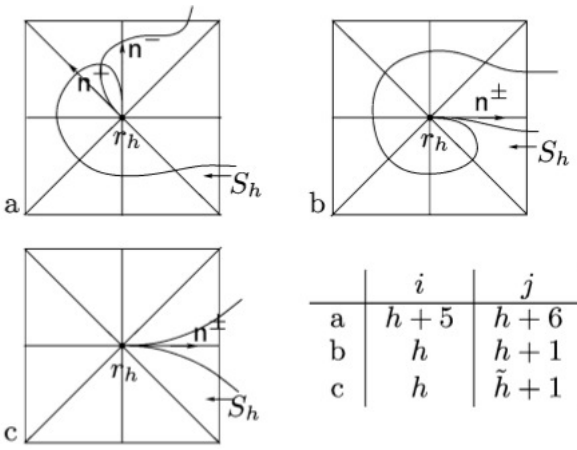

	i	j	θ
a	$h+5$	$h+6$	$-\frac{\pi}{4}$
b	h	$h+1$	0
c	h	$\tilde{h}+1$	2π

Figure 7: Definition of i, j, θ.

while t increases from $t_c - 1/\lambda$ to $t_c + 1/\lambda$ the map $v^\lambda_{\beta,I}(t)$ given by (1.44) crosses one after the other at times $t^\lambda_k \to t_c$ the walls S_k corresponding to $i < k < j$. Therefore, $v^\lambda_{\beta,I}$ is a local perturbation of $u_{*,I}$ that in the interval $(t_c - 1/\lambda, t_c + 1/\lambda)$ has the same wall crossing properties as $\hat{u}^\ell_I$, thus they belong to the same free homotopy class. This argument and the equation (1.45) conclude the proof of the Proposition 1.14.

Excluding partial collisions by uniqueness

In the case of collisions of type $(\rightrightarrows)$ we can not exclude singularity by choosing between direct and indirect arcs, because the indirect arc is not available: therefore, we use a uniqueness result for the solutions of the equation (1.32) with singular initial data, stated in the following Proposition.

PROPOSITION 1.15 - *Let* $w_i : (0, \bar{t}_i) \to \mathbb{R}^3$, $\bar{t}_i > 0$, $i = 1, 2$ *be two maximal solutions of* (1.32) *such that*

$$\lim_{t \to 0^+} w_i(t) = 0.$$

If h_i, b_i, n_i *are the corresponding values of the energy, of* b *and* n *given by equations* (1.35) *and* (1.36)*, then* $h_1 = h_2, b_1 = b_2, n_1 = n_2$ *implies that* $\bar{t}_1 = \bar{t}_2$ *and* $w_1 = w_2$.

The proof of this fact can be found in [5], Proposition 5.9. An analogous uniqueness result holds for collision solutions. So, let us consider $w : (0, \bar{t}) \to \mathbb{R}^3$ a maximal ejection solution for equation (1.32) and assume that $n^+ = n^- = n$ and that the plane $\pi_{r,n}$ generated by r and n is fixed by some reflections $\tilde{R} \in \tilde{\mathcal{R}}$, that is the collision is of type $(\rightrightarrows)$. From the symmetry (1.34), we have that also $\tilde{R}w$ is a solution of equation (1.32) with the same values of b and n: the Proposition 1.15 implies that $\tilde{R}w = w$. This means that the motion is planar, that is $w(t) \in \pi_{r,n}$ for all $t \in (0, \bar{t})$. Then follows that the generating particle u_I of a solution u that presents a partial collision at a time t_c of type $(\rightrightarrows)$, must move on a reflection plane, between two rotation axes. This contradicts the membership to $\overline{\mathcal{K}}$, except for particular topological constraints, defined by sequences ν winding around two adjacent axes only.

We conclude that, provided the cone $\mathcal{K}$ is simple and the related sequence ν does not wind around one axis, nor two axes only, the minimizers $u_* \in \overline{\mathcal{K}}$ of the action $\mathcal{A}$ are free of partial collisions. This result concludes the discussion about collisions and finally gives sufficient conditions to establish if a minimizer $u_* \in \overline{\mathcal{K}}$ is actually a smooth solution of the classical Newtonian N-body problem. We remark that these conditions that excludes both total and partial collisions uses only the two characterizations of the free homotopy classes of $\mathbb{R}^3 \setminus \Gamma$ given by the Propositions 1.5 and 1.6: on the basis of this observation, we want to develop an automatic procedure that finds all the cones that satisfy all the sufficient conditions. This will be the topic of the next Chapter.

2

SEARCHING FOR ADMISSIBLE CONES

On the basis of the results seen in Chapter 1, we want to develop an automatic procedure that generates sequences ν on the Archimedean polyhedron $\mathcal{Q}_{\mathcal{R}}$ that define the cones $\tilde{K}^{\nu}$, on which there exists a collision-free minimizer u_* of the action $\mathcal{A}$. Therefore, finding such sequences ν, we find classical periodic solutions of the Newtonian N-body problem, as seen in the previous Chapter. The strategy used here works fine in the case of the tetrahedron, instead computational problems occur in the cases of the cube and the icosahedron, that have not been fully solved.

AN AUTOMATIC PROCEDURE

To find admissible sequences ν we can use the following strategy: we generate all the paths ν of length l (for certain admissible l), we select only the closed ones and then we control if they satisfy all the conditions that exclude collisions. So, what we have to do is:

1. Find a strategy to construct paths on the Archimedean polyhedron $\mathcal{Q}_{\mathcal{R}}$ that start at the vertex numbered with 1. This condition is not restrictive, since the numbering of the vertexes is arbitrary. After that, we must select only the closed paths.
2. Exclude total collisions by means of the Proposition 1.9 and equation (1.30): these two conditions are converted into a constraint on the length of the path ν.
3. Exclude paths that wind around one axis only, so that condition (C) is satisfied.
4. Exclude paths that wind around two axes only, that give rise to a non-simple cone: in this way we avoid partial collisions.
5. Exclude paths that do not respect the additional symmetry imposed by equation (1.17).

First we see each of these steps and at the end we shall gather them all together, in such a way to describe the entire procedure.

Excluding total collisions and constraints on the length

Let ν be a sequence of vertexes on the Archimedean polyhedron $\mathcal{Q}_{\mathcal{R}}$ that satisfies equation (1.17) for some $k \in \mathbb{N}$ and $R \in \mathcal{R}$, and let ν be the associated

piecewise linear loop defined by (1.16). If ν has k_1 and k_2 sides of type one and two respectively, from the Proposition 1.9 and equation (1.30) we impose that

$$\mathcal{A}(\nu) = \frac{3}{2 \cdot 4^{1/3}} N \ell^{2/3} (k_1 \zeta_1 + k_2 \zeta_2)^{2/3} T^{1/3} \leqslant \alpha_{\mathcal{R},M}, \tag{2.1}$$

so that the minimizer on the cone $\tilde{\mathcal{K}}^{\nu}$ is free of total collisions. We note that the values of $N, \ell, \zeta_1, \zeta_2$ are known (see Table 2) and, fixing the period to $T = 1$, also the values of $\alpha_{\mathcal{R},M}$ are known, for the allowable values of M (see Table 1). Leaving k_1, k_2 on the left hand side of (2.1), we have

$$(k_1 \zeta_1 + k_2 \zeta_2)^{2/3} \leqslant \alpha_{\mathcal{R},M} \frac{2 \cdot 4^{1/3}}{3T^{1/3}} \frac{1}{N} \frac{1}{\ell^{2/3}} := K,$$

and since $K > 0$, the previous inequality becomes

$$k_1 \zeta_1 + k_z \zeta_2 \leqslant K^{2/3}. \tag{2.2}$$

Since $\zeta_1, \zeta_2 > 0$, in the case $\zeta_1 \neq \zeta_2$ (that is, in the case of the cube and the icosahedron), the equation $k_1 \zeta_1 + k_2 \zeta_2 = K^{2/3}$ represents a line in the plane (k_1, k_2) and the piece of the plane that satisfies (2.2) is the one that lies under this line. Because of $k_1, k_2 \geqslant 0$ and $k_1, k_2 \in \mathbb{N}$, we obtain a finite set of *admissible couples* (k_1, k_2) of non-negative integers that satisfy the inequality (2.2): these couples of integers are shown in Figures 8 and 9.

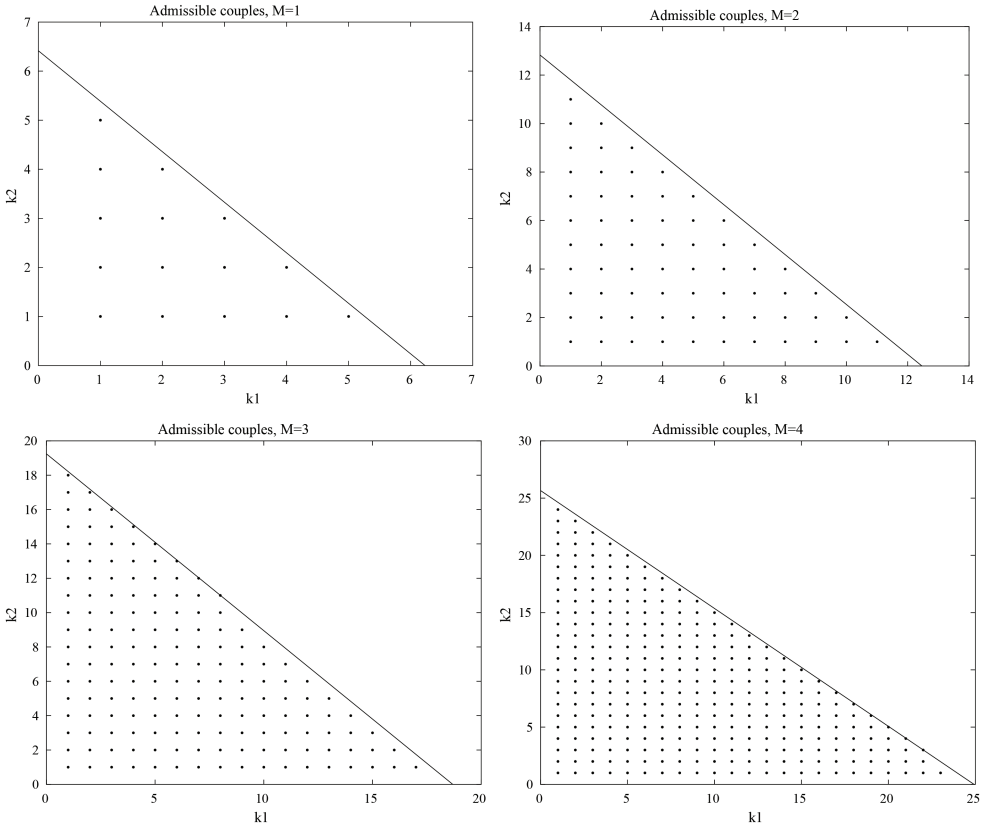

Figure 8: Admissible couples for the cube.

In the case of the tetrahedron, we have $\zeta_1 = \zeta_2$ and the inequality (2.2) becomes $l\zeta_1 \leqslant K^{2/3}$, where $l = k_1 + k_2$ is the length of the sequence ν. In

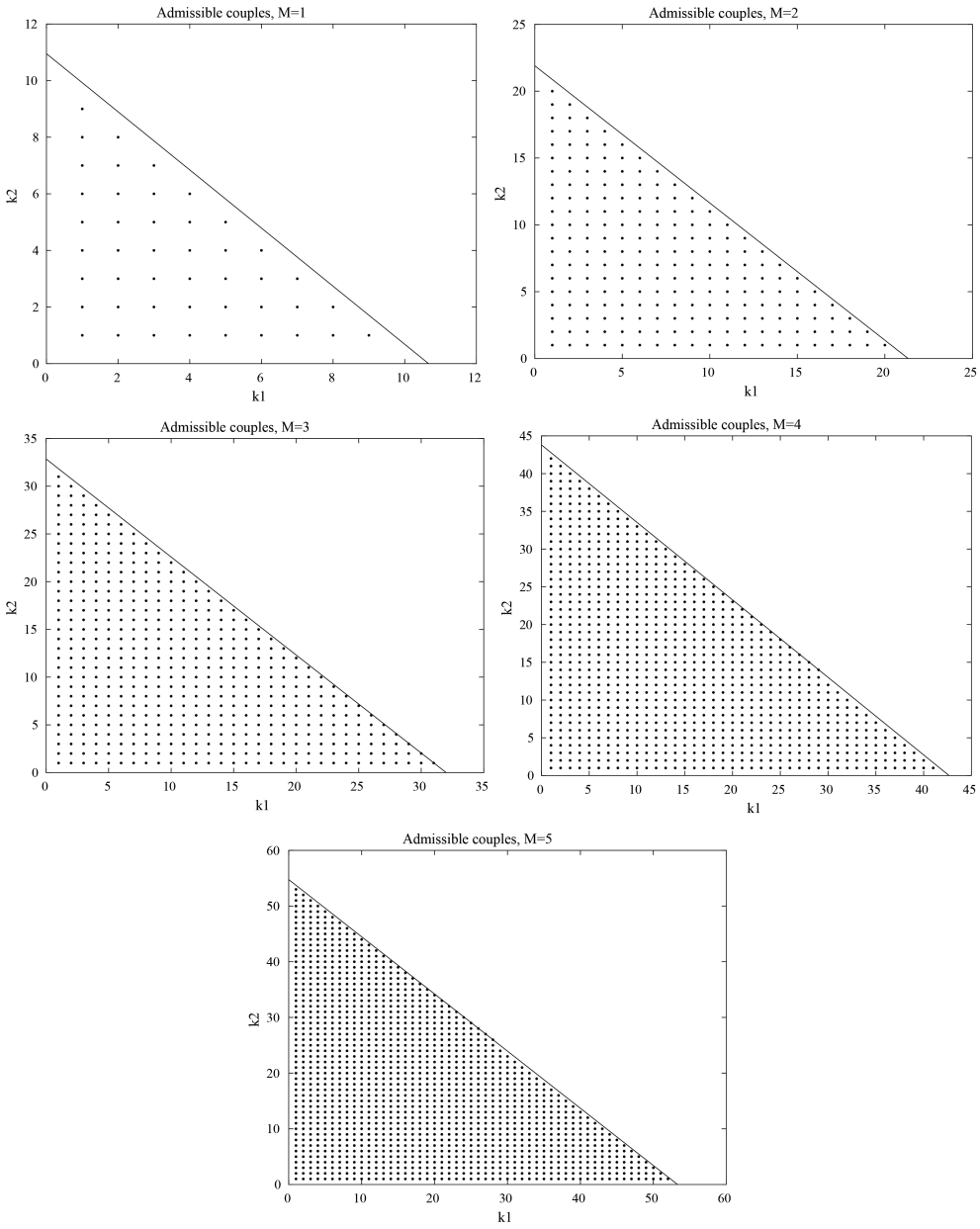

Figure 9: Admissible couples for the icosahedron.

this case we obtain constraints on the maximal length l_{max} of the paths: these values are listed in Table 3.

On the other hand, we can give some constraints on the minimal length l_{min} of the sequence ν. For example, we exclude sequences of length 3 or 4, since such paths wind around one axis only: this gives $l_{min} \geqslant 5$. We can exclude also paths of length 5: in fact in this case we obtain only paths that wind around two axes, therefore $l_{min} \geqslant 6$. On the contrary, admissible sequences of length 6 exists (see Table 4), so we set $l_{min} = 6$.

The argument on the minimal length shows that, in the case of the tetrahedron, we are not able to prove the existence of orbits with $M = 1$, since the maximal length of paths with this property is $l_{max} = 4$. Actually, the same is true also for the cube. In fact, paths with $k_1 = 0$ (or $k_2 = 0$) are not admissible: therefore, since $k_1 + k_2 \geqslant 6$, to obtain $M = 1$ we have only the

Table 3: Maximal length of paths for the tetrahedron.

M	l_{max}
1	4
2	8
3	12

couples $(k_1, k_2) = (4,2), (3,3), (2,4)$ (see Figure 8, top left). But to obtain closed paths of length exactly 6 on $\mathcal{Q}_{\mathcal{O}}$, the sequence ν must touch at most three different faces. However, paths that touch exactly two faces are not admissible, since in this case we can not exclude partial collisions. On the other hand, with a simple argument we can prove that, among the paths that travel through three different faces, the only one that has length exactly 6 is the one shown in Figure 10 (ν_1 in Table 5) that has $M = 2$. Therefore, also in the case of the cube we are not able to prove the existence of periodic orbits with $M = 1$.

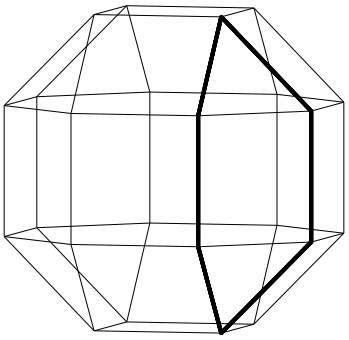

Figure 10: The only path of length 6.

Closed paths construction

From now on, with l_{max} we refer to the maximal admissible length of the sequence ν. What we want to do now is to find a strategy to generate all the sequences of vertexes ν on the Archimedean polyhedron $\mathcal{Q}_{\mathcal{R}}$ of length $l \in \{6, \dots, l_{max}\}$, and then select only the closed ones.

To know which vertexes are reachable from a fixed vertex j, we can interpret the polyhedron as a connected graphs: in this manner we can construct the *adjacency matrix* A of the graph. Furthermore, we want to store the information about what kind of side connects the vertex i to the vertex j into this matrix. Therefore, in the case of the tetrahedron, the generic enter of A will be

$$A_{ij} = \begin{cases} 1 & \text{if vertex } i \text{ and vertex } j \text{ are connected by a side,} \\ 0 & \text{otherwise,} \end{cases} \tag{2.3}$$

while in the other cases the generic enter will be

$$A_{ij} = \begin{cases} 1 & \text{if vertex } i \text{ and vertex } j \text{ are connected by a side of type 1,} \\ 2 & \text{if vertex } i \text{ and vertex } j \text{ are connected by a side of type 2,} \\ 0 & \text{otherwise.} \end{cases} \tag{2.4}$$

Now, fixed the length $l \in \{6, \dots, l_{max}\}$, we want to generate all the sequences ν of length l that start from the vertex numbered with 1. We note that at the first step we can choose among 4 different vertexes, while in the other steps we can choose only among 3 different vertexes, since the Proposition 1.5 forbid to turn back on the same side (that is $\nu_{k-1} \neq \nu_{k+1}$). It follows that the total number of sequences of length l is $4 \cdot 3^{l-1}$. To generate all these different paths, we proceed in two steps:

1. We generate an array of choice, say $\mathbf{c}$, of length l such that $\mathbf{c}(1) \in \{1, 2, 3, 4\}$ and $\mathbf{c}(j) \in \{1, 2, 3\}$ for $j = 2, \dots, l$. Each enter $\mathbf{c}(j)$ tells which way we have to follow at the step j. In other words, if $[V_1, V_2, V_3]$ are the numbered vertexes (sorted in ascending order) reachable from the generic vertex ν_j, the vertex ν_{j+1} in the sequence will be $V_{\mathbf{c}(j)}$.

2. Assigned the array of choice $\mathbf{c}$, we reconstruct the sequence ν starting from the vertex numbered with 1 following the rule explained above, making use of the adjacency matrix A to recover the reachable vertexes.

All the $4 \cdot 3^{l-1}$ arrays of choice $\mathbf{c}$ can be generated in this manner:

1. The last $l-1$ enters are encoded with an integer number $k \in \{0, \dots, 3^{l-1} - 1\}$. In fact, writing k in base 3 we obtain a sequence of $0, 1, 2$ symbols of length $l-1$: now it suffice to transform this in a sequence of $1, 2, 3$ symbols. Clearly, each k identifies a different sequence.

2. We choose the first enter $\mathbf{c}(1)$ in four different manners.

In conclusion, with two nested for cycles ($l = 6, \dots, l_{max}$ and $k = 0, \dots, 3^{l-1} - 1$) we can generate all the paths on the Archimedean polyhedron starting from vertex 1, and among all of them we select only the closed ones: at this point, we have to perform the controls explained before.

One axis control

To verify condition (C), we must check if ν does not wind around one axis only. In the case of the tetrahedron and the cube this can be done simply counting the number m of different vertexes appearing in the sequence: if $m = 3, 4$ it means that ν travels across the sides of a face $\mathcal{F}$ of the polyhedron and therefore it winds around one axis only. In the case of the icosahedron it is not so simple: in fact in the Archimedean polyhedron pentagonal faces appear and they must be treated in a different way. However, from now on, we will not enter into details for the case of the cube and the icosahedron, but we give only some ideas of the problems that come out: the reasons of this choice is explained in Section 2.3.

Two axes control

In the case of the tetrahedron, in $\Omega_{\mathcal{T}}$ two square faces never share a side. For this reason, paths that wind around two axes only can be only of three different types (see Figure 11).

1. A triangular face and a square face that share a side. We exclude these paths excluding those that touch only five different vertexes.
2. Two triangular faces that share a vertex.
3. Two square faces that share a vertex.

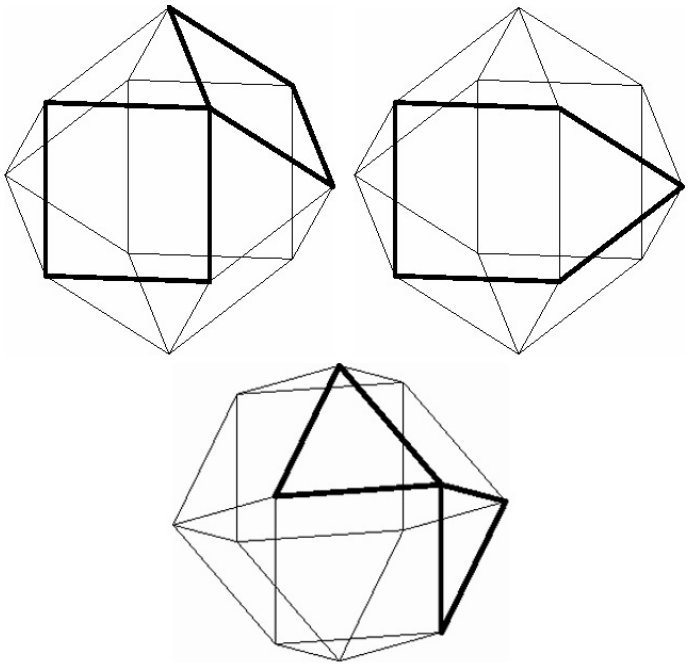

Figure 11: Paths that wind around two axes.

We can exclude the last two cases counting the faces appearing in the sequence ν and then check the length of the path: if it touches two square faces and the minimal period is 8, or if it touches two triangular faces and the minimal period is 6, we exclude the path.

In the case of the cube there are two other situations for paths that wind around two axes.

1. Two square faces that share a side.
2. A square face and a triangular face that share a vertex.

In the case of the icosahedron more situations are possible, since pentagonal faces appear in the associated Archimedean polyhedron, and a careful control is needed.

Additional symmetry control

To verify the additional symmetry condition (1.17), we must write the permutation η_R induced by a rotation $R \in \mathcal{R}$ on the vertexes of $\mathcal{Q}_{\mathcal{R}}$: first we see how to construct it. Let $V_1, \ldots, V_N \in \mathbb{R}^3$ the coordinates of the N vertexes of the Archimedean polyhedron and let $R \in \mathcal{R}$ a rotation. The permutation η_R can be represented with a *permutation matrix* of order $N \times N$, that is a binary matrix that has exactly one unitary entry in each row and each column and

zeros elsewhere. Since the rotation R leaves $\mathcal{Q}_{\mathcal{R}}$ unchanged, it sends vertexes in vertexes, therefore if $RV_i = V_j$ we set $(\eta_R)_{ji} = 1, i = 1, \dots, N$. All the other entries of η_R are zero. To read the effective permutation on the numeration of vertexes, we construct the vector $\boldsymbol{\nu} = (1, \dots, N) \in \mathbb{R}^N$ of the integers from 1 to N: the vector resulting from the product $\eta_R \boldsymbol{\nu}$ provides the permutation we wanted. The permutation matrices are computed once and stored in a text file.

Let now ν be a periodic sequence of vertexes, κ_ν its minimal period and l its length. For all the rotations $R \in \mathcal{R} \setminus \{\mathrm{Id}\}$ we compute the sequence ν_R resulting from the application of the permutation η_R to ν. After that, for all the divisors k of κ_ν, we perform a *circular shift* on the first $l-1$ entries of ν of k positions and let η_k the sequence (of length $l-1$) resulting from this operation. If the first $l-1$ entries of ν_R correspond to those of η_k, the sequence ν satisfies the additional symmetry (1.17) with the couple (k, R). After that, if there are different couples that satisfy (1.17), we select only the least k.

Simple cone control

The Definition 1.12 is expressed through the sequence of triangles of the tessellations of the sphere, that identifies the topological class that we are considering. To decide if the sequence of vertexes ν on the Archimedean polyhedron gives rise to a simple cone, we must traduce the condition on the sequence of the tessellation into a condition on the sequence of vertexes.

In the case of the tetrahedron we see that if the sequence ν contains a subsequence of vertexes that travels across a square face of $\mathcal{Q}_{\mathcal{T}}$, then it gives rise to a non-simple cone, regardless from the direction of travel. Therefore, we must reject paths with this property. On the contrary, when ν contains a subsequence that travels across a triangular face the discussion is not so simple, since the simple cone condition depends on the way we travel that face. Four different situations are possible.

1. The subsequence does not exit from the face after one wind (Figure 12, top left).
2. The subsequence enters and exits the face on the same side (Figure 12, top right).
3. The subsequence enters and exits the face on two different sides, but it performs a knot (Figure 12, bottom left).
4. The subsequence enters and exits the face on two different sides, without performing knots (Figure 12, bottom right).

The situations $1, 2, 3$ have to be excluded, since they produce non-simple cones, while the last is the only admissible. This argument conclude the discussion for the tetrahedron.

In the case of the cube and the icosahedron more situations are possible. For example, in the case of the cube, the above argument on the triangular faces works fine, but the one on the square faces is different: in fact it depends on the order of the pole centered at the face. If the order is 2, then the

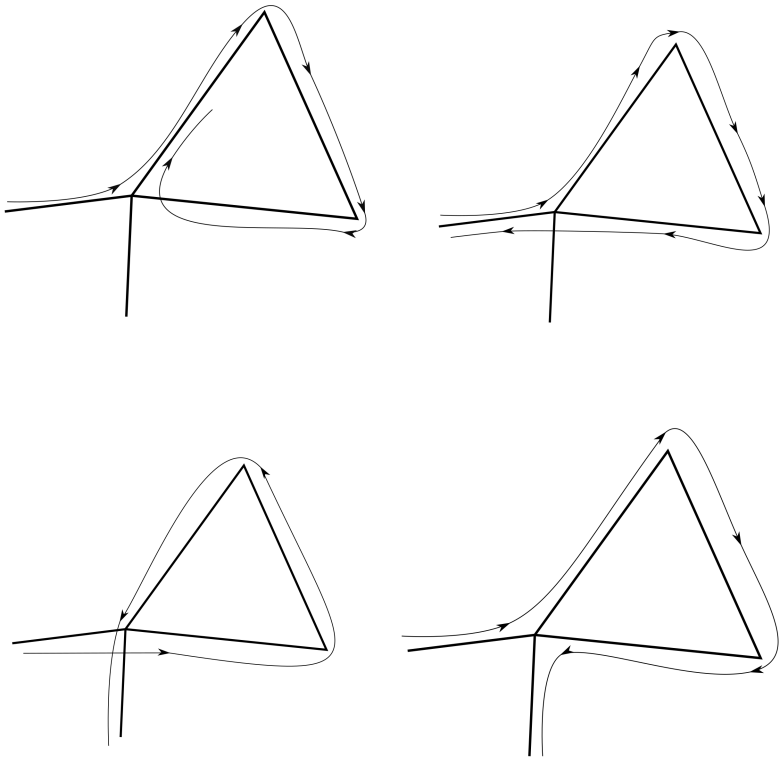

Figure 12: Paths that give rise to non-simple cone.

previous argument still works fine, otherwise when the order is 4 it is possible to travel the square face without produce non-simple cone. In this latter case we must do an analysis similar to the one done for the triangular faces. Of course, these various possibilities complicate the writing of a routine that excludes non admissible paths, since we have to take into account even the order of the pole identified by the square face.

To avoid this difficulty we could use a different Archimedean polyhedron that describes the free homotopy classes of $\mathbb{R}^3 \setminus \Gamma$, obtained again with the Wythoff construction starting from a point lying at the center of the Möbius triangle: the polyhedra obtained are shown in Figure 13. These new polyhedra permit to identify easily the paths that give rise to non-simple cone in all the three different cases: in fact it is sufficient that the sequence ν contains a subsequence that travels an entire face, regardless from the direction of travel. However, the estimates for the maximum length of the path ν now are different and we have to recompute all the admissible couples. Moreover, the new polyhedra have $2 \cdot \#\mathcal{P}$ faces and this may increase the computational

cost of the final algorithm: for these reasons we have decided to continue with the previous characterization of the homotopy classes.

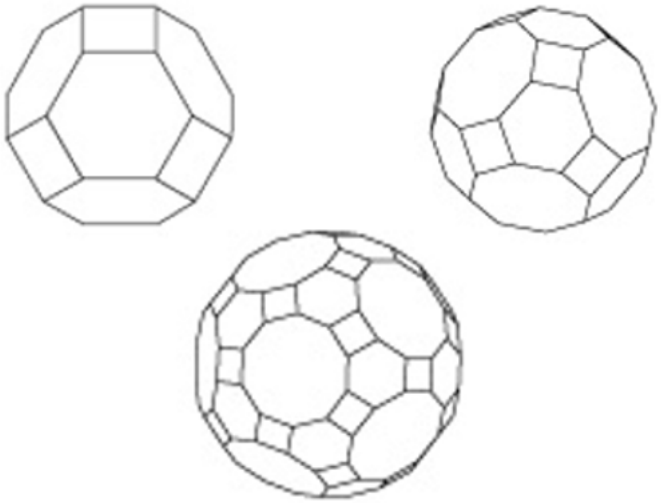

Figure 13: The new Archimedean polyhedron.

Final procedure

Now we can summarize all the above controls and write down the effective procedure to find all the sequences ν desired. For all $l = 6, \dots, l_{max}$ and for all $k = 0, \dots, 3^{l-1} - 1$ we perform the following steps:

1. Convert k in base 3 and generate the corresponding sequence ν, starting from vertex 1.
2. Control if ν is closed.
3. Compute the minimal period κ_ν of ν.
4. Control if ν winds around one axis only.
5. Control if ν winds around two axes only.
6. Additional symmetry control: if ν does not satisfy the condition (1.17) we reject it, otherwise we compute the values M, k and we identify the rotation R that produces the additional symmetry.
7. Check if the couple (k_1, k_2) corresponding to ν is admissible.
8. Control if the cone produced by ν is simple.

If the sequence ν passes all the above controls, then there exists a collision free minimizer of the action $\mathcal{A}$ that belongs to the cone $\tilde{\mathcal{K}}^\nu$. Therefore, we store ν in a list of admissible paths, together with the related informations l, k, κ_ν, M, R.

We will see that this approach works fine in the case of the tetrahedron, but already in the case of the cube computational problems occur.

RESULTS IN THE CASE OF THE TETRAHEDRON

For the case of the tetrahedron we have written the algorithm of the previous Section in MATLAB language. The program ends in about 4 minutes: the main reason of this long execution time is that MATLAB is an interpreted language. However, since the complexity of our algorithm grows exponentially with the maximum length l_{max}, this language is not suitable for the other cases, where l_{max} is 25 for the cube and 58 for the icosahedron. Up to rotations

Table 4: Sequences on $\Omega_{\mathcal{T}}$, with geometrical informations.

Name	Sequence	l	k	κ_ν	M	R
ν_1	[1, 9, 4, 11, 6, 7, 1]	6	3	6	2	11
ν_2	[1, 8, 3, 11, 6, 7, 1]	6	2	6	3	3
ν_3	[1, 7, 2, 6, 11, 4, 12, 9, 1]	8	4	8	2	11
ν_4	[1, 5, 2, 6, 4, 9, 7, 2, 10, 11, 6, 7, 1]	12	4	12	3	4
ν_5	[1, 9, 4, 12, 8, 3, 11, 10, 5, 2, 6, 7, 1]	12	4	12	3	8
ν_6	[1, 8, 3, 10, 2, 6, 4, 9, 1]	8	4	8	2	2
ν_7	[1, 8, 3, 11, 6, 7, 1, 8, 3, 11, 6, 7, 1]	12	2	6	3	3
$\mathcal{K}_1^{\mathcal{T}}$	[1, 7, 2, 5, 10, 3, 8, 12, 9, 1]	9	3	9	3	5
$\mathcal{K}_3^{\mathcal{T}}$	[1, 7, 2, 5, 10, 2, 6, 11, 4, 6, 7, 9, 1]	12	4	12	3	10

of the Archimedean polyhedron (and obviously up to bugs of the software), we found a total of 9 sequences ν: these are listed in Table 4. We remark that all of them, except for ν_6 and ν_7, are equivalent to the one present in Table 1 and Table 6 of [5]: our work expand and complete those lists. The Table 4 shows also the geometrical properties of the sequences: the number in the column labeled with R denotes the number of the rotation that realizes the additional symmetry (1.17).

COMPUTATIONAL PROBLEMS

When we implement the algorithm described above for the case of the cube and the icosahedron, computational problems, due to the exponential complexity, occur. We have tried to write it in FORTRAN95 language for the cube, performing only the steps 1 and 2 of the procedure, that is we looking for closed paths, without perform any control. Moreover, we have exchanged the order of the two nested for cycles, in such a way to speed up the procedure. Varying the maximum length of the path, we note that for small values of l_{max} (that is $l_{max} = 12, 13$, see Figure 14) the execution time is of the order of seconds: this confirms the well known fact that to use a compiled language is better than to use an interpreted language such as MATLAB, in terms of execution time. However, increasing l_{max} the execution time grows exponentially with a factor approximately 3: following this rule, we have that to obtain all the closed paths with $l_{max} = 25$ we must wait about one month. For the icosahedron, where $l_{max} = 58$, we obtain that the program ends in about 3.5×10^{14} years, more than the current age of the Universe (13.8×10^9 years).

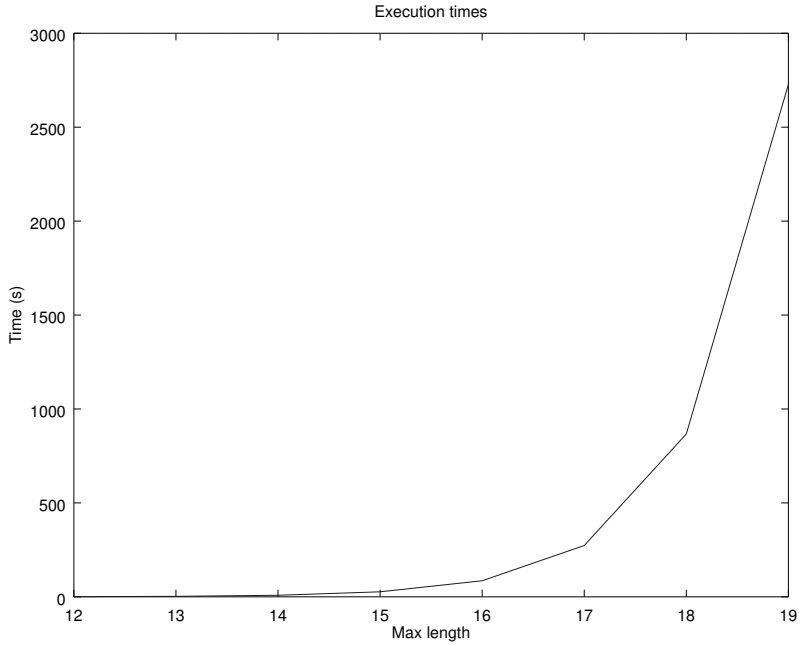

Figure 14: Execution times in function of l_{max}.

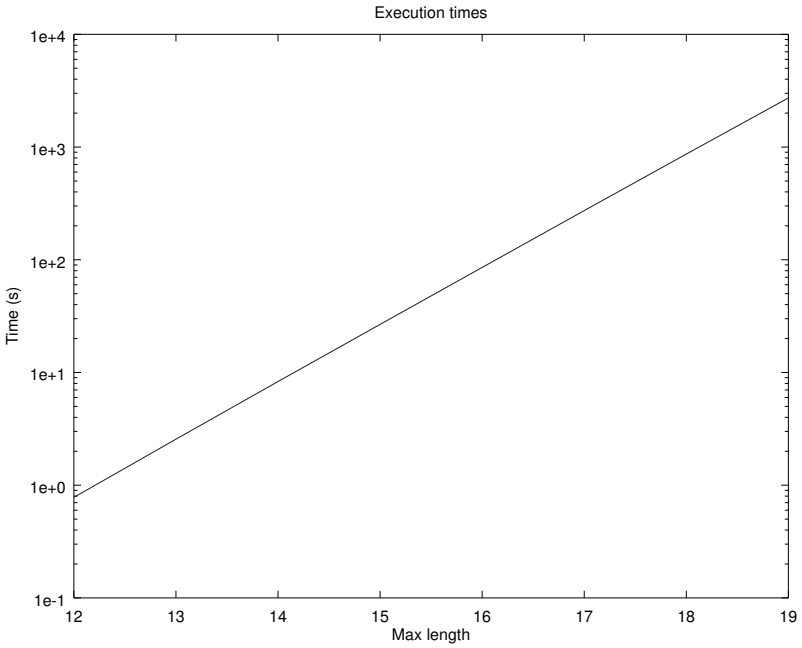

Figure 15: Execution times in function of l_{max}, semi-logarithmic scale.

For this reason we renounce to write the algorithm for the cases of the cube and the icosahedron: we limit ourselves to report here (see Tables 5 and 6) the sequences listed in [5], that we will study in Chapter 4.

Table 5: Sequences on $\Omega_{\mathcal{O}}$, with geometrical informations.

Name	Sequence	l	k	M	R
ν_1	[1, 14, 23, 11, 5, 16, 1]	6	3	2	11
ν_2	[1, 16, 10, 3, 7, 20, 23, 14, 1]	8	4	2	7
ν_3	[1, 5, 16, 1, 3, 7, 18, 20, 7, 14, 1]	10	5	2	7
ν_4	[16, 5, 11, 14, 23, 20, 18, 8, 3, 10, 16]	10	5	2	7
ν_5	[1, 16, 10, 8, 18, 7, 3, 10, 6, 15, 8, 3, 1]	12	4	3	6
ν_6	[9, 22, 6, 15, 8, 3, 7, 20, 23, 11, 19, 17, 9]	12	4	3	16
ν_7	[11, 5, 2, 22, 16, 10, 6, 15, 8, 18, 13, 24, 20, 23, 21, 19, 11]	16	4	4	14
ν_8	[4, 15, 8, 10, 3, 7, 18, 20, 23, 14, 11, 19, 21, 17, 9, 2, 22, 6, 4]	18	6	3	16
$\mathcal{K}_1^{\mathcal{C}}$	[5, 1, 16, 10, 3, 8, 18, 7, 20, 23, 14, 11, 5]	12	3	4	14
$\mathcal{K}_2^{\mathcal{C}}$	[5, 16, 10, 8, 18, 20, 23, 11, 5]	8	2	4	14
$\mathcal{K}_3^{\mathcal{C}}$	[1, 5, 16, 1, 3, 10, 8, 3, 7, 18, 20, 7, 14, 23, 11, 14, 1]	16	4	4	14
$\mathcal{K}_1^{\mathcal{O}}$	[3, 1, 16, 10, 6, 15, 8, 18, 7, 3]	9	3	3	18
$\mathcal{K}_2^{\mathcal{O}}$	[1, 16, 22, 6, 15, 13, 18, 7, 14, 1]	9	3	3	18
$\mathcal{K}_3^{\mathcal{O}}$	[3, 10, 16, 22, 6, 10, 8, 15, 13, 18, 8, 3, 7, 14, 1, 3]	25	5	3	18

Table 6: Sequences on $\Omega_{\mathcal{J}}$, with geometrical informations.

Name	Sequence	l	k	M	R
ν_1	[11, 48, 34, 14, 42, 28, 11]	6	2	3	2
ν_2	[11, 48, 34, 42, 28, 11, 6, 15, 48, 28, 45, 19, 11]	12	4	3	20
ν_3	[11, 19, 43, 50, 1, 3, 7, 47, 6, 11, 28, 45, 19, 1, 54, 59, 3, 6, 15, 48, 11]	20	4	5	6
ν_4	[1, 54, 59, 3, 6, 11, 28, 42, 14, 24, 2, 58, 60, 4, 8, 14, 34, 48, 11, 19, 1]	20	10	2	2
ν_5	[15, 48, 34, 42, 28, 45, 31, 32, 43, 50, 36, 51, 54, 59, 52, 12, 7, 47, 33, 25, 15]	20	4	5	3
ν_6	[26, 49, 38, 34, 14, 8, 20, 31, 27, 16, 37, 36, 35, 23, 53, 52, 13, 40, 21, 33, 26]	20	4	5	3
ν_7	[26, 49, 24, 38, 34, 42, 14, 8, 41, 20, 31, 32, 27, 16, 46, 37, 36, 51, 35, 23, 22, 53, 52, 12, 13, 40, 38, 21, 33, 25, 26]	30	6	5	3
$\mathcal{K}_1^{\mathcal{D}}$	[1, 54, 59, 3, 7, 47, 6, 15, 48, 11, 28, 45, 19, 43, 50, 1]	15	3	5	3
$\mathcal{K}_2^{\mathcal{D}}$	[54, 59, 7, 47, 15, 48, 28, 45, 43, 50, 54]	10	2	5	3
$\mathcal{K}_3^{\mathcal{D}}$	[54, 1, 3, 59, 7, 3, 6, 47, 15, 6, 11, 48, 28, 11, 19, 45, 43, 19, 1, 50, 54]	20	4	5	3
$\mathcal{K}_1^{\mathcal{J}}$	[28, 45, 19, 11, 6, 15, 48, 34, 42, 28]	9	3	3	25
$\mathcal{K}_2^{\mathcal{J}}$	[45, 19, 1, 3, 6, 15, 25, 38, 34, 42, 20, 31, 45]	12	4	3	25
$\mathcal{K}_3^{\mathcal{J}}$	[45, 28, 11, 19, 1, 3, 6, 11, 48, 15, 25, 38, 34, 48, 28, 42, 20, 31, 45]	18	6	3	25

3

STABILITY OF PERIODIC ORBITS

In this chapter we discuss the linear stability of periodic orbits. First we see general concepts and results valid for general autonomous systems, introducing the variational equation associated to a fixed solution of the system, defining the monodromy matrix and the Floquet multipliers: this latter are fundamental for the stability of a fixed and periodic orbit. After that, since we are interested in periodic orbits of the N-body problem, we focus our study on the additional properties of Hamiltonian systems and we treat the orbital stability in this particular case. The reference for these topics is [10]. Additional symmetric properties of choreographies can be exploited to factor the monodromy matrix: these results are introduced in Section 3.5. The reference for this section is [19]. As last topic we define the Poincaré map, another important tool for studying periodic orbits: see [17].

VARIATIONAL EQUATION

Let us consider an autonomous dynamical system

$$\dot{x} = f(x), \tag{3.1}$$

where $f : \Omega \to \mathbb{R}^n$ is a $C^2(\Omega, \mathbb{R}^n)$ vector field, defined on a nonempty open set $\Omega \subseteq \mathbb{R}^n$, and let $p(t) = \phi^t(p_0)$ be the solution of the Equation (3.1) with initial condition $x(0) = p_0$. We want to study the behaviour of the system in the vicinity of this solution, considering perturbed initial conditions of the form $p_0 + \xi_0$, where ξ_0 is supposed to be small. The new solution $p'(t)$, obtained with this conditions, can be expressed in the form

$$p'(t) = p(t) + \xi(t), \tag{3.2}$$

where $\xi(t)$ is the deviation vector between the solution (3.1) and the perturbed solution (3.2), for the same time t. The behaviour of the system in the vicinity of the solution $p(t)$ depends on the deviation vector $\xi(t)$.

If we assume that the initial perturbation ξ_0 is small, because of the continuity of the flow, the deviation vector $\xi(t)$ should be also small, at least for a finite time interval. For this reason we linearize the system (3.1) to the first term in $\xi(t)$, by substituting the perturbed solution. In this manner, we obtain the system of *variational equation*

$$\dot{\xi}(t) = \frac{\partial f(p(t))}{\partial x}\xi(t), \tag{3.3}$$

which describes the evolution of the system (3.1) in the neighborhood of the solution $p(t)$, to the first order terms in the deviation. The variational equation (3.3) is a linear system of n differential equations with time dependent coefficients. Note that if $p(t)$ is a periodic solution of the system (3.1), that is exists $T > 0$ such that $p(t+T) = p(t)$ for all $t \in \mathbb{R}$, then the variational equation is a linear system with periodic coefficients. The theory related to the study of such systems is the Floquet Theory, introduced in [4] by G. Floquet.

The fundamental matrix of solutions

The general solution of (3.3) is expressed as a linear combination of n linearly independent solutions. In particular, we can consider the $n \times n$ matrix $\Delta(t)$ whose columns are n linearly independent solutions of the variational equation corresponding to the initial condition $\Delta(0) = \mathrm{Id}$, where Id is the $n \times n$ unit matrix. The matrix $\Delta(t)$ is called *fundamental matrix of solutions* and the general solution of the variational equation is expressed in the form

$$\xi(t) = \Delta(t)\xi_0. \tag{3.4}$$

Sometimes in the next we will write the variational equation in the matrix form

$$\begin{cases} \dfrac{d}{dt}\Delta(t) = \dfrac{\partial f(p(t))}{\partial x}\Delta(t) \\ \Delta(0) = \mathrm{Id}\,. \end{cases} \tag{3.5}$$

PROPOSITION 3.1 - *The fundamental matrix of solutions is the Jacobian matrix of the general solution.*

Proof. By definition, we have that

$$\frac{\partial}{\partial t}\phi^t(p_0) = f\big(\phi^t(p_0)\big),$$

and if we differentiate this with respect to the initial condition x_0, using the continue differentiability of the flow and Schwarz's theorem to exchange the order of the derivatives, we obtain

$$\begin{aligned} \frac{\partial}{\partial t}\left(\frac{\partial}{\partial x_0}\phi^t(p_0)\right) &= \frac{\partial}{\partial x_0}\left(\frac{\partial}{\partial t}\phi^t(p_0)\right) \\ &= \frac{\partial}{\partial x_0}\Big(f\big(\phi^t(p_0)\big)\Big) \\ &= \frac{\partial f}{\partial x}\big(\phi^t(p_0)\big)\frac{\partial \phi^t(p_0)}{\partial x_0}. \end{aligned}$$

Since $p(t) = \phi^t(p_0)$ and

$$\left.\frac{\partial}{\partial x_0}\phi^t(p_0)\right|_{t=0} = \mathrm{Id} = \Delta(0),$$

we obtain that

$$\Delta(t) = \frac{\partial \phi^t(p_0)}{\partial x_0}.$$

□

REMARK 3.2 - Since $\Delta(t)$ is a solution of a linear ordinary differential equation, it has the property

$$\Delta(t+s) = \Delta(t)\Delta(s). \tag{3.6}$$

Our goal is to study the behaviour of the system (3.1) near a given periodic orbit, therefore from now on we will assume that $p(t)$ is a T-periodic orbit. To do this, we must study the solutions of the variational equation: a first result is the following Proposition.

PROPOSITION 3.3 - *The time derivative* $\dot{p}(t)$ *of the periodic solution* $p(t)$ *is a solution of the variational equation.*

Proof. To prove the result it is sufficient to compute the second derivative

$$\begin{aligned}\frac{d}{dt}\dot{p}(t) &= \frac{d}{dt}\Big(f(p(t))\Big) = \frac{d}{dt}f\Big(\phi^t(p_0)\Big)\\ &= \frac{\partial f}{\partial x}\big(\phi^t(p_0)\big)\frac{\partial}{\partial t}\phi^t(p_0) = \frac{\partial f}{\partial x}\big(\phi^t(p_0)\big)\dot{p}(t).\end{aligned}$$

□

We conclude that the variational equation corresponding to a T-periodic orbit has always a T-periodic solution, which is the time derivative $\dot{p}(t)$ of the periodic solution. In order to study the stability of the periodic orbit, we introduce a definition, that will be fundamental in the following.

DEFINITION 3.4 - If p_0 is the initial condition of a periodic orbit, the matrix

$$M = \Delta(T) = \frac{\partial \phi^T(p_0)}{\partial x_0} \tag{3.7}$$

is called *monodromy matrix*.

In the next Section we will see that the eigenvalues of this matrix play an important role in the stability of the periodic orbit.

LINEAR STABILITY AND FLOQUET MULTIPLIERS

Let $p(t)$ be a periodic orbit and $p'(t)$ a perturbed orbit which, to a linear approximation, can be expressed in the form $p'(t) = p(t) + \xi(t)$, where $\xi(t)$ is the solution of the variational equation. This latter solution is expressed by means of the fundamental matrix solution, that is set $\xi(0) = \xi_0$

$$\xi(t) = \Delta(t)\xi_0, \tag{3.8}$$

and for $t = T$

$$\xi(T) = \Delta(T)\xi_0. \tag{3.9}$$

By induction, we obtain that

$$\xi(nT) = \big(\Delta(T)\big)^n\xi_0. \tag{3.10}$$

In fact, if we assume that this property holds for n, then using (3.6) we have

$$\xi\big((n+1)T\big) = \xi(nT+T) = \Delta(nT+T)\xi_0 = \Delta(nT)\Delta(n)\xi_0 = \big(\Delta(T)\big)^{n+1}\xi_0,$$

and (3.10) holds. Equations (3.9) and (3.10) give the deviation, to a linear approximation, of the perturbed orbit $p'(t)$ from the periodic orbit $p(t)$ after a time interval equals to n times the period T, due to an initial deviation $\xi_0 = p'_0 - p_0$. Hence, equation (3.10) defines a linear map of the initial deviations ξ_0 at integer multiples of the period T, represented by the monodromy matrix $\Delta(T)$ (see Figure 16). It is clear that the stability depends on the properties of this matrix, in particular depends on its eigenvalues: these values are often called *Floquet's multipliers*.

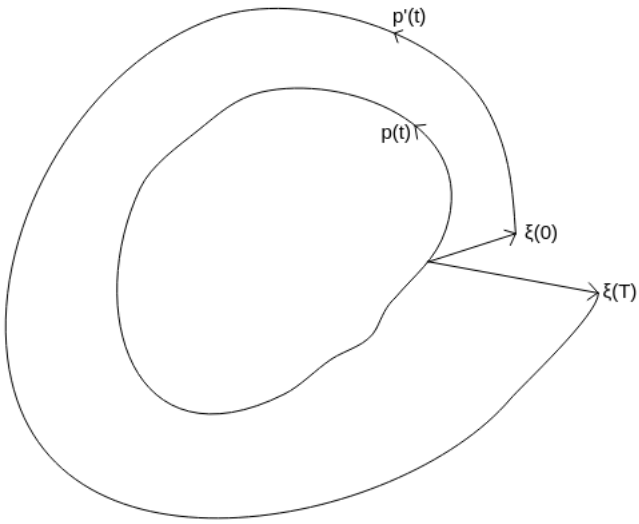

Figure 16: The map on the initial deviations defined by $\Delta(T)$.

We observe that a unitary eigenvalue always exists. In fact, if $\xi(t)$ is a T-periodic solution of the variational equation, we have that $\xi(t+T) = \xi(t)$, in particular $\xi(T) = \xi_0$. Then, by equation (3.9)

$$\xi_0 = \xi(T) = \Delta(T)\xi_0.$$

From the Proposition 3.3 we know that if $p(t)$ is a T-periodic solution of the equation (3.1), then $\dot{p}(t)$ is a T-periodic solution of the corresponding variational equation, hence we conclude that a unitary eigenvalue of the monodromy matrix always exists, and the corresponding eigenvector is $\xi_0 = \dot{p}(0)$: it represents a tangent displacement along the periodic orbit.

On the other hand, if the monodromy matrix $\Delta(T)$ has a unitary eigenvalue with ξ_0 a corresponding eigenvector, then there exists a T-periodic solution of the variational equation. In fact, let $\xi(t) = \Delta(t)\xi_0$ be the solution with initial conditions ξ_0, then

$$\xi(t+T) = \Delta(t+T)\xi_0 = \Delta(t)\Delta(T)\xi_0 = \Delta(t)\xi_0 = \xi(t),$$

that is a periodic solution of the variational equation. In general, if there exist k unitary eigenvalues with k linearly independent eigenvectors respectively, then the system of variational equation has k independent periodic solutions.

Existence of an integral of motion

Let $G : \Omega \to \mathbb{R}$ be an integral of motion, hence we have $G(\phi^t(p_0)) = G(p_0)$ for all initial conditions $p_0 \in \Omega$. If we differentiate this expression we obtain

$$\frac{\partial G(p_0)}{\partial x} = \frac{\partial}{\partial x}\Big(G(\phi^t(p_0))\Big) = \frac{\partial G(\phi^t(p_0))}{\partial x}\frac{\partial \phi^t(p_0)}{\partial x_0}.$$

Set $t = T$, taking into account that $\phi^T(p_0) = p_0$, we have

$$\frac{\partial G(p_0)}{\partial x} = \frac{\partial G(p_0)}{\partial x}\frac{\partial \phi^T(p_0)}{\partial x_0} = \frac{\partial G(p_0)}{\partial x}\Delta(T),$$

and rearranging the terms,

$$\big(\Delta^\tau(T) - \mathrm{Id}\,\big)\nabla G(p_0) = 0, \tag{3.11}$$

where Δ^τ denotes the transpose of Δ. We have that, if $\nabla G(p_0) \neq 0$, $\Delta^\tau(T)$ has a unitary eigenvalue. We conclude that, if the dynamical system has an integral of motion which is not stationary along the periodic orbit, the monodromy matrix has an additional unitary eigenvalue: in particular if we have an Hamiltonian system, there exist two unitary eigenvalues, but only one eigenvector. We shall discuss later the case of Hamiltonian systems with more details.

Characteristic exponents

Let us assume that the variational equation has a special solution with the property

$$\xi(t + T) = \lambda\xi(t), \tag{3.12}$$

that for $t = 0$ becomes

$$\xi(T) = \lambda\xi_0, \tag{3.13}$$

which means that the initial condition ξ_0 is mapped, after a period T, to a multiple of it. This latter equation is a difference equation, and its solution is of the form

$$\xi(t) = g(t)\lambda^{t/T} \tag{3.14}$$

where g is a T-periodic function that satisfies the initial condition. From equations (3.13) and (3.9) we obtain $\Delta(T)\xi_0 = \lambda\xi_0$, that is λ is an eigenvalue of the monodromy matrix and ξ_0 is a corresponding eigenvector.

On the other hand, if λ is an eigenvalue of $\Delta(T)$ and ξ_0 is a corresponding eigenvector, then it is the initial condition of a solution with the property (3.12), that is $\xi(t) = \Delta(t)\xi_0$. From this hypothesis and from the equation (3.9) we get

$$\xi(T) = \lambda\xi_0. \tag{3.15}$$

Setting the time at $t+T$ in the equation (3.8), and using the equation (3.15) and the property (3.6), we prove the result. In fact

$$\begin{aligned}\xi(t+T) &= \Delta(t+T)\xi_0 \\ &= \Delta(t)\Delta(T)\xi_0 \\ &= \Delta(t)\lambda\xi_0 \\ &= \lambda\Delta(t)\xi_0 \\ &= \lambda\xi(t).\end{aligned}$$

Therefore we have proven the following Lemma.

LEMMA 3.5 - *For each eigenvalue λ of the monodromy matrix $\Delta(T)$ there exists a solution of the form $g(t)\lambda^{t/T}$, where $g(t)$ is a T-periodic function, whose initial condition is an eigenvector $g(0)$ corresponding to the eigenvalue λ.*

Hence, we can define a parameter α as

$$\alpha = \frac{1}{T}\log\lambda, \tag{3.16}$$

where the principal value of the logarithm is taken. The solution (3.14) can be expressed as

$$\xi(t) = g(t)e^{\alpha t}. \tag{3.17}$$

The parameter α is called *characteristic exponent* and it is related to the eigenvalue λ; note that for $\lambda = 1$ we have $\alpha = 0$.

REMARK 3.6 - The monodromy matrix $\Delta(T)$ is a $n \times n$ matrix and it has n eigenvalues. If there exist n independent eigenvectors corresponding to the n eigenvalues of $\Delta(T)$ (this may not be the case if some eigenvalues are multiple), then there exist n independent solutions of the variational equation with the property (3.12) and consequently of the form (3.17). From this, it is clear that the periodic orbit $p(t)$ is linearly stable if and only if

$$\mathfrak{Re}(\alpha) \leqslant 0 \tag{3.18}$$

for all the characteristic exponents of the monodromy matrix $\Delta(T)$.

THE HAMILTONIAN CASE

Since we are interested it the stability of periodic orbits of the N-body problem (which has an Hamiltonian formulation), we now study the Floquet Theory is Hamiltonian case. A Hamiltonian system is defined by a Hamilton function

$$H(y, x), \tag{3.19}$$

where $x \in \mathbb{R}^n$ are the coordinates and $y \in \mathbb{R}^n$ are the momenta. The Hamiltonian equations of motion are

$$\begin{pmatrix}\dot{y} \\ \dot{x}\end{pmatrix} = J\nabla H, \tag{3.20}$$

where J is the $2n \times 2n$ symplectic matrix

$$J = \begin{pmatrix} 0 & -\mathrm{Id}_n \\ \mathrm{Id}_n & 0 \end{pmatrix}. \tag{3.21}$$

We recall that this matrix has the property that $J^\tau = J^{-1} = -J$, and $\det J = 1$.

Variational equation for Hamiltonian systems

To make the notation simpler, we put together the coordinates and the momenta into a unique vector $x = (y; x) \in \mathbb{R}^{2n}$, so that equation (3.20) becomes $\dot{x} = J\nabla H(x)$. The variational equation of the system (3.20) becomes

$$\dot{\xi} = \frac{\partial}{\partial x}\big(J\nabla H\big)\xi = J\frac{\partial^2 H}{\partial x^2}\xi = JA\xi, \tag{3.22}$$

where $A = A(t)$ is the Hessian matrix of the Hamilton function H, evaluated in a given solution $(y(t), x(t))$ of (3.19). This system can be expressed in the Hamiltonian form through the Hamilton function $K(\xi, t) = \xi^\tau A(t)\xi/2$: in fact if we write the Hamilton equations, we obtain

$$\dot{\xi} = J\nabla K(\xi) = JA(t)\xi,$$

since $A(t)$ is a symmetric matrix. In the Hamiltonian case, the fundamental matrix solution has an important property, stated in the following Lemma.

LEMMA 3.7 - *The determinant of the fundamental matrix solution $\Delta(t)$ is equal to one. In particular, for $t = T$*

$$\det \Delta(T) = 1, \tag{3.23}$$

that is, the monodromy matrix has unitary determinant.

Proof. From the Proposition 3.1 we know that the fundamental matrix solution is the Jacobian matrix of the general solution. Since our system is a Hamiltonian one, Liouville's Theorem holds, that is the volume in the phase space is conserved by the general solution. This property means that the Jacobian matrix of the general solution has unitary determinant, hence the thesis. □

Another important property of the monodromy matrix of a Hamiltonian system is the symplectic property, stated in the following Lemma.

LEMMA 3.8 - *If ξ and ξ' are two solutions of the variational equation, then*

$$\xi'^\tau J\xi = \mathrm{const}, \tag{3.24}$$

that is, $\xi'^\tau J\xi$ is an integral of motion for the variational equation.

Proof. The proof is obtained computing the derivative with respect to the time, and remembering that $A = A^\tau$ and $J^2 = -\mathrm{Id}$. In fact

$$\begin{aligned} \frac{d}{dt}\big(\xi'^\tau J\xi\big) &= \dot{\xi}'^\tau J\xi + \xi'^\tau J\dot{\xi} \\ &= (JA\xi')^\tau J\xi + \xi'^\tau J(JA\xi) \\ &= \xi'^\tau A^\tau J^\tau J\xi + \xi'^\tau JJA\xi \\ &= \xi'^\tau A\xi - \xi'^\tau A\xi = 0. \end{aligned}$$

□

We note that, since $\xi(t) = \Delta(t)\xi_0$, the equation (3.24) becomes (for $\xi = \xi'$)

$$\xi_0^\tau \Delta(t)^\tau J \Delta(t) \xi_0 = \xi_0^\tau J \xi_0,$$

for all initial conditions ξ_0. This means that $\Delta(t)^\tau J \Delta(t) = J$ for all t, in particular for $t = T$ we obtain

$$\Delta(T)^\tau J \Delta(T) = J, \tag{3.25}$$

that is the monodromy matrix of a Hamiltonian system is symplectic. This property implies some special features of the eigenvalues. In fact, we can rewrite (3.25) as

$$\Delta(T)^\tau = J\Delta(T)^{-1}J^{-1},$$

that is the matrix $\Delta(T)^\tau$ is related to the matrix $\Delta(T)^{-1}$ by a similarity transformation, then they have the same set of eigenvalues. Since $\Delta(T)$ and $\Delta(T)^\tau$ are also related by a similarity transformation, and the matrix $\Delta(T)$ is real, we have proven the following Lemma.

LEMMA 3.9 - *The eigenvalues of the monodromy matrix are in reciprocal pairs and they are also in complex conjugate pairs.*

We note that if $\mathbf{p}(t) = (y(t), x(t))$ is a periodic solution of the system (3.20), we had seen that $\xi(t) = \dot{\mathbf{p}}(t)$ is a periodic solution of the variational equation and then the monodromy matrix has a unit eigenvalue $\lambda_1 = 1$. Because of Lemma 3.9, there exists an eigenvalue λ_2 such that $\lambda_1\lambda_2 = 1$, that is $\lambda_2 = 1$: the monodromy matrix of an Hamiltonian system corresponding to a periodic orbit has a double unit eigenvalue.

ORBITAL STABILITY IN HAMILTONIAN SYSTEMS

To to understand the linear stability in the case of Hamiltonian systems, let us consider first the case of two degrees of freedom. After that we will extend these results to more degrees of freedom.

The case of two degrees of freedom

In two degrees of freedom the monodromy matrix is a 4×4 matrix with eigenvalues $\lambda_1, \lambda_2, \lambda_3, \lambda_4$ such that $\lambda_1 = \lambda_2 = 1$ and $\lambda_3\lambda_4 = 1$, with $\lambda_3 = \bar{\lambda}_4$. From this constraints we conclude that the eigenvalues λ_3, λ_4 are either on the unit circle (on the complex plane), or on the real axis, one inside and the other outside the unit circle (see figure 16). A special case is when they are both $+1$ or -1. It is evident that the orbit is stable only in the case where these eigenvalues are complex conjugate, on the unit circle. If they are real, the orbit is unstable. Asymptotic stability never occurs, because it is not possible for λ_3, λ_4 to be both inside the unit circle: this is also a consequence of the fact that the volume in the phase space is conserved.

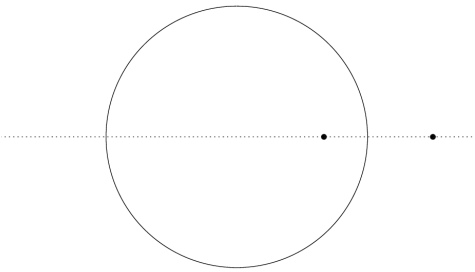

(a) Real eigenvalues inside and outside the unit circle.

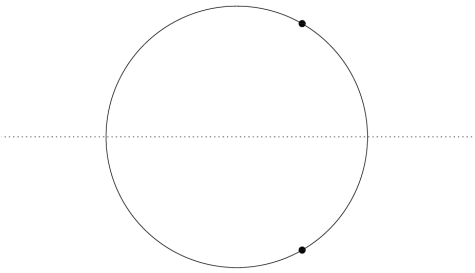

(b) Complex conjugate eigenvalues on the unit circle.

Figure 16: Positions of the eigenvalues λ_3, λ_4.

Let now try to understand the behaviour of the system in the vicinity of a periodic orbit $\mathbf{p}(t)$, and the meaning of the double unit eigenvalue. A perturbed orbit $\mathbf{p}'(t)$ is expressed in the form

$$\mathbf{p}'(t) = \mathbf{p}(t) + \boldsymbol{\xi}(t), \tag{3.26}$$

to a linear approximation in the deviation, where $\boldsymbol{\xi}(t)$ is the solution of the variational equation. The properties of the orbit $\mathbf{p}'(t)$ are determined from the properties of the solution $\boldsymbol{\xi}(t)$ of the variational equation, in particular if it is bounded, then also $\mathbf{p}'(t)$ will be bounded. In order to write the general solution of the variational equation, we remember that to each eigenvalue of $\Delta(T)$ there corresponds a solution $\boldsymbol{\xi}(t)$, hence we have four linear independent solutions, but to the double unit eigenvalue corresponds only one eigenvector $\boldsymbol{\xi}_0 = \dot{\mathbf{p}}(0)$. The two linear independent solutions corresponding to this eigenvalue are

$$\begin{cases} \boldsymbol{\xi}^1(t) = \mathbf{f}_1(t) \\ \boldsymbol{\xi}^2(t) = \mathbf{f}_2(t) + t\mathbf{f}_1(t) \end{cases} \tag{3.27}$$

where $\mathbf{f}_1(t), \mathbf{f}_2(T)$ are T-periodic functions. For the other two eigenvalues we have the solutions for different cases:

(i) Real and positive eigenvalues, $\xi^{3,4}(t) = f_{3,4}e^{\pm\alpha t}$;

(ii) Real and negative eigenvalues, $\xi^{3,4}(t) = f_{3,4}e^{\pm\alpha t}e^{\pm i\pi t/T}$;

(iii) Complex conjugate eigenvalues on the unit circle, $\xi^{3,4}(t) = f_{3,4}e^{\pm i\beta t}$;

where $f_3(t), f_4(t)$ are T-periodic functions. The initial conditions for the above special solutions are $f_i(0), i = 1, \dots, 4$ and are given by

$$\begin{cases} (\Delta(T) - Id)f_1(0) = 0, \\ (\Delta(T) - Id)f_2(0) = Tf_1(0), \\ (\Delta(T) - \lambda_{2,3})f_{2,3}(0) = 0. \end{cases} \tag{3.28}$$

The general solution is a linear combination of this four solutions, that is

$$\xi(t) = c_1\xi^1(t) + c_2\xi^2(t) + c_3\xi^3(t) + c_4\xi^4(t).$$

We have that, in the cases (i) and (ii) the orbit $p(t)$ is unstable, because of the real exponential term due to the real eigenvalues. In the case (iii) a secular term, due to the double unit eigenvalue, may appears in $\xi(t)$, but it generates only a phase shift in the orbit $p'(t)$, as we shall see in the following: therefore in this case $p(t)$ is stable.

Secular term and orbital stability

Now we want to understand the meaning of the secular term appearing in the special solution ξ^2. For this we have the following Proposition.

PROPOSITION 3.10 - *The displacement vector ξ_0 can be expressed as a linear combination of the four vectors $f_i(0), i = 1, \dots, 4$*

$$\xi_0 = c_1f_1(0) + c_2f_2(0) + c_3f_3(0) + c_4f_4(0),$$

where $c_i, i = 1, \dots, 4$ are arbitrary constants. We have that the displacement ξ_0 is isoenergetic (that is, the Hamiltonian is not changed passing form p_0 to $p_0 + \xi_0$) if $c_2 = 0$.

Proof. The change in H due to a displacement ξ_0 is

$$\delta H = \nabla H(p_0) \cdot \xi_0.$$

Consider first $c_1 \neq 0, c_2 = c_3 = c_4 = 0$. Then $\xi_0 = c_1f_1(0) = c_1\dot{p}(0)$, and since $\dot{p}(0) = J\nabla H(p_0)$ we have that

$$\delta H = \nabla H(p_0) \cdot (c_1 J\nabla H(p_0)) = 0,$$

that is, there is not change in the energy. Consider now $c_3 \neq 0, c_1 = c_2 = c_4 = 0$, so that $\xi_0 = c_3f_3(0)$: the change in the energy is given by

$$\delta H = c_3\nabla H(p_0) \cdot f_3(0).$$

From the Hamilton equation, $\dot{p}(0) = f_1(0) = J\nabla H(p_0)$ and then $\nabla H(p_0) = J^{-1}f_1(0) = -Jf_1(0)$. Consequently, the change in the Hamiltonian is

$$\delta H = -c_3(Jf_1(0)) \cdot f_3(0).$$

From the previous results, we have that $\mathbf{f}_1(0) = \Delta(T)\mathbf{f}_1(0)$ and $\mathbf{f}_3(0) = \Delta(T)\mathbf{f}_3(0)/\lambda_3$. Therefore, the scalar product becomes

$$\begin{aligned}
(J\mathbf{f}_1(0)) \cdot \mathbf{f}_3(0) &= (J\Delta(T)\mathbf{f}_1(0)) \cdot \left(\frac{1}{\lambda_3}\Delta(T)\mathbf{f}_3(0)\right) \\
&= \frac{1}{\lambda_3}\mathbf{f}_1(0)^\tau \Delta(T)^\tau J^\tau \Delta(T)\mathbf{f}_3(0) \\
&= -\frac{1}{\lambda_3}\mathbf{f}_1(0)^\tau \Delta(T)^\tau J\Delta(T)\mathbf{f}_3(0) \\
&= -\frac{1}{\lambda_3}\mathbf{f}_1(0)^\tau J\mathbf{f}_3(0) \\
&= \frac{1}{\lambda_3}\mathbf{f}_1(0)^\tau J^\tau \mathbf{f}_3(0) \\
&= \frac{1}{\lambda_3}(J\mathbf{f}_1(0)) \cdot \mathbf{f}_3(0),
\end{aligned}$$

where we have used the fact that the monodromy matrix is symplectic. This latter equation, for $\lambda_3 \neq 1$, gives $(J\mathbf{f}_1(0)) \cdot \mathbf{f}_3(0) = 0$ and then $\delta H = 0$. A similar proof holds when $c_4 \neq 0, c_1 = c_2 = c_3$. □

Hence, we conclude that:

- Any perturbation which is a linear combination of $\mathbf{f}_1(0), \mathbf{f}_3(0), \mathbf{f}_4(0)$ is isoenergetic.
- For an isoenergetic displacement, no secular term appears in the general solution of the variational equation.
- To obtain a change of energy we must have a displacement along the vector $\mathbf{f}_2(0)$.

The stability that we have mentioned before refers to the evolution of the deviation vector $\xi(t) = \mathbf{p}'(t) - \mathbf{p}(t)$ between the perturbed solution $\mathbf{p}'(t)$ and the periodic orbit $\mathbf{p}(t)$ at the same time t. We have seen that if $\xi(t)$ is bounded, then the periodic orbit is stable. However, in the case of Hamiltonian systems this condition is not enough for stability, because a secular term, due to the double unit eigenvalue, always appears in the general solution of the variational equation, making the general solution $\xi(t)$ unbounded. From the Proposition 3.10, we have that this secular term appears only if the vector ξ_0 of the initial displacement has a component along the direction $\mathbf{f}_2(0)$.

To understand the meaning of the secular term, we consider the initial conditions

$$\mathbf{p}'(0) = \mathbf{p}_0 + \varepsilon\mathbf{f}_2(0), \tag{3.29}$$

for ε small. As we saw before, the corresponding solution is

$$\mathbf{p}'(t) = \mathbf{p}(t) + \varepsilon\mathbf{f}_2(t) + \varepsilon t\mathbf{f}_1(t),$$

and using the fact that $\mathbf{f}_1(t) = \dot{\mathbf{p}}(t)$ we obtain

$$\mathbf{p}'(t) = \mathbf{p}(t) + \varepsilon t\dot{\mathbf{p}}(t) + \varepsilon\mathbf{f}_2(t), \tag{3.30}$$

and to a linear approximation in ε

$$\mathbf{p}'(t) = \mathbf{p}(t + \varepsilon t) + \varepsilon \mathbf{f}_2(t + \varepsilon t). \tag{3.31}$$

If we define the time $t' = t + \varepsilon t$, we finally come to the conclusion that $\mathbf{p}'(t) - \mathbf{p}(t')$ is bounded: thus the secular term introduces a phase shift only along the orbit. This means that the two orbits $\mathbf{p}(t), \mathbf{p}'(t)$, considered as geometrical curves, are close to each other (see Figure 17). In this case we say that we have orbital stability, provided that the eigenvalues λ_3, λ_4 are on the unit circle, and consequently the corresponding solution is bounded.

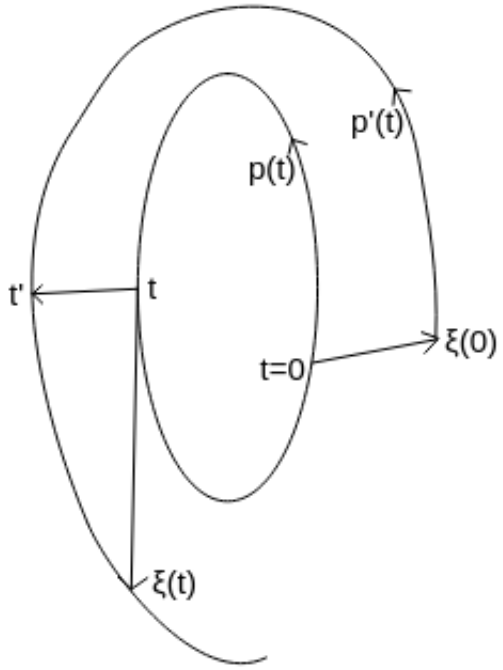

Figure 17: Orbital stability.

Extension to three or more degrees of freedom

All the above results concerning the eigenvalues and the stability of a periodic orbit, obtained in systems with two degrees of freedom, can be easily extended to three or more degrees of freedom. We have seen that in a general Hamiltonian system the monodromy matrix is a $2n \times 2n$ symplectic matrix, and the eigenvalues are in reciprocal pairs and in complex conjugate pairs. Then there are the following possibilities for the eigenvalues:

- Complex conjugate on the unit circle, $e^{\pm i\phi}$: in this case we have stability.
- Real, on the real axis and in reciprocal pairs $\lambda, 1/\lambda$: in this case we have instability.
- Complex, inside and outside the unit circle, in reciprocal and in complex conjugate pairs (see Figure 18), $Re^{\pm i\phi}, R^{-1}e^{\pm i\phi}$: in this case we have complex instability.

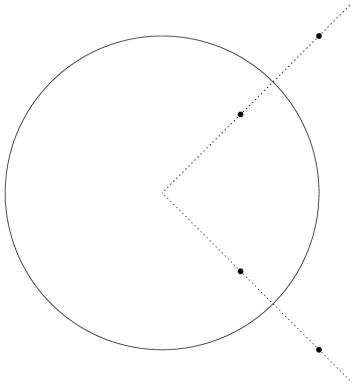

Figure 18: Eigenvalues inside and outside the unit circle in reciprocal pairs and in complex conjugate pairs.

Note that in three, or more, degrees of freedom we have a new type of instability, namely complex instability, which cannot appears in systems with only two degrees of freedom.

In conclusion, given a periodic orbit $p(t)$ of a system, to study the stability we compute the associated monodromy matrix and we find its eigenvalues. To establish the stability of such orbit, it is sufficient to verify that $\mathfrak{Re}(\alpha) \leqslant 0$ for all the characteristic exponents. Moreover, for Hamiltonian systems we have seen that to obtain orbital stability, all the eigenvalues of the monodromy matrix must lie on the unit circle.

STABILITY REDUCTION USING SYMMETRIES

In this section we present some results described in [19]: in particular we will focus on the factorization of the monodromy matrix, that arises from special symmetries of the periodic solution. This reduction will be useful also in the numerical integration: in fact, it allows to compute the full monodromy matrix integrating the variational equation over a time span smaller than the entire interval $[0, T]$. The main result is the following Lemma, presented with previous notations for general Hamiltonian systems.

LEMMA 3.11 - *Let* $\mathbf{p}(t)$ *a* T*-periodic solution of an Hamiltonian system with Hamiltonian* $H(\mathbf{x})$, $\mathbf{x} \in \Omega \subseteq \mathbb{R}^n \times \mathbb{R}^n$. *If there exists an orthogonal matrix* $S \in SO(2n, \mathbb{R})$ *such that:*

1. *The orbit has a direct symmetry, that is for some* $N \in \mathbb{N}$, *we have* $\mathbf{p}(t + T/N) = S\mathbf{p}(t)$ *for all* t*;*
2. S *commutates with* J, *that is* $SJ = JS$*;*
3. S *leaves the Hamiltonian unchanged, that is* $H(S\mathbf{x}) = H(\mathbf{x})$ *for all* $\mathbf{x}$,

then the fundamental matrix solution $\Delta(t)$ *of the variational equation* (3.22) *satisfies the relation*

$$\Delta\left(t + \frac{T}{N}\right) = S\Delta(t)S^{\tau}\Delta\left(\frac{T}{N}\right). \tag{3.32}$$

Proof. Set $A = \Delta(T/N), Y(t) = \Delta(t + T/N)$ and $Z(t) = S\Delta(t)S^\tau\Delta(T/N)$. Consider the matrix differential equation

$$\begin{cases} \dot{\Xi} = SJ\dfrac{\partial^2 H(\mathbf{p}(t))}{\partial \mathbf{x}^2}S^\tau\Xi \\ \Xi(0) = A. \end{cases} \tag{3.33}$$

Since each column of $\Delta(t)$ solves the variational equation (3.22), we have that

$$\dot{Y}(t) = \dot{\Delta}(t + T/N) = J\frac{\partial^2 H(\mathbf{p}(t + T/N))}{\partial \mathbf{x}^2}\Delta(t + T/N) = SJ\frac{\partial^2 H(\mathbf{p}(t))}{\partial \mathbf{x}^2}S^\tau Y(t),$$

where in the second and the third passes we have used all the three properties of S. On the other hand, the time derivative of Z is

$$\dot{Z}(t) = SJ\frac{\partial^2 H(\mathbf{p}(t))}{\partial \mathbf{x}^2}\Delta(t)S^\tau A = SJ\frac{\partial^2 H(\mathbf{p}(t))}{\partial \mathbf{x}^2}S^\tau Z(t),$$

where we have used the fact that S is an orthogonal matrix. Since $Y(0) = Z(0) = A$, then $Y(t), Z(t)$ both solve the equation (3.33) and therefore, by uniqueness, we have $Y(t) \equiv Z(t)$, hence the thesis. □

Therefore, under the above hypotheses, for all $k \in \mathbb{N}$ the following factorization holds

$$\Delta\left(\frac{kN}{T}\right) = S^k\left(S^\tau\Delta\left(\frac{T}{N}\right)\right)^k. \tag{3.34}$$

We can prove this by induction: the relation (3.34) is trivially true for $k = 0$. Suppose now that it holds for k, then from the Lemma 3.11 we have

$$\begin{aligned} \Delta\left(\frac{(k+1)T}{N}\right) &= \Delta\left(\frac{T}{N} + \frac{kT}{N}\right) \\ &= S\Delta\left(\frac{kT}{N}\right)S^\tau\Delta\left(\frac{T}{N}\right) \\ &= SS^k\left(S^\tau\Delta\left(\frac{T}{N}\right)\right)^k S^\tau\Delta\left(\frac{T}{N}\right) \\ &= S^{k+1}\left(S^\tau\Delta\left(\frac{T}{N}\right)\right)^{k+1}, \end{aligned}$$

that is, the relation (3.34) holds also for $k + 1$. In addition, we see that if the symmetry matrix S satisfies $S^N = \mathrm{Id}$, the monodromy matrix factors as

$$\Delta(T) = \left(S^\tau\Delta\left(\frac{T}{N}\right)\right)^N, \tag{3.35}$$

that is, we can recover the monodromy matrix from the fundamental matrix solution valued at the time $t = T/N$. These results are particularly useful not only in our case study, but whenever we are considering a choreography of the N-body problem, see [19] for details.

The monodromy matrix can be further factored if the periodic solution has a time-reversing symmetry. In fact, the following Lemma holds.

LEMMA 3.12 - *Let* $\mathbf{p}(t)$ *a* T*-periodic solution of an Hamiltonian system with Hamiltonian* $H(\mathbf{x})$, $\mathbf{x} \in \Omega \subseteq \mathbb{R}^n \times \mathbb{R}^n$. *If there exists an orthogonal matrix* $S \in SO(2n, \mathbb{R})$ *such that:*

1. *The orbit has a time-reversing symmetry, that is for some* $N \in \mathbb{N}$, *we have* $\mathbf{p}(-t + T/N) = S\mathbf{p}(t)$ *for all* t;
2. S *anti commutates with* J, *that is* $SJ = -JS$;
3. S *leaves the Hamiltonian unchanged, that is* $H(S\mathbf{x}) = H(\mathbf{x})$ *for all* $\mathbf{x}$,

then the fundamental matrix solution $\Delta(t)$ *of the variational equation* (3.22) *satisfies the relation*

$$\Delta\left(-t + \frac{T}{N}\right) = S\Delta(t)S^{\tau}\Delta\left(\frac{T}{N}\right). \tag{3.36}$$

Proof. The proof is similar to that of the Lemma 3.11. Set $A = \Delta(T/N), Y(t) = \Delta(-t + T/N)$ and $Z(t) = S\Delta(t)S^{\tau}\Delta(T/N)$. Consider the matrix differential equation

$$\begin{cases} \dot{\Xi} = SJ\dfrac{\partial^2 H(\mathbf{p}(t))}{\partial \mathbf{x}^2}S^{\tau}\Xi, \\ \Xi(0) = A. \end{cases} \tag{3.37}$$

Since column of $\Delta(t)$ solves the variational equation (3.22), we have that

$$\dot{Y}(t) = -\dot{\Delta}(t + T/N) = -J\frac{\partial^2 H(\mathbf{p}(-t + T/N))}{\partial \mathbf{x}^2}\Delta(-t + T/N) = SJ\frac{\partial^2 H(\mathbf{p}(t))}{\partial \mathbf{x}^2}S^{\tau}Y(t),$$

where in the second and the third passes we have used all the three properties of S. On the other hand, the time derivative of Z is

$$\dot{Z}(t) = SJ\frac{\partial^2 H(\mathbf{p}(t))}{\partial \mathbf{x}^2}\Delta(t)S^{\tau}A = SJ\frac{\partial^2 H(\mathbf{p}(t))}{\partial \mathbf{x}^2}S^{\tau}Z(t),$$

where we have used the fact that S is an orthogonal matrix. Since $Y(0) = Z(0) = A$, then $Y(t), Z(t)$ both solve the equation (3.37) and therefore, by uniqueness, we have $Y(t) \equiv Z(t)$, hence the thesis. □

Under the hypotheses of the above lemma, the fundamental matrix solution at the time $t = T/N$ factors as

$$\Delta\left(\frac{T}{N}\right) = SB^{-1}S^{\tau}B, \quad B = \Delta\left(\frac{T}{2N}\right). \tag{3.38}$$

In fact, using (3.36) we have

$$\Delta\left(\frac{T}{2N}\right) = \Delta\left(\frac{T}{N} - \frac{T}{2N}\right) = S\Delta\left(\frac{T}{2N}\right)S^{\tau}\Delta\left(\frac{T}{N}\right),$$

and solving this equation for $\Delta(T/N)$ we have (3.38).

In conclusion, if $\mathbf{p}(t)$ has a symmetry S_d and a time-reversing symmetry S_r that satisfies the hypotheses of the Lemmas 3.11, 3.12 with the same integer N and moreover $S_d^N = \mathrm{Id}$, combining the equations (3.35) and (3.38), we obtain that the monodromy matrix factors as

$$\Delta(T) = (S_d^{\tau}S_r B^{-1}S_r^{\tau}B)^N, \quad B = \Delta\left(\frac{T}{2N}\right), \tag{3.39}$$

that is, we can write $\Delta(T)$ in terms of the symmetry matrices and the fundamental matrix solution valued at the time $t = T/(2N)$. Consequently, to find the full monodromy matrix, it is sufficient to solve the variational equation only over the time span $[0, T/N]$ if the periodic orbit has a symmetry only, and over the time span $[0, T/(2N)]$ if it has also the time-reversing symmetry.

Symmetry of Platonic polyhedra

For the periodic orbits found in the Chapters 1 and 2, we had imposed the constraint (1.18), then there exists a rotation $R \in \mathcal{R} \setminus \{Id\}$ such that the generating particle satisfies $u_I(t + T/M) = Ru_I(t)$. Therefore, if we set $S_d \in SO(6, \mathbb{R})$ to be

$$S_d = \begin{pmatrix} R & 0 \\ 0 & R \end{pmatrix}, \tag{3.40}$$

in the Hamiltonian formalism this matrix gives a symmetry for the periodic orbit. Clearly S_d is an orthogonal matrix , satisfies $JS_d = S_d J$ and leaves the Hamiltonian unchanged, since in our case H depends only from the norms of the coordinates and the momenta. Moreover, we have that $S_d^M = Id$. In fact,

$$\begin{aligned} R^M u_I(t) &= R^{M-1} u_I\left(t + \frac{T}{M}\right) \\ &= R^{M-2} u_I\left(t + \frac{2T}{M}\right) \\ &\vdots \\ &= u_I\left(t + \frac{MT}{M}\right) = u_I(t + T) = u_I(t), \end{aligned}$$

and since $u_I(t)$ is not a stationary orbit, we must have $R^M = Id$ and therefore $S_d^M = Id$. Consequently, our periodic orbit with the matrix S_d satisfies all the hypotheses of Lemma 3.11 and then, from the equation (3.35), the monodromy matrix factors as

$$\Delta(T) = \left(S_d^\tau \Delta\left(\frac{T}{M}\right)\right)^M. \tag{3.41}$$

What we shall do in the next Chapter is a numerical study of the stability of these latter orbits. In particular, we will exploit the symmetry (1.18) to reduce the integration time span from $[0, T]$ to $[0, T/M]$ and we will use the factorization (3.35) to compute the full monodromy matrix. We will not use the time-reversing symmetries because it is not clear if all our orbits have this property: we have not fully investigated this situation yet. However, it is clear that some of the orbits of Chapter 2 have the time-reversing symmetry, since in [5] the authors have found them imposing also this latter constraint. In these particular cases it is possible to use this additional property to reduce the integration time span to $[0, T/(2M)]$, but we have not followed this way because we wanted to write a software that uses only the general properties of the orbit.

POINCARÉ MAPS

The Poincaré map is a method to transform a continuous system in dimension n to a discrete system in dimension $n - 1$. Let us consider the system (3.1) and let $p(t)$ be a T-periodic orbit, such that $f(p(t)) \neq 0$, and let p_0 be an initial condition for the periodic orbit. Let now $\Sigma \subseteq \mathbb{R}^n$ be a manifold

of dimension $n-1$ such that $p_0 \in \Sigma$. We say that Σ is a *surface of section* (or cross section) if the flow crosses transversally Σ at the point p_0 (see Figure 19), that is if

$$\mathbb{R}^n = T_{p_0}\Sigma \oplus \langle f(p_0)\rangle. \tag{3.42}$$

Near p_0 it is always possible to write the surface of section as a level set of a function, that is

$$\Sigma = \{x \in \Omega : G(x) = 0\} \tag{3.43}$$

where $G : \Omega \to \mathbb{R}$ is a differentiable function, such that $\nabla G(x) \neq 0$ for all $x \in \Sigma$. In this case the transversality condition (3.42) can be written as

$$\langle \nabla G(p_0), f(p_0)\rangle = \frac{d}{dt} G(\phi^t(p_0))\Big|_{t=0} \neq 0. \tag{3.44}$$

Because of the continuity of the flow, the surface of section Σ will be remain

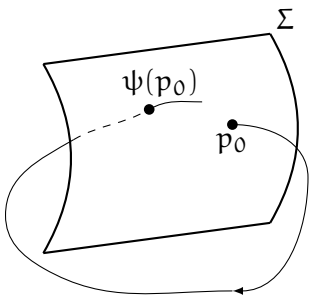

Figure 19: The Poincaré map on the surface of section.

transversal to the flow in a whole open neighborhood $U \cap \Sigma$ of p_0, where $U \subseteq \Omega$ is an open neighborhood of p_0. What we would do now is to define a map $\psi : U \cap \Sigma \to \Sigma$, that associate at every point of $U \cap \Sigma$ the first return on the cross section through the flow. To construct this map, first we see the following Lemma.

LEMMA 3.13 - *In the above hypothesis, there exists an open neighborhood* $U \subseteq \Omega$ *of* p_0 *and a differentiable function* $\tau : \Sigma \cap U \to \mathbb{R}$ *such that* $\tau(p_0) = T$ *and* $\phi^{\tau(x)}(x) \in \Sigma$ *for all* $x \in U \cap \Sigma$.

Proof. The equation $G(\phi^t(x)) = 0$ is satisfied for $t = T$ and $x = p_0$, and from the periodicity of $p(t)$ and the transversality condition (3.44) we obtain

$$\frac{d}{dt} G(\phi^t(p_0))\Big|_{t=T} \neq 0.$$

Then, from the implicit function theorem, there exist an open neighborhood $U \subseteq \Omega$ of p_0 and a differentiable function $\tau : U \to \mathbb{R}$ such that $\tau(p_0) = T$ and $G(\phi^{\tau(x)}(x)) = 0$ for all $x \in U$. In particular, this latter condition holds for all $x \in U \cap \Sigma$, and $\tau|_{U\cap\Sigma}$ is still differentiable, hence the thesis. □

Through the Lemma 3.13 we can define a map $\psi : U \cap \Sigma \to \Sigma$ such that $\psi(x) = \phi^{\tau(x)}(x)$: this is called *first return map* or *Poincaré map*. From its definition, it is clear that ψ is a differentiable function. Moreover, it is a diffeomorphism with its image: indeed its inverse is obtained simply by

following the flow with reversing the time. Hence, this map defines a $(n-1)$-dimensional discrete system.

The first return map is another instrument to study the stability of a periodic orbit, since the fixed points or the periodic points (that is, if exists $n \in \mathbb{N}$ such that $\psi^n(x) = x$) of ψ correspond to periodic orbits of the continuous system. However, we will see that the stability of the fixed point is the same as the stability of the corresponding periodic orbit, then the theory of Poincaré maps is analogue to the Floquet Theory of the previous section.

Stability of the fixed points

To determine the stability of a fixed point p_0 of the first return map $\psi : \Sigma \to \Sigma$, we have to study the eigenvalues of the differential map $d\psi_{p_0} : T_{p_0}\Sigma \to T_{p_0}\Sigma$. First we see that this set of eigenvalues does not depend from the initial condition p_0 and from the cross section Σ. In fact, taken p, q two points of the periodic orbit and Σ_1, Σ_2 two cross sections in p and q respectively, we have two Poincaré maps $\psi_i : \Sigma_i \to \Sigma_i$, $i = 1, 2$. Following the flow from the first section Σ_1 to the second one Σ_2, we obtain a local diffeomorphism $\chi : \Sigma_1 \to \Sigma_2$ such that $\chi \circ \psi_1 = \psi_2 \circ \chi$, because of the semigroup property of the flow. If we differentiate this latter equation at the point p, we obtain

$$d\chi_{\psi_1(p)} \circ d(\psi_1)_p = d(\psi_2)_{\chi(p)} \circ d\chi_p,$$

but $\chi(p) = q$ and $\psi_1(p) = p$, then

$$d\chi_p \circ d(\psi_1)_p = d(\psi_2)_q \circ \chi_p. \tag{3.45}$$

From this equation we conclude that $d(\psi_1)_p$ and $d(\psi_2)_q$ are related by a similarity transformation, hence these two operators have the same set of eigenvalues.

Now, given an initial point p_0 of the periodic orbit $p(t)$ and a cross section Σ, we want to study the eigenvalues of the map $d\psi_p$. From the chain rule and the definition of the first return map ψ, we obtain that

$$d\psi_x = d(\psi^\tau)_x = d(\phi^{\tau(x)})_x + \frac{\partial \phi^{\tau(x)}(x)}{\partial t} d\tau_x.$$

Evaluating at the fixed point $x = p_0$ we find the differential operator

$$d\psi_{p_0} = d(\phi^T)_{p_0} + f(p_0) d\tau_{p_0}. \tag{3.46}$$

We know that the matrix that represents the operator $d(\phi^T)_{p_0}$ in the canonical basis of $\mathbb{R}^n$ is the Jacobian matrix of the flow at the time T, that is it is the monodromy matrix $\Delta(T)$ corresponding to the periodic orbit $p(t)$. If we split the whole space $\mathbb{R}^n$ as in the equation (3.42), we obtain that $d(\phi^T)_{p_0}$ is represented by the matrix

$$\begin{pmatrix} 1 & -\tau_{p_0} \\ 0 & d\psi_{p_0} \end{pmatrix}.$$

Hence, we have proven the following Lemma.

LEMMA 3.14 - *The following relation holds*

$$\det(\Delta(T) - \lambda \,\mathrm{Id}) = (1-\lambda)\det(d\psi_{p_0} - \lambda \,\mathrm{Id}). \tag{3.47}$$

That is, the eigenvalues set of the differential $d\psi_{p_0}$ *is the same of the monodromy matrix* $\Delta(T)$*, except for the unitary eigenvalue.*

We conclude that the stability of the fixed point p_0 of the first return map ψ is the same as the stability of the periodic orbit $p(t)$. Moreover, as seen above, the eigenvalues of the monodromy matrix does not depend on the initial point p_0, so the stability is well determined.

The Hamiltonian case

In the case of Hamiltonian systems, let $H(y,x)$ be the Hamilton function, defined on a nonempty open set $\Omega \subseteq \mathbb{R}^n \times \mathbb{R}^n = \mathbb{R}^{2n}$. Let again $\boldsymbol{x} = (y,x) \in \mathbb{R}^{2n}$. Fixed a value $h \in \mathbb{R}$, we know that the level surface

$$S_h = \left\{\boldsymbol{x} \in \Omega : H(\boldsymbol{x}) = h\right\} \tag{3.48}$$

is invariant under the flow: what we want to do is to construct a Poincaré map on this invariant manifold. Let now $\mathbf{p}(t) = (y(t), x(t))$ be a periodic solution of the system with initial conditions $\mathbf{p}_0 = (y_0, x_0)$ and let $h = H(\mathbf{p}_0) = H(\mathbf{p}(t))$ be the corresponding value of the Hamiltonian function. The tangent space to S_h in $\mathbf{p}_0$ is

$$T(S_h)_{p_0} = \left\{\boldsymbol{x} \in \mathbb{R}^{2n} : \langle \nabla H(\mathbf{p}_0), \boldsymbol{x}\rangle = 0\right\}.$$

In particular we have that $f(\mathbf{p}_0) \in T(S_h)_{\mathbf{p}_0}$, since

$$\langle \nabla H(\mathbf{p}_0), f(\mathbf{p}_0)\rangle = \langle H(\mathbf{p}_0), J\nabla H(\mathbf{p}_0)\rangle = 0.$$

To compute the eigenvalues of the monodromy matrix, we can choose local coordinates $\mathbf{y} = (y_1, \dots, y_{2n})$ in a neighbourhood of $\mathbf{p}_0$ such that $H(\mathbf{y}) = y_1$. If we split $\mathbf{y} = (y_1, \mathbf{y}')$, then the map ϕ^T is expressed by $\phi^T(y_1, \mathbf{y}') = (y_1, \phi'(\mathbf{y}'))$. Thus, the linearized map $d\phi^T_{\mathbf{p}_0}$ will be

$$\begin{pmatrix} 1 & 0 \\ * & \hat{\Phi} \end{pmatrix}, \tag{3.49}$$

where $\hat{\Phi} = d\phi^T_{\mathbf{p}_0}|_{T(S_h)_{\mathbf{p}_0}}$. Now if we choose a cross section $\sigma \subseteq S_h$ of dimension $n-2$ near $\mathbf{p}_0$, transversal to $f(\mathbf{p}_0)$, we can define a *reduced Poincaré map* $\psi : \sigma \to \sigma$ as before. Splitting the tangent space as

$$T(S_h)_{\mathbf{p}_0} = T_{\mathbf{p}_0}\sigma \oplus \langle f(\mathbf{p}_0)\rangle,$$

we have

$$d\phi^T_{\mathbf{p}_0}|_{T(S_h)_{\mathbf{p}_0}} = \begin{pmatrix} 1 & \ell \\ 0 & d\psi_{\mathbf{p}_0} \end{pmatrix}.$$

Thus, there is a double unit Floquet multiplier and the remaining are the eigenvalues of the reduced Poincaré map. In conclusion, in the case of Hamiltonian systems, we can reduce a continuous system in dimension n

to a $(n-2)$-dimensional discrete system. We note that the time shift along the perturbed orbit (due to the double unit eigenvalue), does not produce instability in the fixed point, since it occurs only when the displacement is not isoenergetic. Consequently, the stability of the fixed point of the reduced Poincaré map is in fact orbital stability.

4

NUMERICAL ANALYSIS OF THE STABILITY

In this Chapter we develop numerical methods to study the stability of the orbits found in Chapters 1 and 2, using the tools reported in Chapter 3. We propose two different methods to estimate the monodromy matrix. The first takes inspiration from [15] and, to the best of our knowledge, it is not present in the literature about stability of choreographies. The second is more classical and it is based on the well known multiple shooting method: as reference we have used [13]. All the methods presented here are implemented in `FORTRAN95` and to solve all the differential equations we have used an explicit Runge-Kutta method of order $8(5,3)$ called `DOP853`, available at [11]. We report some tests and results obtained with these two methods, focusing on the advantages and disadvantages and the performances of each one. At the end of the Chapter we list the results for the orbits in the Tables 4, 5 and 6.

VARIATIONAL EQUATION AND EIGENVALUES OF THE MONODROMY MATRIX

In this section, first we write the equation of motion for our problem, together with the variational equation, that we have to solve to study the stability of the periodic orbits. Second, we see how to decide the stability of the orbit without computing numerically the eigenvalues of the monodromy matrix.

Variational equation

The Lagrangian function for the generating particle is determined by the action functional (1.8). In general, if we consider also non-gravitational potentials of the form $1/r^\alpha$, the Lagrangian function for our problem is

$$L(u,\dot{u}) = |\dot{u}_I|^2 + \sum_{R\in\mathcal{R}\setminus\{Id\}} \frac{1}{|(R-Id)u_I|^\alpha}, \tag{4.1}$$

where we have used the notation of Chapter 1. If $g(x) = |Bx|^\beta$, where $\beta \in \mathbb{R}, x \in \mathbb{R}^n$ and B is a $n \times n$ matrix, its Jacobian matrix is

$$\frac{\partial g}{\partial x} = \beta |Bx|^{\beta-2} B^\tau B x,$$

therefore we can write the corresponding Euler-Lagrange equation of (4.1). The relevant equation is the one relative to the generating particle, since

the motion of the other particles is obtained by equivariance. This latter equation of motion results to be

$$\ddot{u}_I = -\frac{\alpha}{2} \sum_{R \in \mathcal{R}\setminus\{Id\}} \frac{(R-Id)^\tau (R-Id) u_I}{|(R-Id)u_I|^{\alpha+2}}, \tag{4.2}$$

where $(R-Id)^\tau$ denotes again the transpose. Now we want to study the stability of periodic orbits found in Chapters 1 and 2, using the tools described in Chapter 3: to do this we must write the equation (4.2) as a first order equation. Hence, let $x = (x_1, x_2) = (u_I, \dot{u}_I) \in \mathbb{R}^6$, the equation (4.2) becomes

$$\begin{cases} \dot{x} = f(x), \quad f(x) = (f_1(x), f_2(x)), \\ \\ f_1(x) = x_2, \\ \\ f_2(x) = -\dfrac{\alpha}{2} \displaystyle\sum_{R \in \mathcal{R}\setminus\{Id\}} \dfrac{(R-Id)^\tau (R-Id) x_1}{|(R-Id)x_1|^{\alpha+2}}. \end{cases} \tag{4.3}$$

To study the stability we must study the spectral properties of the monodromy matrix, hence we must write and solve the associated variational equation. To write this latter equation we have to compute the Jacobian matrix of the vector field (4.3). We recall that if $g : \mathbb{R}^n \to \mathbb{R}^n$ and $h : \mathbb{R}^n \to \mathbb{R}$, the Jacobian matrix of the product $g(x)h(x)$ results to be

$$\frac{\partial}{\partial x}(hg) = h\frac{\partial g}{\partial x} + g\left(\frac{\partial h}{\partial x}\right)^\tau.$$

Using this fact, we obtain that the Jacobian matrix of f, and therefore the vector field of the variational equation, is

$$\frac{\partial f}{\partial x} = \begin{pmatrix} 0 & Id \\ 0 & r(x) \end{pmatrix}, \tag{4.4}$$

where

$$\begin{cases} r(x) = & \dfrac{\partial f_2}{\partial x_1}, \\ \\ \dfrac{\partial f_2}{\partial x_1} = & -\dfrac{\alpha}{2} \displaystyle\sum_{R \in \mathcal{R}\setminus\{Id\}} \left[\dfrac{(R-Id)^\tau (R-Id)}{|(R-Id)x_1|^{\alpha+2}} \right. \\ & \left. -(\alpha+2) \dfrac{(R-Id)^\tau (R-Id) x_1 x_1^\tau (R-Id)^\tau (R-Id)}{|(R-Id)x_1|^{\alpha+4}} \right]. \end{cases} \tag{4.5}$$

What we shall do now is to find a way to solve numerically the variational equation relative to a T-periodic solution $x(t) = (u_I(t), \dot{u}_I(t))$, that is we want to solve numerically the differential equation

$$\begin{cases} \dfrac{d\Delta(t)}{dt} = \dfrac{\partial f(x(t))}{\partial x} \Delta(t), \\ \\ \Delta(0) = Id\,. \end{cases} \tag{4.6}$$

Once we have found the numerical solution, we have an estimate of the monodromy matrix $\Delta(T)$: to decide the stability of the periodic orbit we only have to study its spectral properties.

Eigenvalues of the monodromy matrix

To study the spectral properties of the monodromy matrix, we can proceed in two ways: the first is to compute numerically the eigenvalues of $\Delta(T)$, using for example the QR method. However, this solution is not optimal, because the monodromy matrix could be badly conditioned. A better way is to use a result similar to the one present in [13]. From what we saw in Chapter 3, we know that $\Delta(T)$ is a real 6×6 matrix with two unitary eigenvalues, one arising from the periodicity of the orbit and the other from the presence of the first integral of the total energy. We note that the angular momentum for our orbits is zero, in fact

$$\begin{aligned} L &= \sum_{R \in \mathcal{R}} (u_R \times \dot{u}_R) \\ &= \sum_{R \in \mathcal{R}} (R u_I \times R \dot{u}_I) \\ &= \sum_{R \in \mathcal{R}} R(u_I \times \dot{u}_I) \\ &= (u_I \times \dot{u}_I) \sum_{R \in \mathcal{R}} R = 0, \end{aligned}$$

hence it does not produce any other unitary eigenvalue, since its derivative is always zero. Moreover, since $\Delta(T)$ is also symplectic, we have only three possibilities for the remaining eigenvalues $\lambda_1, \lambda_2, \lambda_3, \lambda_4$, up to relabeling:

1. Some of $\lambda_1, \lambda_2, \lambda_3, \lambda_4$ are real and $\lambda_1\lambda_2 = \lambda_3\lambda_4 = 1$.
2. $\lambda_1, \lambda_2, \lambda_3, \lambda_4 \in \mathbb{C} \setminus \mathbb{R}$ and $\lambda_1 = \lambda_2^{-1} = \bar{\lambda}_3 = \bar{\lambda}_4^{-1}$.
3. $\lambda_1, \lambda_2, \lambda_3, \lambda_4 \in \mathbb{C} \setminus \mathbb{R}$ and $\lambda_1 = \lambda_2^{-1} = \bar{\lambda}_2$, $\lambda_3 = \lambda_4^{-1} = \bar{\lambda}_4$.

If we set $T_1 = \lambda_1 + \lambda_2, T_2 = \lambda_3 + \lambda_4$, we can write the characteristic polynomial as

$$\begin{aligned} p(\lambda) &= (\lambda - 1)^2(\lambda - \lambda_1)(\lambda - \lambda_2)(\lambda - \lambda_3)(\lambda - \lambda_4) \\ &= (\lambda - 1)^2(\lambda^2 - T_1\lambda + 1)(\lambda^2 - T_2\lambda + 1) \\ &= \lambda^6 - (T_1 + T_2 + 2)\lambda^5 + (T_1T_2 + 2(T_1 + T_2) + 3)\lambda^4 + \dots. \end{aligned}$$

If we denote with d_{ij} the element of $\Delta(T)$ in the i-th row and j-th column, $a = \operatorname{tr}\Delta(T)$ and $b = \sum_{1 \leqslant i \leqslant j \leqslant 6}(d_{ii}d_{jj} - d_{ij}d_{ji})$, from the well known expression of the coefficients of the characteristic polynomial, we obtain the relations

$$\begin{cases} T_1 + T_2 + 2 = a, \\ T_1T_2 + 2(T_1 + T_2) + 3 = b, \end{cases} \tag{4.7}$$

and because of the symmetry of these two equations, it results that T_1 and T_2 are the roots of the polynomial

$$q(s) = s^2 - (a - 2)s + (b - 2a + 1). \tag{4.8}$$

The stability of the orbit can be assessed finding the roots of this latter polynomial, as expressed in the following Lemma.

LEMMA 4.1 - *Let* T_1, T_2 *the roots of* $q(s)$ *and suppose that*

$$\begin{cases} \Delta = (a-2)^2 - 4(b-2a+1) > 0, \\ |T_1| < 2, \quad |T_2| < 2. \end{cases} \tag{4.9}$$

Then the eigenvalues of the monodromy matrix lie on the unit circle and the periodic orbit is therefore linear stable.

Proof. The hypothesis $\Delta > 0$ says that T_1 and T_2 are real and distinguished: this excludes immediately the condition 2 above, since in this case we would have $T_1 = T_2$ or $\mathfrak{Im}(T_1) \neq 0$. In the case of condition 1 we would have that

$$|T_1| = |\lambda_1 + \lambda_2| = |\lambda_1 + \lambda_1^{-1}| > 2, \quad |T_2| = |\lambda_3 + \lambda_4| = |\lambda_3 + \lambda_3^{-1}| > 2,$$

in contradiction with the hypotheses: the only possibility is the third, that is the eigenvalues of the monodromy matrix lie on the unit circle. The stability of the orbit follows from results of Chapter 3. □

In conclusion, through this Lemma we can avoid the numerical computation of the eigenvalues and we can establish the stability of the orbit simply by computing the roots of a polynomial of degree two, whose coefficients depend only on the entries of the monodromy matrix.

MONODROMY MATRIX VIA RELAXATION DYNAMICS

A first way to integrate the variational equation is to find some approximation of the trajectory of the generating particle, without using any initial condition of the orbit. A method to do this is described in [15] and is called *relaxation dynamics*. After that we have only to propagate numerically the variational equation to produce an estimate of the monodromy matrix: as said before, this step make use of the `DOP853` integrator.

Relaxation dynamics

From the principle of least action, we know that the solutions of a Hamiltonian system are extremal points of the action functional

$$\mathcal{A}(q) = \int_0^T L(q, \dot{q}, t)dt.$$

We can look for periodic orbits belonging to a given topological class through an iterative numerical procedure that minimizes the action functional $\mathcal{A}$. If we introduce an auxiliary time variable τ that parametrizes such curves, so that $q = q(t, \tau)$, the action functional will depends also on this new parameter. The gradient dynamics of the action functional is expressed by the equation

$$\frac{\partial q}{\partial \tau} = \nabla \mathcal{A},$$

where ∇ denotes the L^2 gradient of the functional. In the case of a mechanical system (which is also our case), the Lagrangian function has the form

$$L(q, \dot{q}) = \frac{1}{2}|\dot{q}|^2 + U(q),$$

where we have supposed unitary masses, and the L^2 gradient results to be

$$\nabla \mathcal{A} = \ddot{q} + \frac{\partial U}{\partial q} = \ddot{q} - F(q),$$

where $F(q)$ denotes the force arising from the potential. Therefore, the gradient dynamics is expressed by

$$\frac{\partial q}{\partial \tau} = \ddot{q} - F(q). \tag{4.10}$$

We note that if $\partial q/\partial \tau = 0$ we get a solution of the equation of motion, that corresponds to an equilibrium point of the gradient dynamics.

The numerical implementation of this is reduced to to a gradient search in some finite-dimensional approximation of the path space (see [20]). In our case, we simply discretize the path at equally spaced values of the time. Starting with an arbitrary path of the desired free homotopy class and applying the relaxation process, only three situations can happen:

1. The masses escape;
2. A collision occurs;
3. Convergence to an equilibrium point.

Since the first two cases are avoided by the theory of Chapter 1 for our topological free homotopy classes, only the third option remains. Therefore, from this step we get an approximation of the motion of the generating particle. The orbits discussed in Chapters 1 and 2 were obtained numerically with this technique, using software written by G. F. Gronchi: videos of some of them are available at [8]. We will use this software to produce an approximation of the motion.

Estimate of the monodromy matrix

The output of the gradient search is a set of points that discretize the trajectory of the generating particle: this finite set of points is interpolated with a cubic spline, in a way to obtain a continuous approximation for the position, together with an estimate for the velocity of the particle. Since the gradient search is an iterative procedure, we produce a sequence $p_h(t)$ of C^2 T-periodic loops that converge to our periodic orbit $p(t)$, solution of Equation (4.3). What we would do now is to use this approximation of the motion to solve the variational equation. The idea is to integrate numerically the problem

$$\begin{cases} \dfrac{d\Delta_h}{dt} = A_h(t)\Delta_h(t), \\ \Delta_h(0) = \mathrm{Id}, \end{cases} \tag{4.11}$$

where

$$A_h(t) = \frac{\partial f(p_h(t))}{\partial x}, \tag{4.12}$$

for an integer h large enough. Since $f(x)$ is a smooth vector field, we have that $A_h(t) \to A(t)$, where

$$A(t) = \frac{\partial f(p(t))}{\partial x}, \tag{4.13}$$

is the linear coefficient of the variational equation. Because of the continuity of the solutions with respect to the coefficients of the system, we have that also the solutions converge, that is $\Delta_h(t) \to \Delta(t)$: in particular for $t = T$ we have that the monodromy matrices computed with the approximated solutions converge to the true monodromy matrix $\Delta(T)$. At this point, we can compute the values T_1 and T_2, introduced in the previous section, to state the stability of the periodic orbit. Furthermore, we can exploit the symmetry (1.18) to reduce the integration time span from the whole $[0, T]$ to $[0, T/M]$ and then obtain the monodromy matrix from the factorization given by the Lemma 3.11.

MONODROMY MATRIX VIA SHOOTING METHODS

Another different way to check the stability of a periodic orbit is to find some initial condition and then solve the equation of motion and the variational equation coupled together. To do this we can see our problem like a boundary value problem, with periodic boundary conditions, that is

$$\begin{cases} \dot{x} = f(x), \\ x(0) = x(T), \end{cases} \tag{4.14}$$

where $f(x)$ is expressed by (4.3). However, solving on the whole period could produce numerical instability due to multiple close approaches: to avoid this problem we can exploit again the symmetry of our orbits. In fact, since the condition (1.18) holds, we can solve the boundary problem only in the fundamental interval $[0, T/M]$. Therefore, it becomes

$$\begin{cases} \dot{x} = f(x), \\ x(T/M) = Sx(0), \end{cases} \tag{4.15}$$

where

$$S = \begin{pmatrix} R & 0 \\ 0 & R \end{pmatrix},$$

and R is the rotation give by (1.18). A well known numerical technique to solve this type of problem is the *multiple shooting method*: we explain here the basic idea, the reader can found more details in [22]. The idea is to subdivide the interval $[0, T/M]$ in $k+1$ *shooting points*, $0 = t_1 < t_2 < \cdots < t_{k+1} = T/M$, shooting on every subinterval and require the continuity of the solutions at the nodes t_i, $i = 2, \ldots, k$. In other words, this approach consists in find some zeros of the function $F(s_1, \ldots, s_k) : \mathbb{R}^{6k} \to \mathbb{R}^{6k}$, whose components are

$$\begin{cases} F_i(s_1, \ldots, s_k) = s_{i+1} - \phi_{t_i}^{t_{i+1}}(s_i), \quad i = 1, \ldots, k-1, \\ F_k(s_1, \ldots, s_k) = Ss_1 - \phi_{t_k}^{T/M}(s_k), \end{cases} \tag{4.16}$$

where $\phi_{t_i}^{t}(s_i)$ denotes the solution starting from s_i at time t_i. In fact, the first $k-1$ conditions express the continuity of the solutions in the nodes, while the last is the boundary condition of the problem. To solve this non-linear system of equations we can use the well known Newton-Raphson method.

This iterative method involves even the Jacobian matrix of the function F, that results to be

$$J(s_1,\dots,s_k)=\begin{pmatrix} -\Delta_{s_1}(t_2) & \mathrm{Id} & & \\ & -\Delta_{s_2}(t_3) & \ddots & \\ & & \ddots & \mathrm{Id} \\ S & & & -\Delta_{s_k}(t_{k+1}) \end{pmatrix} \tag{4.17}$$

The matrices $\Delta_{s_j}(t)$ are obtained solving numerically the equation of motion and the variational equation coupled together, with the appropriate initial condition, that is we solve

$$\begin{cases} \dot{x}(t)=f(x(t)), \\ \dfrac{d}{dt}\Delta_{s_j}(t)=\dfrac{\partial f(x(t))}{\partial x}\Delta_{s_j}(t), \quad j=1,\dots,k. \\ x(t_j)=s_j, \\ \Delta_{s_j}(t_j)=\mathrm{Id}, \end{cases} \tag{4.18}$$

Again, for this step we have used the `DOP853` integrator. Since this is an iterative method, to obtain convergence we must start with a first guess near to the zero: to do this we choose as initial points s_j the one produced by the relaxation dynamics, described in the previous section. The iterative process is stopped when the sup norm of $F(\mathbf{s}^j)$ (where $\mathbf{s}^j=(s_1^j,\dots,s_k^j)$ is the initial condition of the $j-$th step) is less than a fixed tolerance or whenever we reach a maximum number of iterations: in the first case we declare the convergence.

If the method has reached the convergence, we get a point $p_0\in\mathbb{R}^6$ such that $\phi^{T/M}(p_0)=Sp_0$: since $SJ=JS$ and $H(Sx)=H(x)$ for all $x\in\mathbb{R}^6$, we have that (1.18) holds for all time t. In fact by the semigroup property of the flow we get

$$\phi^{t+T/M}(p_0)=\phi^t(\phi^{T/M}(p_0))=\phi^t(Sp_0)=S\phi^t(p_0).$$

The latter equality follows from the properties listed above: if we set $p_1(t)=\phi^t(Sp_0)$ and $p_2(t)=S\phi^t(p_0)$, we have that $p_1(0)=p_2(0)$. Moreover, $p_1(t)$ is a solution of Hamilton equation by definition, but it is also p_2: it is sufficient to compute the derivative with respect to the time

$$\dot{p}_2(t)=SJ\nabla H(\phi^t(p_0))=JS\nabla H(\phi^t(p_0))=J\nabla H(S\phi^t(p_0))=J\nabla H(p_2(t)).$$

Therefore, by uniqueness of the solution, we have $p_1(t)=p_2(t)$, that is we can move the matrix S out of the flow.

At this point we only have to solve numerically the equation of motion and the variational equation coupled together, with initial condition equal to p_0 for the orbit. Again, we can solve on the whole interval $[0,T]$ and get directly the monodromy matrix, or solve on the fundamental interval $[0,T/M]$ and compute the monodromy matrix by the decomposition obtained in Chapter 3. At last we check the stability of the orbit by computing the values of T_1 and T_2 and using Lemma 4.1.

TESTS

In this section we want to test our software on some specific orbits of Chapter 2, in order to understand pros and cons of the two different methods described above. In particular, we want to find which method produces better results and how do they behave when some close approaches occur. As indexes of the goodness of the results produced we can use some values. First, we compute the sup norm of the matrix $\Delta(T)^\tau J \Delta(T) - J$, that we know be 0. Second, we compute the eigenvalues of the monodromy matrix with the QR algorithm, using the routine `dgeev` of the `LAPACK` library. From this set we check the presence of the double unitary eigenvalue, arising from the periodicity of the orbit and from the Hamiltonian structure.

Orbit without close approaches

As test orbit without close approaches we choose ν_2 on $\mathcal{Q}_\mathcal{T}$ (see Table 4). Once we have obtained the trajectory with the relaxation dynamics method, we can make our test. First we compute the estimate of the monodromy matrix without the factorization, that is we solve numerically the variational equation on the entire interval $[0, T]$. Exploiting the symmetry of the orbit, we can propagate the variational equation only over the interval $[0, T/M]$ and we recover the monodromy matrix through the factorization given in Chapter 3. The results, truncated at some decimal digit, are listed in the Table 7. The monodromy matrix results to be symplectic with a good approximation,

Table 7: Results of the integration of the variational equation for ν_2, using the relaxation dynamics.

Fact.	Symp. check	Eigenvalues
No	0.1×10^{-8}	1445 0.0006 $0.994 \pm 0.107i$ $0.997 \pm 0.077i$
Yes	0.7×10^{-9}	1445 0.0006 $0.994 \pm 0.104i$ $0.997 \pm 0.077i$

that becomes better when we use the decomposition. The results obtained in the two cases are very similar: in particular we note that the double unitary eigenvalue is not present, but there is a couple of complex conjugate eigenvalues that have a small imaginary component. Since the numerical implementation of the relaxation dynamics is an iterative procedure, we can try to go ahead with the process: in this manner we see that, in both cases, the couple of unitary complex conjugate eigenvalues still lie on the unit circle, but the imaginary part decrease in the successive iterations, therefore we can think that they converge to the double unitary eigenvalue. However, the convergence is very slow and we were unable to obtain the couple of unitary eigenvalues. We can proceed with the tests of the shooting method.

The shooting method converges in two steps, with a tolerance of 10^{-10} and 700 equispaced shooting points, producing an initial point of the orbit. Therefore we integrate the equation of motion and the variational equation coupled together. Again, we get first the monodromy matrix integrating on the whole $[0, T]$ and then we compare this with those obtained using the factorization. The results are listed in the Table 8. In both cases the

Table 8: Results of the integration of the variational equation for ν_2, using the shooting method.

Fact.	Symp. check	Eigenvalues
No	0.7×10^{-9}	1445 0.0006 $0.994 \pm 0.107i$ $0.999 \pm 0.002i$
Yes	0.4×10^{-9}	1445 0.0006 $0.994 \pm 0.107i$ 1 ± 0.001

monodromy matrix still results symplectic with a good approximation. A couple of unitary complex conjugate eigenvalues with a small imaginary component appears again when we do not use the factorization. Instead, using the factorization, a couple of reciprocal real eigenvalues appears but however they are still close to 1. We conclude that the shooting method seems to produce better results than the precedent method, at least in this particular case.

Since in the numerical implementation of the relaxation dynamics we have to select a certain number of points that discretize the trajectory of the generating particle, we want to understand if taking a larger number of points produces better results. In the tests mentioned above we have used 1000 points per side of the sequence ν_2, for a total of 6000 points. As second test we take 300 points per side, for a total of 1800 points. The results obtained are listed in the Table 9: we can see that they are very similar, except for

Table 9: Results of the integration of the variational equation for ν_2, using the relaxation dynamics with 300 time points per side.

Fact.	Symp. check	Eigenvalues
No	0.3×10^{-8}	1445 0.0006 $0.994 \pm 0.107i$ $0.999 \pm 0.021i$
Yes	0.5×10^{-9}	1445 0.0006 $0.994 \pm 0.104i$ $0.999 \pm 0.021i$

the symplectic check, that is better when we use the factorization. Moreover, it seems that the results are better than the previous one: this can be explained by the fact that using more approximation points slows down the convergence of the gradient method. However, the convergence of the pro-

cess is still slow and we have to use the shooting method to improve our analysis. In fact, this latter method converges with a tolerance of 10^{-13} with 1000 equispaced shooting points in two steps. The results obtained from the numerical integration of the equation of motion and the variational equation coupled together are listed in the Table 10. We see that, integrating on

Table 10: Results of the integration of the variational equation for ν_2, using the shooting method ($\texttt{tol} = 10^{-13}$).

Fact.	Symp. check	Eigenvalues
No	0.6×10^{-9}	1445 0.0006 $0.994 \pm 0.107i$ $0.9999 \pm 0.0001i$
Yes	0.4×10^{-9}	1445 0.0006 $0.994 \pm 0.104i$ 1 ± 10^{-5}

the whole $[0, T]$, the unitary complex conjugate pair of eigenvalues is even more close to 1. Finally, when we use the factorization, we get the couple of double unitary eigenvalues with a good approximation. As last comment, the values obtained to check the stability are $T_1 \simeq 1443.85, T_2 \simeq 7.78$ and therefore this orbit seems to be unstable.

From this first test we conclude that:

1. We can use a not too high number of approximation points in the relaxation dynamics process, in order to get a faster (but still slow) convergence.
2. Integrating the variational equation over the interval $[0, T/M]$ and using the factorization seems to produce better results than integrating over the entire period.
3. The shooting method seems to produce more reliable results than the first method.

In the following we see how these two methods behave in the case of close approaches.

Close approaches: a good case

As example of orbit with some close approaches we take ν_1 on $\mathcal{Q}_\mathcal{T}$ (see Table 4): for this orbit the generating particle presents two close approaches per period. The trajectory is being approximated with 1500 points. The results of the integration of the variational equation using our first method are reported in Table 11. From these values we can see that, using or not the factorization of the monodromy matrix, the eigenvalues are real and in reciprocal couples. Moreover, continuing with the iterations of the gradient method, we see that the third eigenvalue decreases and the fourth increases. However, the convergence to the double unit eigenvalue is very slow and

Table 11: Results of the integration of the variational equation for ν_1, using the relaxation dynamics.

Fact.	Symp. check	Eigenvalues
No	0.6×10^{-8}	1055
		317
		38
		0.0259
		0.0009
		0.0031
Yes	0.3×10^{-9}	1055
		317
		38
		0.0259
		0.0009
		0.0031

Table 12: Results of the integration of the variational equation for ν_1, using the shooting method.

Fact.	Symp. check	Eigenvalues
No	0.3×10^{-9}	658
		0.0015
		$0.086 \pm 0.996i$
		$1 \pm 3 \times 10^{-4}$
Yes	0.3×10^{-10}	658
		0.0015
		$0.086 \pm 0.996i$
		$0.9999 \pm 10^{-4}i$

clearly far: in this case the results produced are not reliable. This fact is due to the slow convergence of the gradient method when the orbit presents one or more close approaches (see [20]).

The only thing to do is try to recover an initial condition using the shooting method. With 2 equispaced shooting points we obtain convergence in 196 steps with tolerance equals to 10^{-8}. Moreover, we see that increasing the number of shooting points do not improve the results, on the contrary, the convergence is not been reached at all with the same tolerance: this fact can be seen as a first sign of the instability of the orbit. The results of the integration are listed in the Table 12. We can see that in both cases there is a couple of eigenvalues that are close to 1: this is a confirm that the shooting method produces more reliable results than the other one. Furthermore, the values computed to check the stability are $T_1 \simeq 658, T_2 \simeq 4.34$ and this seems to confirm our conjecture on the instability.

In conclusion, when we are able to get the convergence of the shooting method, the results produced by this latter are more accurate and reliable than the other one, produced by the method based on the relaxation dynamics.

Close approaches: exploiting the symmetry

As last test orbit we choose ν_4 on $\mathcal{Q}_\mathcal{T}$ (see Table 4): for this orbit the generating particle presents three close approaches per period. The trajectory is being approximated with 12000 points. The results of the integration of the variational equation using our first method are reported in Table 13. The values produced seem to do not have any sense and they completely disagree with the theory of Chapter 3: this fact confirms that this approach is not effective when the orbit passes close to a collision. However, the shooting

Table 13: Results of the integration of the variational equation for ν_4, using the relaxation dynamics.

Fact.	Symp. check	Eigenvalues
No	0.6×10^{-1}	-16995792 $-3179.317 \pm 692.498i$ $-0.0003 \pm 0.00006i$ -6×10^{-8}
Yes	0.4×10^{0}	22522389 -390957 $0.920 \pm 0.390i$ -2.56×10^{-6} 5×10^{-8}

method is convergent with 2 shooting points and a tolerance of 10^{-7}, performing 7 steps. The results obtained are listed in the Table 14: we see that,

Table 14: Results of the integration of the variational equation for ν_4, with the shooting method.

Fact.	Symp. check	Eigenvalues
No	0.2×10^{-1}	935745 1.788 $0.243 \pm 0.969i$ 0.559 10^{-6}
Yes	0.7×10^{-3}	928092 $0.273 \pm 0.961i$ 1.010 0.990 10^{-6}

when we solve numerically on the whole $[0, T]$, we do not recover the double unitary eigenvalue: this is a consequence of the presence of multiple close approaches during the entire period, that cause a strong deviation from the true orbit. However, when we exploit the factorization of the monodromy matrix, we find a couple of near unitary eigenvalues: this fact confirm our prediction that integrating only over $[0, T/M]$ produces better results. The values computed to check the stability are $T_1 \simeq 928092$ and $T_2 \simeq 4.29$ and then it seems that this orbit is unstable.

A similar behaviour is found also in the orbits $\mathcal{K}_1^c$ and $\mathcal{K}_3^c$ on $\mathcal{Q}_\mathcal{O}$. We conclude that, when multiple close approaches occur during the entire period of the orbit, exploiting the symmetry to factor the monodromy matrix

provide more reliable results that obtaining directly the monodromy matrix by numerical integration.

RESULTS

In the previous Section we have seen that using the multiple shooting method we produce more reliable results than using the method based on the relaxation dynamics: for this reason we decided to report only these values. The results obtained are listed in the Tables 15, 16 and 17: we see that all the orbits result to be unstable, with a large value of the root T_1. This also means that one of the Floquet multipliers is very large in absolute value, causing a strong instability of our periodic orbits. We remark that in the case of the Icosahedron (Table 17) we have not obtained the results of the stability for all the orbits listed in Table 6, since we had some problems in the convergence of the gradient method: this means that we do not have an initial first guess good enough to ensure the convergence of the multiple shooting method. However, in order to make these results a true computer assisted proof, a rigorous estimate of the numerical error is needed: we claim that this step should not be very problematic, because of the large values of Δ and T_1.

Table 15: Stability results for $\Omega_{\mathcal{O}}$, using the shooting method.

Seq.	Tol.	Nr. pts.	Nr. steps	Fact.	Δ	T_1	T_2
ν_1	10^{-7}	2	4	No	3707347	1925	−0.20
				Yes	3707418	1925	−0.20
ν_2	10^{-6}	2	8	No	685205338	26176	0.36
				Yes	685188753	26176	0.36
ν_3	10^{-7}	2	6	No	88727489	9422	2.56
				Yes	88725613	9421	2.56
ν_4	10^{-9}	2	11	No	52198072319	228474	5.70
				Yes	52198126551	228474	5.70
ν_5	10^{-7}	2	7	No	64284472441410	8017762	2.77
				Yes	64252542203824	8015771	2.85
ν_6	10^{-12}	1000	2	No	147035784654	383460	7.90
				Yes	147035807080	383460	7.95
ν_7	10^{-10}	2	10	No	293604893	17142	7.98
				Yes	293604965	17142	7.98
ν_8	10^{-9}	2	5	No	$\sim 2.4 \times 10^{17}$	491885581	5.46
				Yes	$\sim 2.3 \times 10^{17}$	482672232	2.41
$\mathcal{K}_1^e$	10^{-6}	1000	2	No	2046983418464	1430731	2.77
				Yes	2254290809856	1501432	3.19
$\mathcal{K}_2^e$	10^{-8}	1000	2	No	293649754	17143	7.34
				Yes	293648416	17143	7.35
$\mathcal{K}_3^e$	10^{-6}	1000	2	No	35895760791592	5991340	33.51
				Yes	12888718668962	3590093	7.00
$\mathcal{K}_1^o$	10^{-7}	2	4	No	11722273880	108269	0.21
				Yes	11723156041	108273	0.21
$\mathcal{K}_2^o$	10^{-14}	2	68	No	50484851	7112	7.13
				Yes	50484857	7112	7.13
$\mathcal{K}_3^o$	10^{-9}	2	25	No	4958837949	70425	6.78
				Yes	4958837586	70425	6.78

Table 16: Stability results for $\mathcal{Q}_{\mathcal{T}}$, using the shooting method.

Seq.	Tol.	Nr. pts.	Nr. steps	Fact.	Δ	T_1	T_2
ν_1	10^{-8}	2	196	No	428323	658	4.21
				Yes	428323	658	4.21
ν_2	10^{-11}	500	2	No	2062282	1443	7.78
				Yes	2062282	1443	7.78
ν_3	10^{-6}	1200	2	No	3896494	1981	8.00
				Yes	3896537	1981	8.00
ν_4	10^{-7}	2	5	No	875609325820	935745	5.06
				Yes	861347364822	928092	4.49
ν_5	10^{-8}	800	2	No	2776597113	52694	0.59
				Yes	2776597055	52694	0.59
ν_6	10^{-12}	300	2	No	56003497	7491	8.10
				Yes	56003499	7491	8.10
ν_7	10^{-12}	1000	2	No	4367612596058	2089891	8.12
				Yes	4367626412333	2089894	7.77
$\mathcal{K}_1^{\mathcal{T}}$	10^{-6}	500	2	No	489717189	22135	5.59
				Yes	489166428	22122	5.59
$\mathcal{K}_3^{\mathcal{T}}$	10^{-5}	1000	2	No	622055864	24948	7.75
				Yes	615384687	24814	7.53

Table 17: Stability results for $\mathcal{Q}_{\mathcal{J}}$, using the shooting method.

Seq.	Tol.	Nr. pts.	Nr. steps	Fact.	Δ	T_1	T_2
ν_3	10^{-6}	2	4	No	$\sim 51 \times 10^{18}$	$\sim 22 \times 10^{7}$	-82
				Yes	$\sim 51 \times 10^{23}$	$\sim 72 \times 10^{10}$	6.46
ν_5	10^{-12}	2	10	No	$\sim 78 \times 10^{17}$	$\sim 28 \times 10^{8}$	6.34
				Yes	$\sim 78 \times 10^{17}$	$\sim 28 \times 10^{8}$	6.32
ν_6	10^{-13}	2	19	No	$\sim 67 \times 10^{16}$	$\sim 82 \times 10^{7}$	7.73
				Yes	$\sim 67 \times 10^{16}$	$\sim 82 \times 10^{7}$	7.73
ν_7	10^{-9}	2	11	No	$\sim 14 \times 10^{25}$	$\sim 12 \times 10^{12}$	41
				Yes	$\sim 20 \times 10^{31}$	$\sim 14 \times 10^{15}$	4.00
$\mathcal{K}_1^{\mathcal{D}}$	10^{-8}	2	3	No	$\sim 64 \times 10^{15}$	$\sim 25 \times 10^{7}$	-0.59
				Yes	$\sim 58 \times 10^{15}$	$\sim 24 \times 10^{7}$	-1.92×10^{-2}
$\mathcal{K}_2^{\mathcal{D}}$	10^{-12}	2	52	No	$\sim 21 \times 10^{11}$	$\sim 14 \times 10^{5}$	1.68
				Yes	$\sim 21 \times 10^{11}$	$\sim 14 \times 10^{5}$	1.68
$\mathcal{K}_3^{\mathcal{D}}$	10^{-10}	2	32	No	$\sim 15 \times 10^{17}$	$\sim 12 \times 10^{8}$	1.30
				Yes	$\sim 15 \times 10^{17}$	$\sim 12 \times 10^{8}$	1.27
$\mathcal{K}_3^{\mathcal{J}}$	10^{-12}	2	5	No	$\sim 76 \times 10^{9}$	$\sim 27 \times 10^{4}$	0.93
				Yes	$\sim 76 \times 10^{9}$	$\sim 27 \times 10^{4}$	0.93

5

CONCLUSIONS AND FUTURE WORKS

First, we have developed an algorithm to find all the free homotopy classes that satisfy the sufficient conditions to obtain a cone on which exist a collision-free minimizer of the Lagrangian action, and therefore a periodic orbit that is a solution of the classical Newtonian N-body problem. Our algorithm works fine in the case of the Tetrahedron, while when we considering the remaining Platonic polyhedra some computational problems occur. In the case of the Archimedean polyhedron $\mathcal{Q}_{\mathcal{O}}$ we may obtain the results in a finite time almost acceptable, since we must run the program only once. However, our approach is not effective in the case of the $\mathcal{Q}_{\mathcal{I}}$ Archimedean polyhedron, because of the exponential computational complexity. A possible strategy that could improve the algorithm is to find all the closed paths up to rotations of $\mathcal{Q}_{\mathcal{I}}$, since the orbits resulting from them are obtained simply rotating the space, in a way to exclude a priori some free homotopy classes. This possibility has not been explored yet, since it is not trivial to understand how to find the paths up to rotations.

Second, we have developed two numerical methods to study the stability of a given periodic orbit with the symmetry of the Platonic polyhedra. The first method is based on the relaxation dynamics, introduced by C. Moore, while the second one uses a multiple shooting method to find an approximation of the initial condition of the orbit: given this initial condition we can solve numerically the equation of motion and the variational equation coupled together, obtaining an approximation of the monodromy matrix. We have written these two numerical methods in `FORTRAN95` and tested the two different approaches: we have concluded that the first method does not produce reliable results when the orbit we are considering presents multiple close approaches, because of the slow convergence of the numerical implementation of the relaxation dynamics. On the contrary, the results obtained with the multiple shooting method, if convergent, are more reliable than the previous one. Moreover, we have seen that exploiting the symmetry of the orbits to factor the monodromy matrix can reduce the errors in the numerical integration, due again to the close approaches. With this method we have computed the values of T_1 and T_2 to check the stability of all the orbits listed in Chapter 2: from the results we have obtained, reported at the end of the Chapter 4, we concluded that they are all unstable. However, in order to make our work a true computer assisted proof, we must perform a study of the numerical error.

Our work can be improved trying to treat better the orbits that present strong close approaches. In the implementation of the relaxation dynam-

ics we have discretized the path at equally spaced values of the time: this implementation can be improved introducing truncated Fourier series, as described in [16] and [18]. With this approach, we write the action as a function of the Fourier components of the choreography curve, truncating the Fourier series at some finite order. Then the extrema of the action can be found with a gradient procedure, analogue to the one we have used: this new approximation of the path produces better results than the previous one (see [16]). However, when the orbit passes close to a collision, the convergence is still slow (see [14]): this fact suggests that we may not be able to obtain better results when we use this approximation of the motion to integrate the variational equation. On the other hand, it could be a more accurate first guess for the shooting method.

The shooting method could be improved both in the method used to integrate ODEs and in the practical implementation. Instead of a classical explicit Runge-Kutta method, we could use a *Taylor method* (see [12]). The idea is quite simple: let $\dot{x} = f(x)$ be an autonomous system and let

$$x(t) = \sum_i x^{[i]} h^i, \quad h = t - t_0, \quad x^{[i]} = \frac{1}{i!} \frac{dx(t_0)}{dt^i}$$

be the Taylor series at the time t_0 of the solution $x(t)$. Substituting x by its series in the system, expanding the function $f(\sum_i x^{[i]} h^i) = \sum_i f^{[i]}(x^{[0]}, \ldots, x^{[i]}) h^i$, and equating the coefficients of the series, we obtain the equation

$$x^{[i+1]} = \frac{f^{[i]}(x^{[0]}, \ldots, x^{[i]})}{i+1}.$$

This gives, in an iterative way beginning from an initial condition for $x^{[0]}$, a method to find the coefficients $x^{[i+1]}$ of the Taylor expansion of the solution of the system. The Taylor methods have been successfully used in [1] to compute some periodic orbits of the Lorenz model.

In the software implementation more improvements can be done, in order to obtain better results and make the algorithm faster. Some of these are the following.

- We have used equispaced shooting points: this may be a bad choice when some close approaches occur. We could introduce an automatic selection of the shooting points, as explained in [22] Section 7.3.6.

- We could exploit the parallel computing to solve the different initial value problems, that are all independent.

- We could use the particular sparse structure of the Jacobian matrix (4.17), in a way to reduce the computational complexity of the resolution of the linear system.

- We could use multiple precision arithmetic or interval arithmetic, as in [13]. We also observe that implementing the Taylor method using interval arithmetic permits to derive a bound for the total error of the numerical integration.

These improvements permits to perform also an accurate study of the numerical error, to produce a true computer assisted proof of the instability of our periodic orbits. Furthermore, we can change the potential from $1/r$ (the classical Newtonian potential) to the generalized potential $1/r^{\alpha}$. The periodic orbits with the symmetry of the Platonic polyhedra still exist for $\alpha \neq 1$ (see [6]), then we can study numerically the stability of such orbits and if some bifurcation occur or not.

BIBLIOGRAPHY

[1] A. Abad, R. Barrio, and A. Dena. Computing periodic orbits with arbitrary precision. *Phys. Rev. E*, 84, 2011.

[2] H. S. M. Coxeter, M. S. Longuet-Higgins, and J. C. P. Miller. Uniform polyhedra. *Philosophical Transactions of the Royal Society of London. Series A, Mathematical and Physical Sciences*, 246(916):401–450, 1954.

[3] L. D. Ferrario and S. Terracini. On the existence of collisionless equivariant minimizers for the classical n-body problem. *Inventiones mathematicae*, 155(2), 2003.

[4] G. Floquet. Sur les équations différentielles linéaires à coefficients périodiques. *Annales de l'École Normale Supérieure*, 12, 1883.

[5] G. Fusco, G. F. Gronchi, and P. Negrini. Platonic polyhedra, topological constraints and periodic solutions of the classical N-body problem. *Inventiones mathematicae*, 185(2), 2010.

[6] Giorgio Fusco and Giovanni F. Gronchi. Platonic polyhedra, periodic orbits and chaotic motions in the n-body problem with non-newtonian forces. *Journal of Dynamics and Differential Equations*, 26(4), 2014.

[7] William B. Gordon. A minimizing property of keplerian orbits. *American Journal of Mathematics*, 99(5), 1977.

[8] G. F. Gronchi. `http://adams.dm.unipi.it/~gronchi/nbody/`.

[9] Gronchi, G. F. *Periodic orbits of the N-body problem with the symmetry of Platonic polyhedra*, 2013.

[10] J. Hadjidemetriou. Periodic orbits in gravitational systems. *Chaotic Worlds: From Order to Disorder in Gravitational N-Body Dynamical Systems*, 2006.

[11] E. Hairer. `http://www.unige.ch/~hairer/software.html`.

[12] A Jorba and M. Zou. A software package for the numerical integration of odes by means of high-order taylor methods. *Experiment. Math.*, 14(1), 2005.

[13] T. Kapela and C. Simó. Computer assisted proofs for nonsymmetric planar choreographies and for stability of the eight. *Nonlinearity*, 20(5), 2007.

[14] R. Montgomery. N-body choreographies. *Scholarpedia*, 5(11), 2010.

[15] C Moore. Braids in classical dynamics. *Physical review letters*, 70(24), 1993.

[16] C. Moore and M. Nauenberg. New periodic orbits for the n-body problem. *Journal of Computational and Nonlinear Dynamics*, 1, 2006.

[17] J. Moser and E. Zehnder. *Notes on dynamical systems*. AMS, 2005.

[18] M. Nauenberg. Periodic orbits for three particles with finite angular momentum. *Physics Letters A*, 292(1), 2001.

[19] G. E. Roberts. Linear stability anlysis of the figure-eight orbit in the three-body problem. *Ergodic Theory and Dynamical Systems*, 27, 2007.

[20] Simó, C. *New families of Solutions in N-body problems*. Proceedings of the ECM, July 2000.

[21] E.L. Stiefel and G. Scheifele. *Linear and regular celestial mechanics*. Springer-Verlag, 1971.

[22] J. Stoer and R. Bulirsch. *Introduction to numerical analysis*. Texts in applied mathematics. Springer, 2002.

[23] A. Venturelli. *Application de la minimisation de l'action au Probléme des N corps dans le plan et dans l'espace*. PhD thesis, Université De Paris, 2002.